Photocopy and Use Authorization

In presenting this thesis in partial fulfillment of the requirements for an advanced degree at Idaho State University, I agree that the Library shall make it freely available for inspection. I further state that permission for extensive copying of my thesis for scholarly purposes may be granted by the Dean of the Graduate School, Dean of my academic division, or by the University Librarian. It is understood that any copying or publication of this thesis for financial gain shall not be allowed without my written permission.

Signature: _____

Date: _____

Interpreting River Incision History using Terraces and Mass Movements along the South Fork Eel River, Northern California

by

Katherine E. Wehrs

A thesis

submitted in partial fulfillment

of the requirements for the degree of

Master of Science in the Department of Geosciences

Idaho State University

Summer 2018

Committee Approval

To the Graduate Faculty:

The members of the committee appointed to examine the thesis of Katherine E. Wehrs find it satisfactory and recommend that it be accepted.

_____

Benjamin T. Crosby,

Major Advisor

_____

Glenn D. Thackray,

Committee Member

_____

Yolonda L. Youngs,

Graduate Faculty Representative

Acknowledgements

I want to thank the California Parks Service and local landowners for access to OSL sampling locations. To the National Science Foundation (EAR-1349261) and Idaho State University Department of Geosciences, Geslin Award for providing funding for fieldwork and sample processing. To Utah State University's Luminescence Laboratory for the multiple hours of processing completed and those still to be done.

To my support system for this project; Dr. Benjamin Crosby, Dr. Glenn Thackray, Dr. Yolonda Youngs, Brandon Crawford, Ian Lauer, Jenny Deering, Anna Radke, Chris Borg, Ashley Shields, Sarah Tetzloff, Hanan Abou Ali, Graham Meese, and everyone else in the department. To my parents, Bobbi and Dave Wehrs, and to my amazing sister Teresa, for all of their support and encouragement. Thank you all for your assistance in getting this thesis completed. For all the hours spent revising and discussing ideas, help with fieldwork, emotional support, and just making these past two years so amazing.

Table of Contents

List of Tables

List of Figures

Interpreting River Incision History using Terraces and Mass Movements

along the South Fork Eel River, Northern California

Thesis Abstract - Idaho State University (2018)

This aim of this study is to understand the coupled relationship between rivers and their surrounding hillslopes during and following base level fall. To do this we examine (1) the placement and longitudinal age variation of strath terraces and (2) the form, frequency and position of mass movements below, at and above a mainstem knickpoint. Our findings from the South Fork Eel River, in northern California indicate that incision initiated ~ 134,000 years ago and was accomplished through progressive upstream knickpoint retreat, as alluvial sediments on terrace treads show two clusters of ages which young upstream. Hillslopes responded to base level fall in a similar progressive manner, as the frequency of mass movements decrease in with distance upstream, with mass movements having a larger impact on the adjusted lower basin of the South Fork Eel River, than the relict upper basin. Translational slides dominate throughout the basin, with a decrease in the number of earth flows present with distance upstream, and an increase in the number of debris flows with distance to the knickzone.

Keywords:

Geomorphology, landscape evolution, landslides, fluvial terraces, OSL dating, hillslope-channel coupling, strath terrace, Northern California, transience, South Fork Eel River, LiDAR, bulk OSL sampling, landslide mapping

Chapter 1 : Introduction

1.1 Problem Statement

Landscapes respond to various disturbances, whether a shift in the rate of tectonic uplift, a change in climate, or human influence. Landscapes adjust to these disturbances, diverging from a relative steady state into a state of transience. Understanding how landscapes respond to disturbances allows us to predict how they may continue to change in the future. This can be done through the study of location and placement of river terraces, knickpoints, and mass movements. River terrace placement can be used to reconstruct channel locations (Merritts et al., 1994; Meyer and Leidecker, 1999; Litchfield and Berryman, 2005), while knickpoints can be used to determine how incision signals have propagated up through the system (Crosby and Whipple, 2006; Foster and Kelsey, 2012), and mass movements can be used to determine how the hillslopes respond to these changes (Gallen et al., 2011; Dibiase et al., 2012; Roering et al., 2015; Bennett et al., 2016). Typically, the formation of knickpoints and terrace placement has dominated the study of how upland and bedrock river networks respond to relative base level fall. Some research has focused on how the adjacent hillslopes respond around propagating knickpoints (Ouimet et al., 2007; DiBiase et al., 2014), but little work has been done on how hillslopes respond on a basin-wide scale to base level fall. I use terrace height and placement along with Optically Stimulated Luminescence techniques, to determine how and when mainstem incision likely occurred. I then use LiDAR for high resolution mass movement mapping to determine how the morphology and frequency of mass movements changes with distance along a channel undergoing active change. The presence of numerous strath terraces, a prominent knickzone, and high-resolution LiDAR along the entire channel, enable this study of hillslope response to base level fall along the South Fork Eel River.

1.2 River Transience – how does a river respond to changing conditions?

1.2.1 Base level changes, a response to tectonic uplift or climatic forcing

The drivers of change within a river system are water discharge, sediment load, and base level. These drivers are impacted by tectonics, climate, vegetation and anthropogenic actions. The magnitude and direction of base level change determines whether a river will incise into its bed or aggrade, and to what degree. Changes in local base level can occur due to rise or fall in sea level which could cause local incision or aggradation (Swenson and Muto, 2007) or increase of precipitation, which could increase the amount of sediment delivered to the channel or increase water discharge, increasing erosive potential (Whipple, 2002). Changes in these factors would likely lead to base level adjustment and propagation changes up the entire channel network (Hack, 1975; Schumm, 1993).

1.2.2 Knickpoints/Knickzones

Rivers respond to base level changes at varying scales, with larger scale changes like tectonic uplift or sea level drop prompting the development of an incision signal which propagates upstream, potentially forming knickpoints or knickzones (Whipple and Tucker, 1999; Crosby and Whipple, 2006; Foster and Kelsey, 2012; Mackey et al., 2014). These knickpoints represent the erosional front from the upstream propagation of base level fall and separate the adjusting and relict portions of the landscape (Schlunegger and Schneider, 2005; Crosby and Whipple, 2006). The formation of knickpoints and knickzones can occur as single events or as progressive alterations, which are recorded via changes in channel gradient along the channel profile, through landscape adjustment and mass wasting events to stabilize the coupled hillslopes to a new river base level (Savi et al., 2013).

1.2.3 Terraces and their Formation

Terrace sequences record river incision through time and are distinguished from floodplains as they lie above the present channel and are disconnected from flood events. There are two forms of terraces; alluvial or fill, and strath.

Alluvial or fill terraces, are characterized by a thick alluvial deposits (Pazzaglia, 2013). These tend to form in alluvial systems, where unconsolidated or weakly consolidated sediments are prominent and envelop the base of the river. These systems are sensitive to active tectonics, and are highly dependent on stream power to move material around and rework the system (Merritts et al., 1994).

A strath terrace is characterized by a beveled surface, commonly carved into bedrock, with a thin mantle of overlying alluvium. Bedrock is any substrate into which the river valley is being cut. This can sometimes include poorly consolidated sediments, which can make it difficult to distinguish between alluvial or strath terraces (Montgomery, 2004; Finnegan and Dietrich, 2011; Pazzaglia, 2013). These bedrock systems can take longer to respond to tectonic change as the bedrock acts as the base of the river, so the river must have the tools and strength to break down and transport the materials away for incision to occur (Fuller et al., 2009; Finnegan and Dietrich, 2011). These features initially form by lateral erosion of the river, which carves the terrace base while systematically depositing fluvial sediments. When sediment load exceeds the transport capacity of the river, causing vertical incision to decrease, and lateral erosion and deposition to dominate. Strath are preserved when stream power exceeds the transport capacity, leading to river incision (Bull, 1990a; Merritts et al., 1994; Hancock and Anderson, 2002).

Terrace location and elevation can be used to reconstruct paleo channel locations and to measure rates of uplift and other tectonic drivers that may be at work within the region (Merritts and Bull, 1989; Meyer and Leidecker, 1999; Gran et al., 2013). The slope of terrace treads can be used to determine the direction of river migration or how quickly incision was accomplished within a system (Finnegan and Dietrich, 2011). The alluvium above strath is assumed to be continually reworked while they exist as the active flood plain, until the plain is abandoned forming the strath terrace. Dating of strath terraces and their fill can then be used to determine vertical incision rates for the system, along with a minimum estimation for placement of the river at that location (Walker, 1986; Meyer and Leidecker, 1999; Tanaka et al., 2001; Litchfield and Rieser, 2005; Fuller et al., 2009; Gran et al., 2013).

1.3 Hillslopes

1.3.1 Coupling to Rivers

There is a coupled relationship between hillslopes and the channel, so as a river incises, it drives a response from the surrounding hillslopes (Mudd and Furbish, 2007; Harvey, 2002; Savi et al., 2013). The strength of this connection affects both the temporal and spatial scale of how and when failures may occur. In poorly coupled systems the hillslope response may stay localized or only be seen at long time scales. In well coupled systems, hillslope response will be transmitted throughout the entire river network as it lowers (Savi et al., 2013). As local incision occurs, the channel experiences increased erosion on the channel bed along with the surrounding banks, typically on the downstream end of a knickpoint. This causes the hillslopes to steepen, and in order to re-establish equilibrium, soils and bedrock fail in the form of mass movements (Korup and Schlunegger, 2007; Ouimet et al., 2007; DiBiase et al., 2014; Roering et al., 2015).

1.3.2 Limiting Factors for Response

As hillslopes respond to river transience, there are a few limiting factors that control what changes can occur. Hillslopes tend to be strength-limited, meaning the mass wasting events are controlled by the rate of channel incision and the mechanical properties of the underlying bedrock. Properties like the strength of the bedrock as determined by bedding plains, fracturing/jointing, seepage, or porosity can resist or promote failure at different scales (Schlunegger et al., 2013; Goudie, 2016). Otherwise, hillslopes are considered transport-limited, meaning that the slope, viscosity, and the availability of the sediment cover drive failure processes and frequency. This is important when analyzing the type of failure one sees, as the variations in setting properties impact whether deep-seated bedrock failures or shallow landslides occur (Korup, 2008). Strength-limited sections of the landscape are dominated by rock falls, rotational, and translational slides while transport-limited areas are dominated by creep, earthflows, and debris flows (Schlunegger et al., 2013). The amount of precipitation, pore pressure, vegetation cover, and rate of incision also impact how quickly hillslopes will respond to base level change (Roering et al., 2015).

1.4 Study Area

1.4.1 Geologic Setting

The South Fork Eel River (SFER), is located within northern California in Humboldt and Mendocino Counties (Figure 1.1). It is located within two major belts of the accreted terrain of the Franciscan Complex (Figure 1.2). These terrains formed over 150 million years of continuous subduction of the Farallon Plate along the western edge of Northern America, spanning from Alaska down into Mexico (Wakabayashi, 2015; Yonkee and Weil, 2015). The eastern, Central Franciscan belt, is comprised of mélange, which consists primarily of

greywackes, shales, conglomerates, sedimentary breccia, with greenstone, and chert. The Central Belt also contains large resistant knockers of blueschist, eclogite or rare limestone that are scattered throughout (Blake Jr et al., 1981; Cloos, 1982; Robert J McLaughlin, 2000; Wakabayashi, 2015). The western belt, the Coastal Franciscan belt, is composed of the Yager and Wildcat group terrains. These terrains contain sheared sandstone, mudstone, and conglomerates and comprise the youngest part of the complex (Blake Jr et al., 1981; USFS and BLM, 1996; Robert J McLaughlin, 2000; Wakabayashi, 2015).

The watershed is dissected by transpressional faults, which strike parallel to subparallel to the northwest strike of the San Andreas fault system (Robert J McLaughlin, 2000; Lock et al., 2006). Uplift rates derived from marine terrace location and ages, suggest that the coast near the southern headwaters experience uplift rates of ~0.4 mm/year (Merritts et al., 1994), with increasing rates north to ~4-3.5 mm/year, due to the northward migration of the Mendocino Triple Junction (Merritts et al., 1994; Snyder et al., 2000; Lock et al., 2006). Further inland, uplift rates have been modelled at 1.3 mm/year for the flight of Mitchell Ranch terraces located south of Garberville (Bickner, 1993), along with a rate of 1 mm/year for the Eel River just to the west of the SFER (Roering et al., 2015).

1.4.2 The South Fork Eel River

The SFER is the largest tributary to the Eel river system, and its watershed covers an area of 1780 km^2, with the river flowing 169 kilometers from Laytonville, CA north to the confluence with the Eel, just north of Weott, CA. The system ranges in elevation from 30 meters above sea level at the Eel River confluence, to 1,369 meters at its highest point, Iron Peak (USFS and BLM, 1996; California Department of Fish and Wildlife, 2014). The river is a dominantly bedrock system, containing one prominent knickzone, ~10 kilometers long, between the tributary

junctions of Tenmile and Rattlesnake Creeks (Fuller et al., 2009). This knickzone, along with the presence of knickpoints within the surrounding tributaries (Foster, 2010), signifies that the SFER is undergoing transience within the basin, and that base level fall has not yet propagated up through the entire system.

The region receives 190-200 centimeters of precipitation annually, (National Center for Atmospheric Research, 2017).This in combination with high uplift rates and weak lithology contributes to high rates of incision and numerous mass movements along the river length.

Chapter 1 Figures

Figure 1.1: Location of the SFER in relation to the surrounding counties, along with major cities and tributaries. The SFER knickzone is outlined in dark blue.

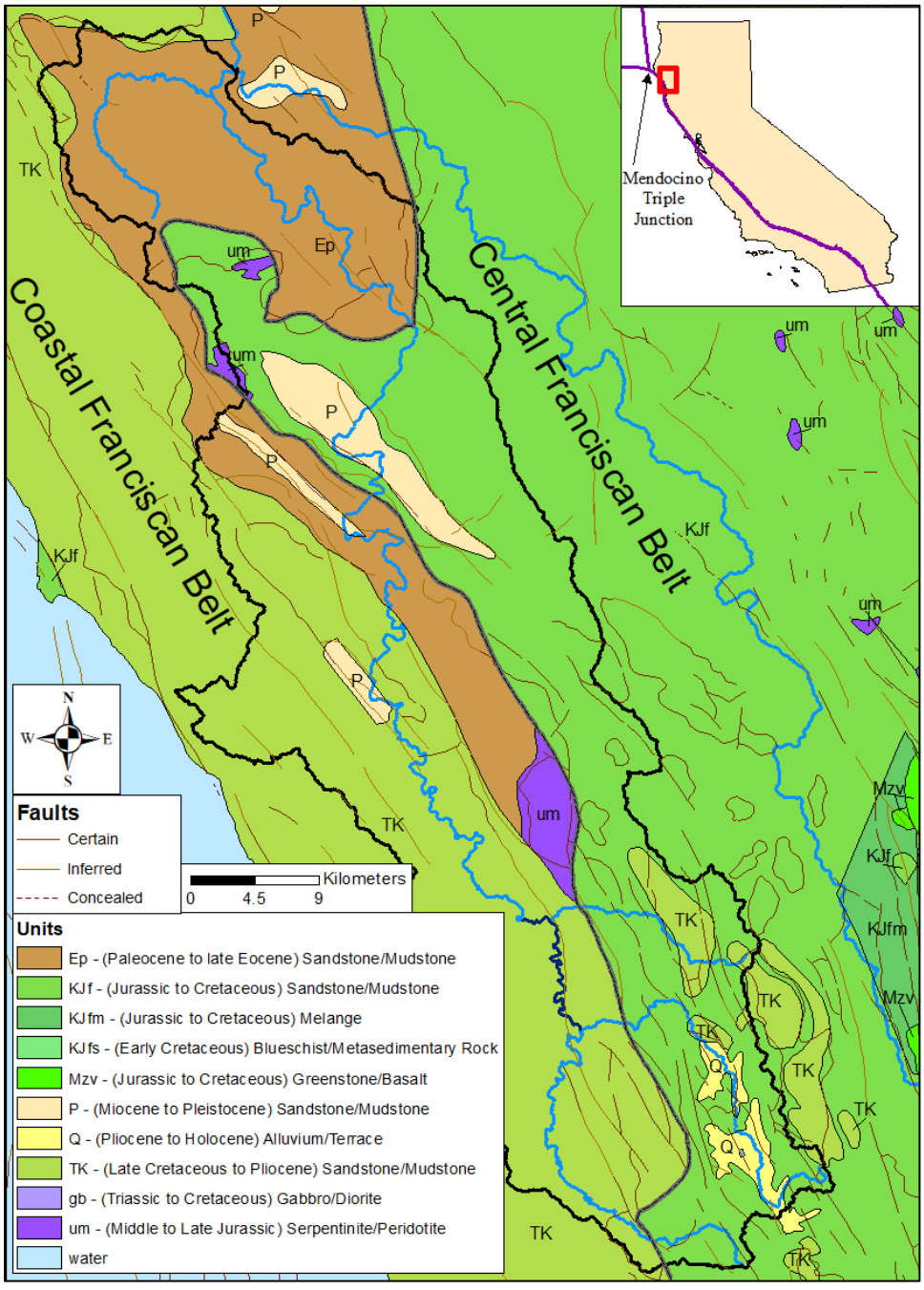

Figure 1.2: Geologic map of the SFER watershed and surrounding areas. Main units of the Franciscan Central Franciscan Belt and Coastal Franciscan Belt terrains are shown and labeled with primary lithologic type. The Franciscan Central Franciscan Belt comprises the eastern half of the watershed, and the Coastal Franciscan Belt comprises the western half – separated by dark gray dashed line. Faults are shown in brown.

References

Bennett, G.L., Miller, S.R., Roering, J.J., and Schmidt, D.A., 2016, Landslides, threshold slopes, and the survival of relict terrain in the wake of the Mendocino Triple Junction: Geology, v. 44, p. 363–366, doi: 10.1130/G37530.1.

Bickner, F.R., 1993, A soil chronosequence of the Mitchell Ranch fluvial terraces on the South Fork Eel River: Age estimates and Tectonic Implications [MS thesis]: Humboldt, California State University, 81 p.

Blake Jr, M.C., Jayko, A.S., and Howell, D.G., 1981, Geology of a subduction complex in the Franciscan assemblage of Northern California: Oceanologica, p. 267–272.

Bull, W.B., 1990, Stream-terrace genesis: implications for soil development: Geomorphology, v. 3, p 351-367, doi: 10.1016/0169-555X(90)90011-E.

California Department of Fish and Wildlife, 2014, South Fork Eel River Watershed Overview: , p. 186.

Cloos, M., 1982, Flow melanges: numerical modeling and geologic constraints on their origin in the Franciscan subduction complex, California: Geological Society of America Bulletin, v. 93, p. 330–345, doi: 10.1130/0016-7606(1982)93<330:FMNMAG>2.0.CO.

Crosby, B.T., and Whipple, K.X., 2006, Knickpoint initiation and distribution within fluvial networks: 236 waterfalls in the Waipaoa River, North Island, New Zealand: Geomorphology, v. 82, p. 16–38, doi: 10.1016/j.geomorph.2005.08.023.

DiBiase, R.A., Heimsath, A.M., and Whipple, K.X., 2012, Hillslope response to tectonic forcing in threshold landscapes: Earth Surface Processes and Landforms, v. 37, p. 855–865, doi: 10.1002/esp.3205.

DiBiase, R.A., Whipple, K.X., Lamb, M.P., and Heimsath, A.M., 2014, The role of waterfalls and knickzones in controlling the style and pace of landscape adjustment in the western San Gabriel Mountains, California: Bulletin of the Geological Society of America, v. 127, p. 539–559, doi: 10.1130/B31113.1.

Finnegan, N.J., and Dietrich, W.E., 2011, Episodic bedrock strath terrace formation due to meander migration and cutoff: Geology, v. 39, p. 143–146, doi: 10.1130/G31716.1.

Foster, M.A., 2010, Knickpoints in tributaries of the south fork Eel River, Northern California [M.S. Thesis]: Humboldt, California State University, 97 p.

Foster, M.A., and Kelsey, H.M., 2012, Knickpoint and knickzone formation and propagation, South Fork Eel River, northern California: Geosphere, v. 8, p. 403–416, doi: 10.1130/GES00700.1.

Fuller, T.K., Perg, L.A., Willenbring, J.K., and Lepper, K., 2009, Field evidence for climate-driven changes in sediment supply leading to strath terrace formation: Geology, v. 37, p. 467–470, doi: 10.1130/G25487A.1.

Gallen, S., Wegmann, K., Frankel, K., Hughes, S., Lewis, R., Lyons, N., Paris, P., Ross, K., Bauer, J., and Witt, A., 2011, Hillslope response to knickpoint migration in the Southern Appalachians: Implications for the evolution of post-orogenic landscapes: Earth Surface Processes and Landforms, v. 36, p. 1254–1267, doi: 10.1002/esp.2150.

Goudie, A.S., 2016, Quantification of rock control in geomorphology: Earth-Science Reviews, v. 159, p. 374–387, doi: 10.1016/j.earscirev.2016.06.012.

Gran, K., Finnegan, N., Johnson, A., Belmont, P., Wittkop, C., and Rittenour, T., 2013, Landscape evolution, valley excavation, and terrace development following abrupt postglacial base-level fall: Bulletin of the Geological Society of America, v. 125, p. 1851–1864, doi: 10.1130/B30772.1.

Hack, J.T., 1975, Dynamic equilibrium and landscape evolution: Theories of Landform Development: Publications in Geomorphology, p. 91–102.

Hancock, G.S., and Anderson, R.S., 2002, Numerical modelling of fluvial strath terrace formation in response to oscillating climate: Geological Society of American Bulletin, v. 114, p. 1131–1142, doi: 10.1130/0016-7606(2002)114<1131.

Harvey, A.M., 2002, Effective timescales of coupling within fluvial systems: Geomorphology, v. 44, p. 175–201, doi: 10.1016/S0169-555X(01)00174-X.

Korup, O., 2008, Rock type leaves topographic signature in landslide-dominated mountain ranges: Geophysical Research Letters, v. 35, p. 1–5, doi: 10.1029/2008GL034157.

Korup, O., and Schlunegger, F., 2007, Bedrock landsliding, river incision, and transience of geomorphic hillslope-channel coupling: Evidence from inner gorges in the Swiss Alps: Journal of Geophysical Research: Earth Surface, v. 112, doi: 10.1029/2006JF000710.

Litchfield, N.J., and Berryman, K.R., 2005, Correlation of fluvial terraces within the Hikurangi Margin, New Zealand: Implications for climate and base level controls: Geomorphology, v. 68, p. 291–313, doi: 10.1016/j.geomorph.2004.12.001.

Litchfield, N.J., and Rieser, U., 2005, Optically stimulated luminescence age constraints for fluvial aggradation terraces and loess in the eastern North Island, New Zealand: New Zealand Journal of Geology and Geophysics, v. 48, p. 581–589, doi: 10.1080/00288306.2005.9515135.

Lock, J., Kelsey, H., Furlong, K., and Woolace, A., 2006, Late Neogene and Quaternary landscape evolution of the northern California Coast Ranges: Evidence for Mendocino triple junction tectonics: Bulletin of the Geological Society of America, v. 118, p. 1232–1246, doi: 10.1130/B25885.1.

Mackey, B.H., Scheingross, J.S., Lamb, M.P., and Farley, K.A., 2014, Knickpoint formation, rapid propagation, and landscape response following coastal cliff retreat at the last interglacial sea-level highstand: Kaua'i, Hawai'i: Bulletin of the Geological Society of America, v. 126, p. 925–942, doi: 10.1130/B30930.1.

McLaughlin, R., Ellen, S., Blake, M., Jayko, A., Irwin, W., Aalto, K., Carver, G., and Clarke Jr, S., 2000, Geology of the Cape Mendocino, Eureka, Garberville, and Southwestern part of the Hayfork 30x60 Minute Quadrangles and Adjacent Offshore Area, Northern California, Plate 3: Garberville Quadrangle: USGS.

Merritts, D., and Bull, W., 1989, Interpreting Quaternary uplift rates at the Mendocino triple junction, northern California, from uplifted marine terraces: Geology, v. 17, p. 1020–1024, doi: 10.1130/0091-7613(1989)017<1020:IQURAT>2.3.CO;2.

Merritts, D.J., Vincent, K.R., and Wohl, E.E., 1994, Long river profiles, tectonism, and eustasy: A guide to interpreting fluvial terraces: Journal of Geophyscial Research, v. 99, p. 1431–1450, doi: 10.1029/94JB00857.

Meyer, G.A., and Leidecker, M.E., 1999, Fluvial terraces along the Middle Fork Salmon River, Idaho, and their relation to glaciation, landslide dams, and incision rates: a preliminary analysis and river-mile guide: Museum, p. 219–235.

Montgomery, D.R., 2004, Observations on the role of lithology in strath terrace formation and bedrock channel width: American Journal of Science, v. 304, p. 454–476, doi: 10.2475/ajs.304.5.454.

Mudd, S.M., and Furbish, D.J., 2007, Responses of soil-mantled hillslopes to transient channel incision rates: Journal of Geophysical Research: Earth Surface, v. 112, p. 1–12, doi: 10.1029/2006JF000516.

National Center for Atmospheric Research, 2017, The Climate Data Guide: PRISM High-Resolution Spatial Climate Data for the United States: Max/min temp, dewpoint, precipitation: NCAR Climate Data Guide.

Ouimet, W.B., Whipple, K.X., Royden, L.H., Sun, Z., and Chen, Z., 2007, The influence of large landslides on river incision in a transient landscape: Eastern margin of the Tibetan Plateau (Sichuan, China): Geological Society of America Bulletin, v. 119, p. 1462–1476, doi: 10.1130/B26136.1.

Pazzaglia, F.J., 2013, Fluvial Terraces, in Shroder, J. ed.: Treatise on Geomorphology Elsevier Inc., v. 9, p. 379–412, doi: 10.1016/B978-0-12-374739-6.00248-7.

Roering, J.J., Mackey, B.H., Handwerger, A.L., Booth, A.M., Schmidt, D.A., Bennett, G.L., and Cerovski-Darriau, C., 2015, Beyond the angle of repose: A review and synthesis of landslide processes in response to rapid uplift, Eel River, Northern California: Geomorphology, v. 236, p. 109–131, doi: 10.1016/j.geomorph.2015.02.013.

Savi, S., Schneuwly-Bollschweiler, M., Bommer-Denns, B., Stoffel, M., and Schlunegger, F., 2013, Geomorphic coupling between hillslopes and channels in the Swiss Alps: Earth Surface Processes and Landforms, v. 38, p. 959–969, doi: 10.1002/esp.3342.

Schlunegger, F., Norton, K., and Caduff, R., 2013, Hillslope processes in Temperate Environments: Treatise on Geomorphology, v. 7, p. 337–354, doi: 10.1016/B978-0-12-374739-6.00183-4.

Schlunegger, F., and Schneider, H., 2005, Relief-rejuvenation and topographic length scales in a fluvial drainage basin, Napf area, Central Switzerland: Geomorphology, v. 69, p. 102–117, doi: 10.1016/j.geomorph.2004.12.008.

Schumm, S.A., 1993, River response to base level Change : implications for sequence stratigraphy: The Journal of Geology, v. 101, p. 279–294.

Snyder, N.P., Whipple, K.X., Tucker, G.E., and Merritts, D.J., 2000, Landscape response to tectonic forcing: digital elevation model analysis of stream profiles in the Mendocino triple junction region, Northern California: Bulletin of the Geological Society of America, v. 112, p. 1250–1263, doi: 10.1130/0016-7606(2000)112<1250:LRTTFD>2.0.CO;2.

Swenson, J., and Muto, T., 2007, Response of coastal plain rivers to falling relative sea-level: Allogenic controls on the aggradational phase: Sedimentology, v. 54, p. 207–221, doi: 10.1111/j.1365-3091.2006.00830.x.

Tanaka, K., Hataya, R., Spooner, N., and Questiaux, D., 2001, Optical dating of river terrace sediments from Kanto plains, Japan: Quaternary Science Reviews, v. 20, p. 825–828, doi: 10.1016/S0277-3791(00)00016-0.

USFS and BLM, 1996, South Fork Eel River Watershed Analysis.

Wakabayashi, J., 2015, Anatomy of a subduction complex: architecture of the Franciscan Complex, California, at multiple length and time scales: International Geology Review, v. 6814, p. 37–41, doi: 10.1080/00206814.2014.998728.

Wakabayashi, J., 2011, Mélanges of the Franciscan Complex, California: Diverse structural settings, evidence for sedimentary mixing, and their connection to subduction processes: Geological Society of America Special Papers, v. 480, p. 117–141, doi: 10.1130/2011.2480(05).

Walker, M., 1986, Quaternary dating methods: West Sussex PO19 8SQ, England, John Wiley & Sons, Ltd, v. 58, 362 p., doi: 10.1016/0168-9622(86)90024-2.

Whipple, K.X., 2002, Implications of sediment-flux-dependent river incision models for landscape evolution: Journal of Geophysical Research, v. 107, p. 2039, doi: 10.1029/2000JB000044.

Whipple, K.X., and Tucker, G.E., 1999, Dynamics of the stream-power river incision model: Implications for height limits of mountain ranges, landscape response timescales, and

research needs: Journal of Geophysical Research: Solid Earth, v. 104, p. 17661–17674, doi: 10.1029/1999JB900120.

Yonkee, W.A., and Weil, A.B., 2015, Tectonic evolution of the Sevier and Laramide belts within the North American Cordillera orogenic system: Earth-Science Reviews, v. 150, p. 531–593, doi: 10.1016/j.earscirev.2015.08.001.

Chapter 2 : Timing and progression of river incision along the South Fork Eel River

Abstract

River networks can provide important clues for understanding how landscapes adjust to changes through time. Analysis of strath terrace placement and age progression, using bulk sampling Optically Stimulated Luminescence, within the South Fork Eel River (SFER) can provide insight into the initiation of mainstem incision, and how incision propagated through this system. Terraces within the SFER were divided into four terrace generations, Qt_o – the oldest terraces that are scattered far above (~80 to 180 m) the present day channel; Qt_1 – the extensive, longitudinally-discontinuous, alluvium-mantled strath terraces elevated around 60-80 meters above the present-day river; Qt_2 – intermediate terraces, with prominent slip off terrace sequences; and Qt_3 – are terraces located just above the present day channel. Several Qt_1 terraces were dated using feldspars, resulting in a central, basin-wide age of 134 ± 29 ka, which represents initiation of incision within the basin. This age indicates that incision for the SFER began during the transition period from a glacial to an interglacial. There are two main clustering's of terrace ages which indicate that incision was likely accomplished through multiple progressive knickpoint retreat events, as the terraces located further upstream are younger than those in the middle of the basin. The age progression and location of SFER terraces reveals that even though there is a significant knickzone located within the system, that the progression of incision is more complicated than the propagation of a singular knickpoint through the system. OSL results from the SFER also showcase that night-sampling of interstitial feldspar grains from between coarse alluvium can yield meaningful ages. This could have a large impact on the surrounding region, and studies across the world which may have been previously overlooked for burial dating.

2.1 Introduction

Transient landscapes are systems that are undergoing change, that are no longer at a dynamic equilibrium, where what is entering the system is balanced by what is leaving, at various spatial and temporal scales. Transient landscapes are constantly responding and adjusting to disturbances. For fluvial systems this means that the output of sediment must be balanced by the delivered sediments, from the removal of alluvial cover or erosion into the bed (Gilbert, 1877). This can be due to a shift in climate (cold/wet to warm/dry) changing the amount of water and sediment fluxing through a fluvial system. Changing climate can also affect global sea level, effectively lowering or raising the base level for streams. Tectonics drive rock uplift or faulting that can also impact the base level of a system, leading to river incision or aggradation within a watershed. Fluvial systems undergoing change can be identified by the presence of terraces, and that change can characterized based on terrace location and fill age (Merritts and Bull, 1989; Merritts et al., 1994; Fuller et al., 2009).

2.1.1 Strath Terrace Formation

Incising landscapes leave behind relict landforms which provide clues to how they have evolved through time. Fluvial terraces are one such landform type. These planar, low-relief surfaces elevated above and adjacent to channels are created by a river's lateral migration and thus can be used to reconstruct the past elevations and positions of the channel as well as the character of the materials in transport. The flat or gently sloping surface of a terrace is called a tread, which is commonly bounded by a steep ascending slope called a riser (Pazzaglia, 2013). Terraces can either be constructed from unconsolidated sediments (an alluvial terrace) or by thin mantles of alluvium overlying a beveled bedrock surface (a strath terrace). Terrace surfaces form when lateral river erosion outpaces vertical incision, creating an active flood plain, and are

preserved when vertical erosion cuts down quickly into the river bed, effectively abandoning the flood plain (Merritts et al., 1994; Finnegan and Dietrich, 2011). This transition from horizontal to vertical erosion can occur due to a number of internal or external controls.

Internal controls on terrace formation can be due to the change in ratio between water and sediment fluxes, which impact stream power and the tools available for erosion or armoring the bed (Bull, 1990b; Merritts et al., 1994; Maddy, 1997). Climate change can drive enhanced sediment production due to freeze-thaw cycles or increased runoff, leading to aggradation-incision cycles which affect channel slope (Merritts et al., 1994; Pazzaglia, 2013; Maddy, 1997). River migration also affects terrace formation within bedrock systems, as meanders grow and then cutoff sections of the channel. This drives internal fluctuations in the channel gradient, affecting the rate of vertical incision (Finnegan and Dietrich, 2011). The underlying lithology also has a strong impact on terrace formation and rates of incision. Weak rocks that undergo cyclic wetting and drying along channel walls will erode faster than the same material that is only being eroded by abrasion and plucking within the channel, leading to higher rates of lateral erosion on channel banks. This process leads to the formation of more extensive terrace treads within environments with weak lithologic materials (Montgomery, 2004; Stock et al., 2005). These internal controls tend to affect the watershed at the reach scale, leading to the formation of isolated terraces that are more difficult to preserve over long time scales (Maddy, 1997).

External controls include regional base level change as the result of either tectonic uplift or subsidence (Merritts et al., 1994; Reneau, 2000), eustatic rise or fall of sea level (Merritts et al., 1994), landslide damming (Ouimet et al., 2007), and climate change (Vandenberghe and Maddy, 2001; Hancock and Anderson, 2002). Low sea levels during cold stages or high rates of tectonic uplift result in downstream incision that may propagate upstream through knickpoint

propagation (Foster and Kelsey, 2012). Rates of uplift directly affect the ratio of lateral versus vertical incision rates within a river system (Finnegan and Dietrich, 2011).

By mapping the location and elevations of fluvial terraces, the paleochannel can be reconstructed for a river system. A timeline for river incision can also be constructed with the dating of the terrace fill or strath material in combination with terrace locations, along with incision rates between several terrace generations along the river (Meyer and Leidecker, 1999), and rates of tectonic deformation (Merritts and Bull, 1989). Marine terraces are extremely helpful in reconstructing sea level and determining rates of tectonic deformation (Merritts et al., 1994; Snyder et al., 2000; Lock et al., 2006; Hartshorn, 2017).

2.1.2 Terraces and Time –Dating Techniques for Terrace Sediments

Various methods can reveal the age of fluvial terraces and their deposits. To determine a minimum time range for terrace abandonment, terrace sediments or materials within these sediments are sampled, as these materials would be deposited while the river was still depositing material, before abandonment. Radiocarbon dating is a well-developed technique that compares the ratio of ^{12}C to ^{14}C within a material. Carbon-14 has a half-life of ~5700 years, meaning carbon-14 dating is reliable tool for dating materials as old as 50 thousand years (Walker, 1986). It can be used on a variety of biogenic materials that can be found within alluvium fill above strath terraces; wood, plant debris and litter, charcoal, and bone. Caution must be taken with ages derived from ^{14}C however, as the resulting ages may not represent time of terrace formation, as the dated material could be much older or younger than when the fluvial surface was abandoned. Plant litter and woody debris within terrace alluvium are ideal materials to date because this material was likely deposited around time of alluvium deposition (Walker, 1986; Wang et al., 1996; Pazzaglia, 2013).

Uranium-series radiometric dating is also a popular method, which is chiefly used for dating marine and terrestrial carbonates. In fluvial systems, these carbonates are found as lacustrine facies or as evaporative deposits within arid soils (Edwards et al., 2003). The U-series is based on the decay of ^{238}U to ^{206}Pb and ^{235}U to ^{207}Pb and is reliable for dating material up to 500 ky (Walker, 1986; Pazzaglia, 2013). These ages are younger than the age of terrace abandonment and provide a minimum age for the landform.

Tephrochronology is the study and age correlation of volcanic ash layers. Tephra is deposited as an air fall deposit on surfaces downwind of the volcanic source. These deposits are isochronous and are found in lake sediments, on peat surfaces, river terraces, and within glacial ice (Walker, 1986; Wulf, 2013). The tephra itself is sometimes dated using argon isotope or fission track dating, to determine the time of volcanic eruption. Once a tephra age is known, the tephra is identified with cheaper geochemical fingerprinting. Tephra is more readily preserved as rivers aggrade and bury the tephra layer. If the system is laterally active or incising, the tephra will likely become reworked within the system, and transported downstream (Walker, 1986; Pazzaglia, 2013). Once the terrace has been abandoned, tephra can accumulate and provide a minimum age for the landform.

Another technique that can be used to determine when terrace surface was abandoned is cosmogenic nuclides. High energy cosmic radiation is constantly entering the earths atmosphere. These high energy rays collide with atoms within the atmosphere and cause a chain of nuclear reactions, leading to the formation of unique meteroic cosmogenic nuclides (^{7}Be, ^{10}Be, ^{14}C, and ^{36}Cl) (Walker, 1986; Pazzaglia, 2013; Von-Blanckenburg and Willenbring, 2014). Some of these nuclides eventually reach Earth's surface, where they are able to pentrate a few meters of rock or sediment. Once there, these nuclides interact with minerals, producing in situ cosmogenic

nuclides. These nuclides remain within rocks and soils until the radioactive nuclides decay (Von-Blanckenburg and Willenbring, 2014). Age of surface exposure can be determined as nuclides accumulate over time, along with determining how long ancient sediments have been buried, by comparing the ratio of decay materials to their radioactive parent. In situ and meteoric nuclides can also be used to indirectly determine the rate at which soil is form or eroded in a landscape, (Walker, 1986; Von-Blanckenburg and Willenbring, 2014).

Optically Stimulated Luminescence dating (OSL) can also be used to establish when fine grained quartz or feldspars were last exposed to light (Rittenour, 2008). When grains are no longer exposed to sunlight they accumulate low levels of natural radiation from surrounding radiogenic elements such as uranium, potassium, thorium, and rubidium, in the form of electrons, within defects in their crystal lattice (Aitken, 1998).The rate of energy accumulation is assumed to be constant, allowing for an estimated time since burial based on the amount of energy released in a laboratory (Aitken, 1998). This technique is useful for dating river terraces as the age of burial for grains should be similar to time of terrace formation (Murray and Olley, 2002), and OSL is reliable between several hundred years to hundreds of thousands of years (Kenworthy et al., 2014).

2.1.3 Study Overview and Rationale

The purpose of this study is to address how base level fall is communicated upstream within a fluvial network and whether it occurs progressively or uniformly through time across the basin. Terrace placement, distance above channel and location along channel length, can be used to determine how a river has responded to change, as terraces represent past channel locations. They can tell us a lot about the history of fluvial systems and how they have evolved through time.

The South Fork Eel River presents an ideal location to answer how rivers may respond to base level fall, as it contains a significant knickzone and numerous strath terraces along its length. It is hypothesized that incision within the SFER was likely accomplished either through uniform lowering (Figure 2.1) or through knickpoint retreat (Figure 2.2). To test this hypothesis terrace placement must be mapped and ages collected for terrace fill. It is assumed that the fill above the beveled strath surfaces would continue to be reworked until they were abandoned by the river. Thus, the age of fill would give us a minimum time of terrace abandonment, and provide additional information into when incision initiated, along with insight into how base level changed over time and how base level fall was accomplished within the system itself. Therefore, if uniform lowering occurred within the lower basin of the SFER, the ages for the uppermost continuous terrace flight would be similar, as these terrace surfaces would be abandoned at a similar time (Figure 2.1). If knickpoint retreat occurred within the basin, incision would be accomplished through the stepping back of a knickpoint, effectively abandoning the terrace surfaces downstream first and systematically stepping back through the basin. The ages of terraces would decrease in age with distance upstream, as these surfaces were abandoned at later times than those downstream (Figure 2.2).

2.2 Study Area and Focus

The focus of this study is the South Fork Eel River (SFER) in northern California. The SFER is a dominantly bedrock river, which flows south to north, and is ~170 kilometers long. It contains one prominent knickzone located ~135 kilometers upstream from its confluence with the main stem of the Eel River. The knickzone, is ~8 kilometers in length, drops the river from 400 to 250 meters above mean sea level, and is located between the tributary junctions of Tenmile and Rattlesnake Creeks (Fuller et al., 2009) (Figure 2.3). There are hundreds of fluvial

terraces along the entire length of the SFER, varying in size and elevation though they have only been discussed at local sites (Bickner, 1993; Fuller et al., 2009; Foster and Kelsey, 2012) and not studied along the entire main stem. Climate for the region is warm-summer Mediterranean, with wet cool winters and dry warm summers. Average annual temperatures for the region are ~13˚C, with an average precipitation of ~200 cm, as calculated over the last 30 years (National Center for Atmospheric Research, 2017). The dominant vegetative cover for the watershed consists of montane hardwood, conifer, Douglas-fir, redwood, montane hardwood, along with scattered grasslands and oak woodlands (USFS and BLM, 1996).

2.2.1 Regional and Terrace lithology

The terraces within the SFER basin are predominately strath terraces, with horizontal strath surfaces capped with 1-5 meters of alluvial fill. The bedrock strath is comprised of central and coastal belt Franciscan accreted terrains (Robert J McLaughlin, 2000).The coastal belt Franciscan consists primarily of sheared sandstone, mudstone, and conglomerates. The central belt Franciscan terrain is a mélange of material that consists primarily of greywackes, shales, conglomerates, sedimentary breccia, with greenstone, chert, and rare limestones (Blake Jr et al., 1981; Wakabayashi, 2015). The alluvium fill is dominantly a gravel to cobble alluvial deposit with intermittent sand lenses, with varying degrees of imbrication. These clasts are composed of the surrounding bedrock, Franciscan greywacke, chert, and mudstone (Figure 2.4). The Franciscan Central Franciscan Belt comprises the eastern half of the watershed, and the Coastal Franciscan Belt comprises the western half.

2.2.2 Paleoclimate

Through analysis of pollen within a lacustrine core from Clear Lake, California a continuous climatic record for California’s northern coast range for the last 130,000 years can be

analyzed (Adam et al., 1981; Adam and West, 1983). The reconstructed temperature and precipitation data indicate a decrease in temperature by ~8°C with an increase of precipitation of about 200 cm, from present, during the last glacial cycles (13,000 – 30,000; 64,000 – 80,000; 128,000 – 130,000 years ago). During the last interglacial period between ~100,000 - 128,000 years B.P, the climate was warmer by ~1.5°C and precipitation decreased by approximately 50 cm (Adam and West, 1983). This suggests that overall, within the last 130,000 years, the climate was colder and much wetter than present. With this changing temperature and precipitation, vegetation cover within the region also changed. The same lake core shows that ~40,000-100,000 years ago coniferous trees dominated as the primary pollen producer within the region, then at ~20,000-40,000 years coniferous pine trees slowly became more of an even producer with the other coniferous species. However, at ~20,000 years ago, during the last glacial maximum, oak pollen became dominant (Adam et al., 1981; Adam and West, 1983). Sea level is also believed to have been changing at this time for the Pacific Ocean (Muhs et al., 2003, 2012), as well as for southern California (Waelbroeck et al., 2002). Between ~120,000 to 20,000 years ago, sea level was progressively lowering from a level close to present to a low of -140 m (Figure 2.5). It then began to rapidly increase for 10,000 years to current day levels, both along the southern coast of California and globally (Waelbroeck et al., 2002; Muhs et al., 2012). These eustatic sea level changes may have affected the base level of the SFER, leading to knickpoint development within the system.

2.2.3 Tectonic Setting

The SFER is located south-east of the Mendocino Triple Junction (MTJ), which lies at the junction between the North American, Pacific, and Juan de Fuca plates. The MTJ is moving northwest at a rate of ~5 cm/year (Sella et al., 2002). This migration of the MTJ leads to

thickening of the crust beneath the Coast Ranges of California, which results in uplift within the North American Plate, as modelled by the Mendocino crustal conveyor (MCC) (Furlong and Govers, 1999; Lock et al., 2006). Uplift resulting from this northwestern migration occurs in a "double-humped" pattern (Lock et al., 2006), which likely began impacting the SFER headwaters approximately 6 million years ago (Figure 2.6). By studying marine terraces along the western coast, which formed in response to tectonic and eustatic processes (Merritts et al., 1994; Snyder et al., 2000; Lock et al., 2006; Crawford, 2015; Hartshorn, 2017), uplift rates can be estimated and correlated with the predicted uplift from the MCC model. Uplift rates are highest closest near the MTJ, with rates ranging from 2.7-4 mm/year south of Cape Mendocino area to the south of the King Range (Figure 2.7) (Bickner, 1993; Merritts et al., 1994; Snyder et al., 2000; Crawford, 2015; Hartshorn, 2017). Uplift rates then decrease slightly north of the MTJ for Cape Mendocino, with rates of ~2.8 mm/year (Merritts et al., 1994). Just south of the King Range, uplift rates fall significantly to 1 mm/year directly west of Garberville (Snyder et al., 2000), and continue to drop to 0.1 mm/year south of Fort Brag (Lock et al., 2006). Uplift rates of 1 mm/year for the middle of Eel River have been modelled using these marine terrace uplift rates (Lock et al., 2006; Roering et al., 2015). A long term estimated uplift rate of 1.3 mm/yr was inferred from the elevations and weathering rind ages of a suite of terraces just south of Garberville, CA within the SFER (Bickner, 1993).

2.3 Methods and Results

2.3.1 Valley Profile and Terrace Digitization

To establish the longitudinal locations of terraces along the SFER, a smoothed valley center line was drawn along the main stem. This line simplified the overall sinuosity of the channel and runs parallel to the present-day valley. Cumulative upstream distances from the

outlet were generated along the line every 30 meters, for interpolation and plotting terrace positions. To provide elevations along the valley center line, we used present day of main stem elevations where the two cross. Between these points, we used a linear interpolation to provide approximate elevations.

Terraces within the SFER were recognized and mapped using a 1m LiDAR slope map collected by NCALM (Power, 2004; Perkins, 2009; Dietrich, 2014). Terraces were recognized as flat or gently sloping surfaces, which form the terrace tread. These treads were then bounded by steeper slopes, called "risers" within the LiDAR (Figure 2.3B insets). Once terrace treads were digitized, two to four points were placed along the length of each terrace tread, placed roughly parallel to the valley profile line to extract elevation values and distance upstream.

The valley profile and terrace elevation points were plotted to create a longitudinal profile (Figure 2.8). Using this profile, longitudinal continuity between terrace treads at similar elevations and size of terraces were used to distinguish between predicted terrace generations (Figure 2.9). One possible correlation, yielded four terrace generations were inferred along the longitudinal profile (Figure 2.10). These generations were distinguished by their height above river, as it is assumed that terraces at similar heights would have formed at similar times. Qt_o, which represents the oldest fluvial terraces that are located far above (80 to 180 m in the lower basin, 40 to 50 m in the upper basin) the current river channel. These terraces are most commonly found below the knickzone and within the upper section of the knickzone itself. Qt_1, are the terraces that comprise the uppermost, extensive, longitudinally-discontinuous surface within the basin, elevated ~60-80m above the present-day channel within the lower basin, and ~15-20 m in the upper basin. Within the upper basin and throughout the upper section of the knickzone, the Qt_1 terraces progressively increase in elevation and become more spread out

horizontally within the lower basin with decreasing elevation towards the mouth of the SFER. It is from this Qt_1 generation of terraces that ages were collected. The next generation of terraces is Qt_2, which represents the intermediate terraces directly below the Qt_1 flight. These intermediate terraces are scattered throughout the lower basin and are not found within the upper basin of the SFER (~ 25-50 m). Slip off terraces are prominent within this section, with no clear continuous surface outside of the knickzone. The last terrace generation is Qt_3, which are located just above the present-day flood plain (~10-25 m). These terraces are clear and continuous near the mouth of the river and become more scattered with distance upstream. Qt_3 terraces are absent within the knickzone and upper basin.

2.3.2 OSL Sampling and Processing

The ages of the terraces were calculated using optically stimulated luminescence (OSL), which establishes when buried grains were last exposed to light. Samples were collected from the uppermost longitudinally extensive and continuous terrace surface, Qt_1, from terraces with >2 meters of river sediment fill. This was done to determine whether this generation of terraces are all the same age or progressively young with distance upstream, allowing us to infer how incision was accomplished for the SFER. The SFER watershed is a highly vegetated area, leading to a high degree of bioturbation (roots, moss, ferns, tree roots, etc.), throughout the terrace surfaces, with small roots growing throughout the alluvial fill, to depths of 4-5 meters. We sampled naturally exposed cut faces or outcrops, at a depth of ≥1.5 meters to minimize the impacts of bioturbation, and zones with a larger amounts of roots were avoided.

Sand sized grains within Qt_1 terraces were collected at 7 locations, along the 140-kilometer river length, from the outlet to just above the knickzone. Fine grained sand lenses (often interbedded between large cobbles and gravel) were sampled as close to the underlying

strath as possible, to collect material that was most likely deposited at time of terrace formation. The reworking of alluvial fill is possible with extended lateral erosion, where younger alluvium replaces previous deposits, so recorded ages area assumed to represent a minimum age for the terrace surface.

Traditional OSL sampling procedure involves collecting sand sized grains by driving metal tubes into well-sorted deposits, then capping the tubes then processing the light safe material from the center of the tube. The alluvium mantling the strath terraces within the SFER however is coarse grained (large number of gravel/boulders/cobbles) with interbedded sand lenses and a fine grained matrix, making this classic OSL sampling technique difficult for this area. A bulk sampling approach was needed to collect samples for processing, the procedure used was based on the processes discussed in Kenworthy et al., 2014, where sampling must be done at night by sampling directly from the deposit and separating the sand from the larger grains, to avoid light contamination for the target sample to be processed. This "ninja" bulk sampling technique (detailed in Appendix 2.1) must be used as samples are light sensitive, so if the sample gets exposed to any sunlight, its age will be "reset" and will not give us an accurate age of how long the grains have been buried.

Collection for samples was typically done in two steps; a day time preparation and a nighttime collection. Once a viable sampling site was located, the outcrop face was cleared during the day. ~40-65 cm of sediment from the face was removed as well as digging down ~40-100 cm toward the strath/alluvium interface. This was to further minimize the impact of any bioturbation, and remove any material that may have experienced creep and mixing of grains. Focusing on the sand-rich portions of the deposit, a radius of ~30 cm was then cleared for where the sample was to be collected. During the night of collection, a tarp was set over the collection

site and tied down to avoid any moonlight, starlight, or other human illumination from reaching the sample. A red headlamp was used under the tarp, as red light is less lightly to reset the grains, however it was worn backwards and never pointed directly on the sample area. Once the tarp was secured, another ~5-10cm was cleared from the sampled surface and surrounding area, to removing material exposed to light earlier in the day. The light sensitive bulk sample was then collected, focusing on the fine sand-rich portions of the deposit (further detailed in Appendix 2.1). After collection, the light sensitive material was stored in a light proof container until processing. A dose rate bulk sample was then collected within 30 cm of the sample site, for determining the local radiation. A film canister of sediment was also collected for water content analysis. Finally, depth to sample, elevation, and latitude/longitudinal measurements were recorded.

Samples were processed at Utah State University Luminescence Laboratory, using standard sample preparation procedures for feldspar and quartz grains. Samples were prepared following the methods of Wintle, (1997). They were wet sieved to a target size range between 75 and 250 μm, with the target fractions treated with 10% hydrochloric acid to dissolve carbonates. They were then treated with hydrogen peroxide to remove organic materials. Quartz and feldspar grains were separated from heavy minerals using sodium polytungstate, at 2.7 g/cm^3 and 2.58 g/cm^3, respectively. Feldspar grains were twice separated, then dried at room temperature (Wintle, 1997). Luminescence measurements were made following Single-Aliquot Regenerative (SAR) protocol (Murray and Wintle, 2000), with heating conditions constant at 250˚C and held for 60 seconds. Infrared measurements were performed on Risø TL/OSL Model DA-20 readers with infrared light-emitting diodes (LEDs) (870±40 nm) and reader dose rates of 0.10-0.11 Gy/sec from a decaying 90 Sr beta source. Dose rates were also taken to calculate their

concentrations of K, Rb, Th, and U, which were determined using ICP-MS and ICP-AES analyses (Aitken, 1998; Guérin et al., 2011). Water content samples were used to determine the influence of water attenuation, Cosmogenic influence was determined using sample depth, elevation, and latitude/longitude position (Prescott and Hutton, 1994).

Preliminary tests using quartz grains yielded weak luminescence signals, therefore pIR-IRSL measurements were made using feldspars, which yielded strong luminescence signals. Quartz derived from metamorphosed materials, like greywackes, have poor crystal lattice structures and therefore do not hold charges as efficiently as un-metamorphosed quartz grains.

The preliminary results (table 2.1, Figure 2.11) show a range of terrace ages, 29.3 ± 7.7 to 166.8 ± 42.2 ka, within the lower basin of the SFER, and up through the knickzone (Figure 2.12). These ages yield a basin wide average age of 139.74 ± 37.08 ka, when excluding anomalously young dates from the two most downstream terraces: Weott and Miranda. These terrace ages were excluded from basin wide average due to their anomalously young ages and a lack of confidence in their collection locations. These samples were collected from poorly defined surfaces, with rounded creep-affected terrace edges, and limited alluvial fill exposed.

The subsequent two terraces, located within the middle of the lower basin, contain the largest error: Leggett Creek Camp road cut terrace with an age of 166.8 ± 42.2 ka and the Garberville – Crazy Horse Ranch terrace with an age of 153.7 ± 50.4 ka. The ~20% uncertainty is also likely due to the limited number of aliquots that have been run (~14 accepted aliquots each). The three uppermost terraces from this study are similar to one another with an average age of 117 ± 23.5 ka, and when compared to the terraces midway up the drainage with an average age of 159.1 ± 23.4, show a decrease in age with distance upstream. The Fuller et al.,

(2009) terraces located directly above the knickzone yield much younger ages of 33.3 ± 4.1 ka and 20.5 ± 3.3 ka.

2.4 Discussion

2.4.1 Longitudinal and Vertical Variation in Terrace Form and Extent

Four terrace tread generations were identified within the SFER; a tread generation as used here represents a grouping of terrace treads that are similar in height above the channel or size (Figure 2.10). Qt_o represent the oldest terraces that are located far above the current river channel. These terraces are smaller in size and are fairly scattered with no clear continuous elevation throughout the basin. Below Qt_o, is Qt_1, which comprises the most extensive and continuous terrace surface throughout the SFER. This generation of terraces represents a clear paleochannel location of the SFER that persisted before significant river incision began. Qt_1 terraces formed when lateral erosion and migration of the channel was dominant, allowing for a broad flood plain to develop. It is assumed that base level then dropped at the mouth of the SFER, due to a change in climate or uplift, causing vertical incision to become the dominant means of erosion. Intermediate terraces, Qt_2, are scattered throughout the lower basin and up through the knickzone. They are not found within the upper basin, which is likely due to the small amount of incision (~15 meters). Qt_2 terraces can be characterized as predominantly slip-off terrace surfaces with similar elevation positions within the lower basin. The final generation of terraces, Qt_3, becomes more scattered in elevation with distance upstream, and does not occur within the knickzone nor in the upper basin. The terrace treads closest to the mouth are the closest in elevation to one another.

The minor amounts of variation in height above the channel within terrace generations are probably due to variations in fill thickness. Some terraces have little to no fill present, where

other terraces have 5+ meters of fill. The larger amounts of variation seen in terrace elevation is likely due to non-uniform base level fall through the basin, along with location of tributaries and meander bends, as these influence where terraces are preserved. A majority of tributary junctions have terraces that likely received sediment from both the tributary and the main stem channel.

2.4.2 Interpretation of Terrace Ages

The overall Qt_1 terrace ages decrease with distance upstream, with the two terraces in the middle of the basin being significantly older than the uppermost three locations, suggesting that incision was progressive and occurred through knickpoint retreat and did not occur uniformly (Figure 2.13). Due to the placement of Qt_2 and Qt_3 terraces and the clustering of ages for Qt_1, singular knickpoint retreat is unlikely, and incision was most likely accomplished through multiple progressive propagating knickpoint retreat events (Figure 2.14). This progressive knickpoint retreat would account for the different terrace generations (Qt_1, Qt_2, and Qt_3), as singular knickpoint retreat is unfavorable for the formation and preservation of intermediate terraces. Progressive knickpoint retreat would also be supported by a decrease in Qt_1 terrace ages with distance upstream (Figure 2.15).

With an overall average age of 134 ± 29 ka, it shows that the Qt_1 terraces are similar in age they are not that statistically different from one another. This therefore makes the central basin wide average Qt_1 terrace age of 134 ± 29 ka important for determining possible disturbances could have led to this incision to occur. The central basin wide age of 134 ± 29 ka correlates with the end of the Penultimate Glaciation (~200-130 ka, PG), which was a time of extreme sea level low (~120 m below present, Figure 2.5). The climate was also expected to become cooler and wetter during glacial periods (Goni et al., 2000; Porter, 2001). These conditions are favorable for sediment aggradation within fluvial systems (Penck and Brückner,

1909), since sediments were collected just above the terrace strath, this suggests that these materials were deposited during the PG while the system was aggrading.

Following the PG, at ~130 ka, there was a rapid rise in sea level for the Pacific Ocean, which rose by ~100 meters over the span of 10,000 years (135,000 – 125,000 years ago; Waelbroeck et al., 2002; Figure 2.5). During this time the local temperatures also increased by ~10˚C (5˚C to +15˚C – compared to present-day conditions with an average temperature of 13˚C) and precipitation decreased by 270 cm (250 cm to -50 cm - compared to present-day conditions of 200 cm/year; Figure 2.16) (Adam and West, 1983). This change in climate, along with continued tectonic uplift for the region, likely lead to a shift from aggradation to incision within the SFER, leading to the abandonment of terrace treads. Whether a river is incising or aggrading can be influenced by a changing climate as it impacts discharge, sediment supply, and sediment storage (Blum and Törnqvist, 2000). Higher amounts of precipitation increase sediment being delivered to a channel, leading to aggradation within a system (Fuller et al., 2009), whereas in dryer, warmer climates, it would be assumed that less sediment is being delivered to the channel. This starves the fluvial system of sediment, where the material armoring the bed is being removed, and the river begins to incise.

At ~125 ka, relative sea level then began to fall ~100 meters over the next 100 ka (125,000 – 30,000 years ago) in a oscillating ‘yo-yo’ pattern, into the Last Glacial Maximum (LGM). This steady lowering in sea level, was aligned with an oscillation of temperature and precipitation back to the conditions observed ~130 kya (5˚C, 310 cm). Coming out of the LGM, ~20 ka, sea level began to rise again at a rate of ~ 0.625 cm/year to present-day levels (Waelbroeck et al., 2002; Muhs et al., 2012).

In river systems, incision is presumed to be controlled by eustatic base level fluctuations, for systems located along an oceanic shoreline, as sea level changes can be large (Merritts et al., 1994; Muhs et al., 2003, 2012; Blum and Törnqvist, 2000). The incision within the SFER, is likely decoupled from this observed eustatic base level change, as the offshore sediments of the Eel River Basin, deposited ~ 140 ky, slope gently towards the shoreline and the canyons which cut through these shelf deposits do not propagate inland but also decrease in relief with distance towards the shoreline (Burger et al., 2002). This suggests, that when sea level was at its lowest, the gradient of the Eel river was not much different than today, at a high stand of 140 meters. As sea level rose and fell, as detailed above, the shoreline moved in and out without changing the gradient of the Eel River and thus never triggered a base level fall incision event to propagate up into the SFER.

Instead it is more likely that the landscape which is comprised of easily erodible mélange, the cycles of aggradation and incision (which created and preserved our terraces), were driven by fluctuations in the terrestrial climate. The large observed changes in precipitation and temperature for the region, would directly impact the production (hillslope erodibility) and transport capacity of sediment. In the SFER, the colder, wetter glacial periods would enhance sediment production (consistent with observations from Bennett et al., (2016) that earthflows slow during periods of drought), overwhelming and armoring the channel, leading to the domination of lateral incision (Figure 2.16). As the climate begins to warm and dry, sediment production drops, stopping the replenishment of sediment to armor the bed, enabling incision to occur.

The terraces located within the upper basin have been labeled at Qt_1, as they are appear to be a continuation of the extensive Qt_1 terraces found within the lower basin. Incision for the upper basin is less well known, and the terraces in the upper basin could potentially be much younger than the terraces within the lower basin, as suggested by the Fuller et al. (2009) ages. Their Elder Creek tributary terrace sample yields and age of 33.3 ± 4.1 ka. Their SFER terrace sample yields an age of 20.5 ± 3.3 ka. These are ~100 ka younger than the terraces we sampled just downstream (Figure 2.12). This suggests an interpretation that these upper basin terraces could actually be Qt_2 intermediate terraces, and not a continuation of the Qt_1 terraces.

More samples would need to be collected throughout the upper basin to determine the age progression of these upper basin terraces to determine how they relate to those found within the lower basin. The terrace ages collected by Fuller et al., (2009) do suggest that those sampled sediments were buried during the Last Glacial Maximum (LGM). Based on their sampling locations however, it is possible that these sediments may not be representative of timing of terrace abandonment. The Elder Creek terrace sample was collected within Elder Creek, upstream from the tributary junction, so these younger sediments could be tributary fan deposits that were deposited during the LGM. The other sample location along the SFER, is located on the outside edge of a meander bend. This is where erosion is localized and if flooding was to occur along this bend, sediment would likely be removed and replaced by younger material. As stated previously, it is more likely that these terrace surfaces were not abandoned until the LGM, ~20 ka.

Future sampling on the Weott and Miranda terraces by trenching would allow for better constraints on lower-basin ages, by minimizing the amount of creep and mixing of grains at terrace edges. By sampling other terraces within the upper basin, we would be able to get a

clearer idea of whether there is truly a large decrease in terrace ages in the upper basin. If intermediate terraces were sampled in the future, then the rate of incision between terrace generations could also be calculated, instead of assuming a lower basin incision rate of 0.57 m/ky.

Terraces showcase a complicated history of how rivers respond to changes through time. These results suggest that by identifying terraces along a similar generation, timing of incision can be determined for that generation, even when sampling conditions are less than ideal. The SFER is heavily vegetated region, meaning that bioturbation rates are high. This implies that mixing of younger grains with older grains is high in areas with roots moving through the alluvium deposits. Mixing of grains can lead to scattering of results within samples (Bateman et al., 2007; Rittenour, 2008; Nelson et al., 2015). In addition to high bioturbation, the alluvium within the SFER is coarse-grained, so conventional OSL techniques are not ideal, when a pipe is hammered into a thick sand or finer grained deposits. As a result, fine grained material must be collected in bulk from either intermittent sand lenses or from within the fine grained matrix surrounding the coarse materials (Kenworthy et al., 2014). Lastly, the quartz grains within the deposits yielded weak luminescence signals, so feldspars were used. These feldspar grains yielded strong luminescence signals with relatively low amounts of scattering.

This study shows that even in less than ideal field settings, like the SFER with high amounts of bioturbation and poor lithology, OSL is still a viable technique for dating alluvium within terrace deposits, when special care is taken when samples are collected. It is then possible to pair with terrace locations to determine when the paleochannel once resided and reconstruct the timing of incision and determine how incision was accomplished. This could have a large impact on the surrounding region, specifically within the Franciscan complex or other accreted

terrains, that while the quartz as derived from the surrounding greywackes has poor luminescence, feldspar grains are a viable option. Furthermore, for areas across the globe that are highly vegetated, resulting in high rates of bioturbation, if samples are collected at deeper depths and avoiding large roots, the amount of mixing can be reduced. With the advancement in OSL processing and sampling techniques, study sites that may have been overlooked for dating in the past could be revisited using bulk OSL sampling techniques and process using feldspars instead of quartz.

2.4.3 River Response to Base Level Fall

Terrace age progression for Qt_1 and placement of intermediate terraces (Qt_2) suggests that the SFER responded to base level fall through progressive knickpoint retreat. This knickpoint propagation would have occurred as a series of knickpoint retreat events (Figure 2.14), with multiple incision steps that then propagated upstream to the current knickzone position, leaving behind a few terrace generations. This data for the SFER suggests that in systems with a large amount of incision, it is likely accomplished in steps instead of all at once (Figure 2.15).

For progressive knickpoint retreat to be accomplished, the present day knickzone is likely 'stuck' at its current location, due to a change to a more resistant lithology, fault activity, or reduction in stream power. There is a significant decrease in total drainage area above the knickzone, as one of the largest tributaries, Tenmile Creek, joins the SFER at this location. The total drainage area above the knickzone comprises ~323 km^2, with Tenmile Creek draining ~52.5% (169.33 km^2) and the SFER draining the remaining 47.6% (153.78 km^2). This is a significant change in available stream power for the system, as the drainage area for the upper basin SFER suddenly drops by over half above its confluence with Tenmile Creek. This reduction in stream power is likely preventing the large amount incision to continue its

propagation up through the upper basin of the SFER. The SFER has experienced ~60-80m of incision, from Qt_1, throughout a majority of the lower basin. The upper basin has only experienced ~15m of incision. This indicates that there is some "spill-over" of the incision wave into the upper basin (Berlin and Anderson, 2009), however due to lack of stream power or a change to a more resistant region of lithology less incision has been accomplished over time. This "spill-over" likely occurred during the LGM, as suggested by the Fuller et al., (2009) terraces, or that the incision within the upper basin only began during the LGM. Once again, to determine the correlation of terraces and timing of incision for the upper basin, more above-knickpoint terrace ages must be determined.

2.5 Conclusions

The SFER hosts extensive, longitudinally-discontinuous, alluvium-mantled strath terraces (Qt_1) elevated around 60-80 meters above the present-day river, along its entire length. There is a prominent low generation of terraces throughout the basin (Qt_3), along with intermediate terraces (Qt_2) and sporadic upper terraces (Qt_o) scattered throughout. These terraces encompass four terrace generations, and the age progression of the uppermost continuous surface of terraces yields an average age of ~130 ka, with two clusters of terrace ages suggesting an overall decrease in terrace age with distance upstream. This age progression, in combination with the elevation of intermediate terraces suggests that progressive knickpoint retreat occurred within the basin, with the knickzone becoming hung up at its current location. With a better constraint on terrace ages, we will get an even better understanding on the pattern of incision through the basin. This research suggests that in systems that experience significant base level fall and subsequent river incision, it is accomplished through stages of knickpoint retreat and not all at once. Results of this study also shows that while the SFER is less than ideal for conventional OSL techniques,

bulk sampling techniques at greater depths, and using feldspar grains instead of quartz yields accurate results. That these alternate methods should not be overlooked in future studies.

Chapter 2 Tables

Table 2.1: Optically Stimulated Luminesce ages for the South Fork Eel River.

Sample ID	Sample elevation	Dist upstream (km)	depth (m)	# disks	IRSL age (ka)	2 SE
Weott	69.27	5.07	2.6	12(14)	70.90	21.20
Miranda	97.31	22.89	1.5	11 (14)	29.30	7.70
Leggett Creek Camp roadcut	142.13	39.96	3.0	15(15)	166.80	42.20
Garberville - Crazy Horse Ranch	159.98	48.93	1.5	13(14)	151.40	32.60
Standish Hickey SP	268.03	84.27	2.8	13(14)	98.50	21.90
So. Leggett - Big Bend roadcut	314.36	93.90	2.2	17(20)	128.90	26.20
Tenmile	394.54	106.92	1.2	17(22)	124.70	22.30
Elder Terrace (Fuller)	405.09	117.93	3.0		33.30	4.10
SFER terrace (Fuller)	394.03	117.39	6.4		20.50	3.30

Chapter 2 Figures

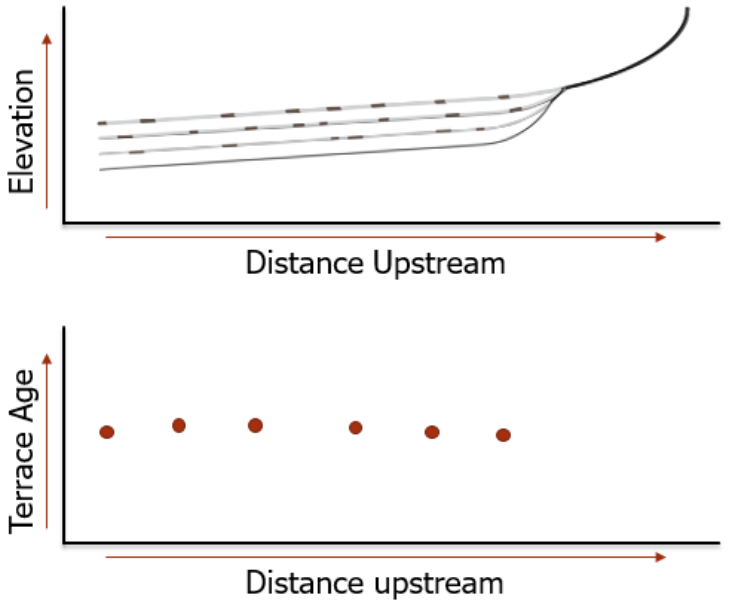

Figure 2.1: Model showing terrace ages for uniform lowering within the lower basin, with several terrace generations. The uppermost terrace generation would yield similar terrace ages with distance upstream.

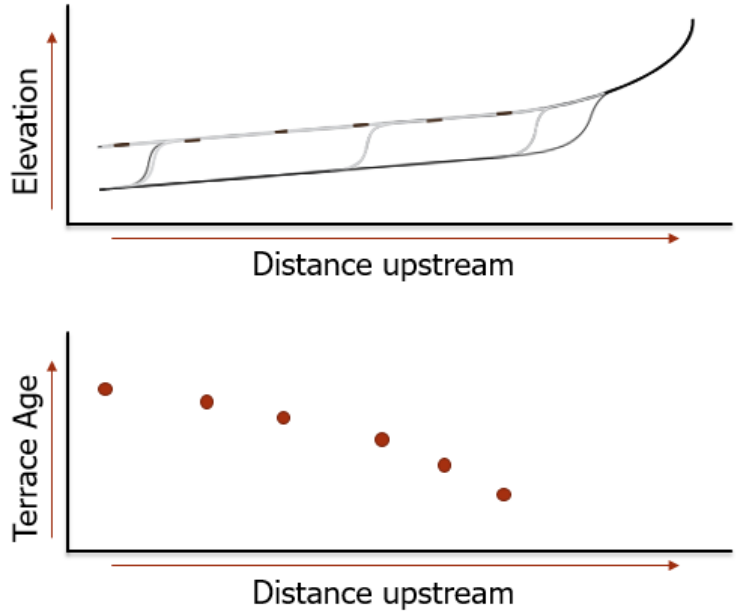

Figure 2.2: Model showing terrace ages for knickpoint retreat within the lower basin, with a singular terrace generation. The uppermost terrace generation for knickpoint retreat in scenario results in terrace ages that progressively young in the upstream direction.

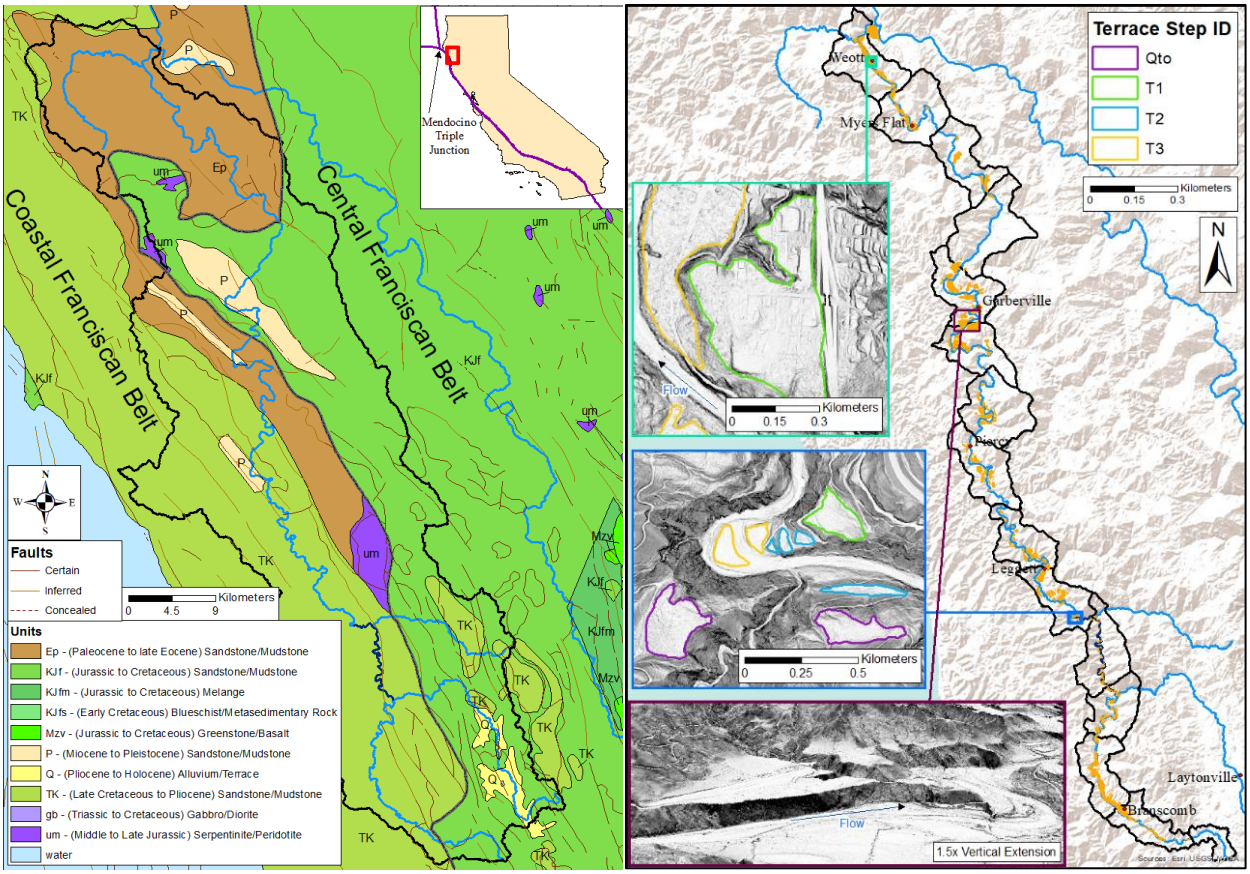

Figure 2.3: A) Geologic map of the SFER watershed and surrounding areas. Main units of the Franciscan Central and Coastal belts are shown and labeled with primary lithologic type. The Franciscan Central Franciscan Belt comprises the eastern half of the watershed, and the Coastal Franciscan Belt comprises the western half. Faults are shown in brown B.) Map of terrace locations along the SFER, with the ridgeline sections outlined in black. Insets are examples of terraces found within the SFER.

Figure 2.4: Digitized image of a terrace outcrop (South Leggett, Big Bend location) showing the variation of clast size within the alluvium fill. Grey represents cobble sized materials and large gravel clasts, brown represents areas dominated by gravel sized clasts, and yellow represents areas dominated by sand sized clasts. Green is vegetation.

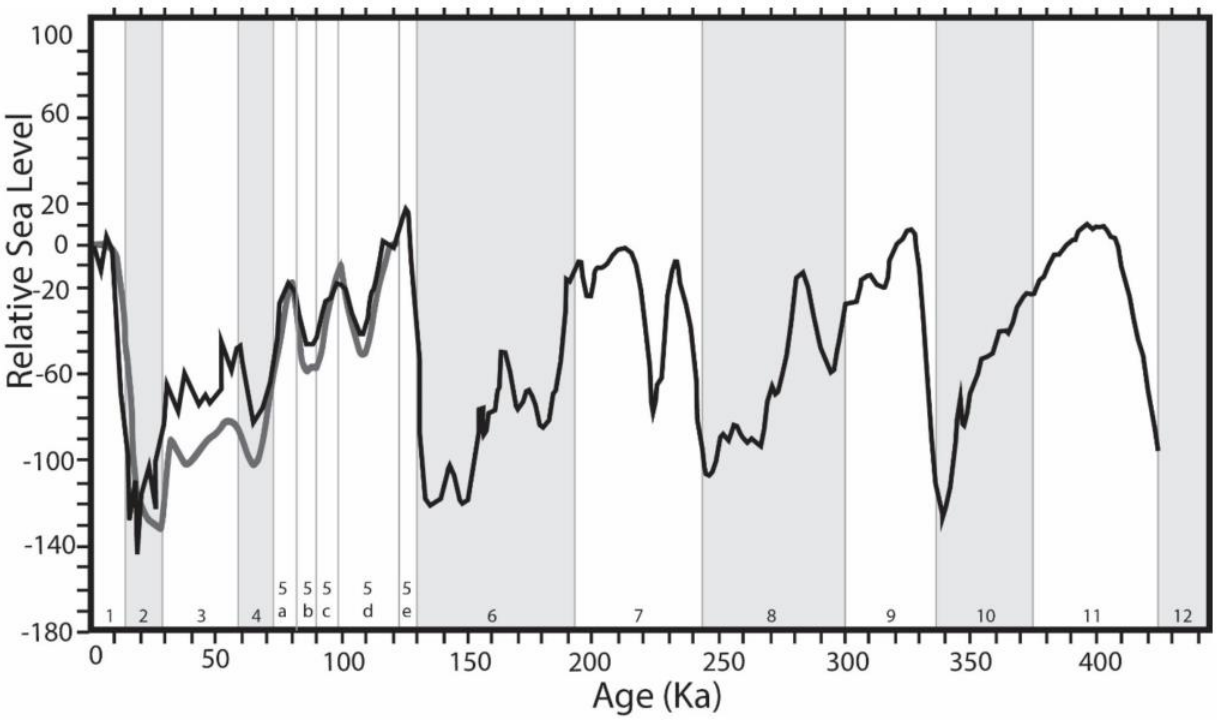

Figure 2.5: Sea Level Curve for Pacific Coast. Figure from Hartshorn, 2017. Showing the relative sea-level change (grey) for San Nicholas Island, CA (Muhs et al., 2012) and eustatic sea level curve from New Zealand (Black) (Waelbroeck et al., 2002). Light grey shading represents glacial periods, and white represents interglacial.

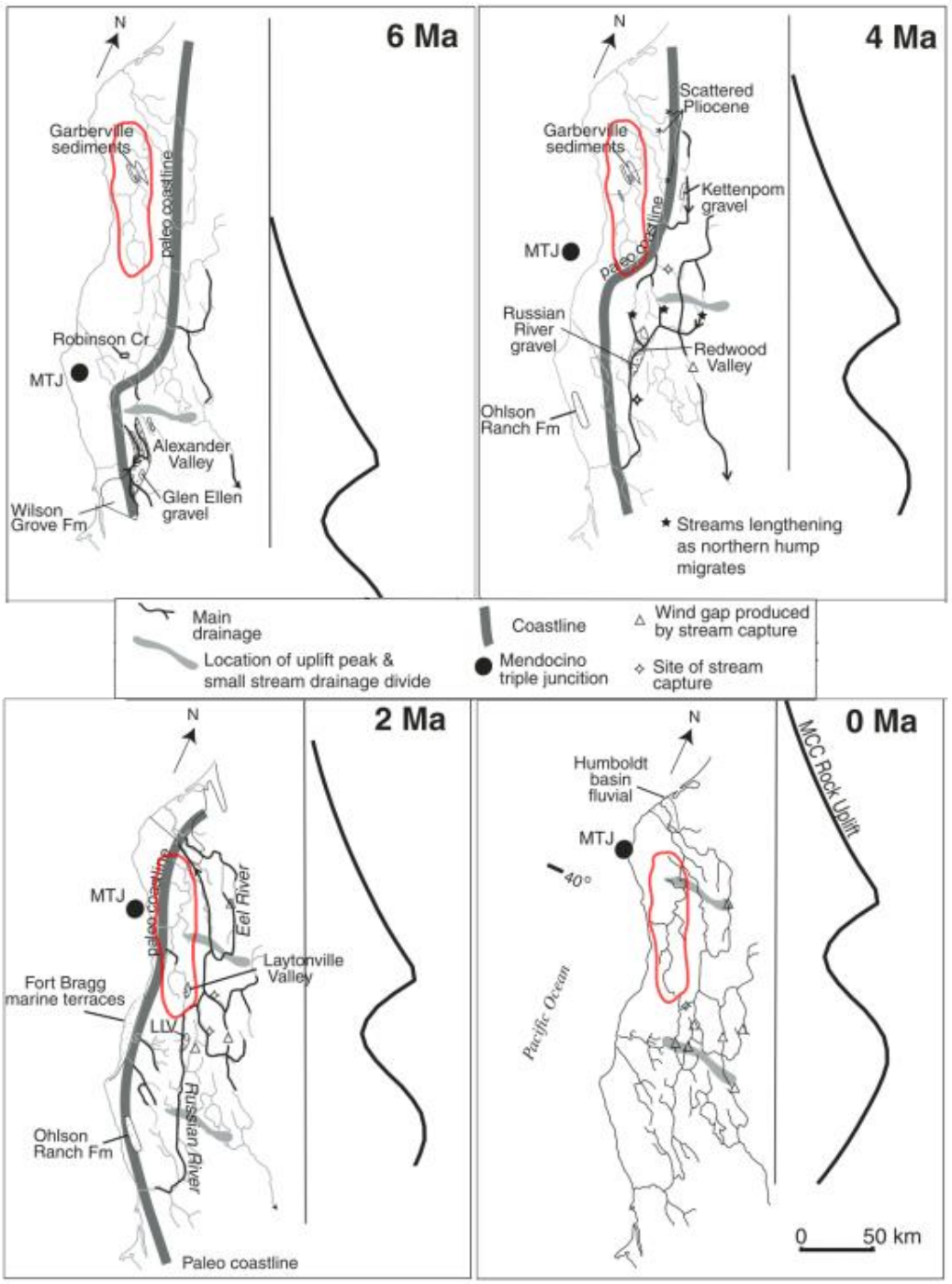

Figure 2.6: "Double-Humped" uplift and migration of the Mendocino Triple Junction (MTJ), modified from Lock et al., (2006).Thick black line on the right of each time step represents the location “double-humped” uplift wave that migrates northwest at a rate of 40-50 mm/yr, which drives averaged uplift rates up to 4 mm/yr. Red outline represents the location of the SFER basin. The relatively consistent northward migration of the MTJ and the location of the SFER shows that uplift within the basin has been relatively consistent over the last 2 million years, and it is unlikely that the migration of the MTJ lead to terrace formation within the SFER.

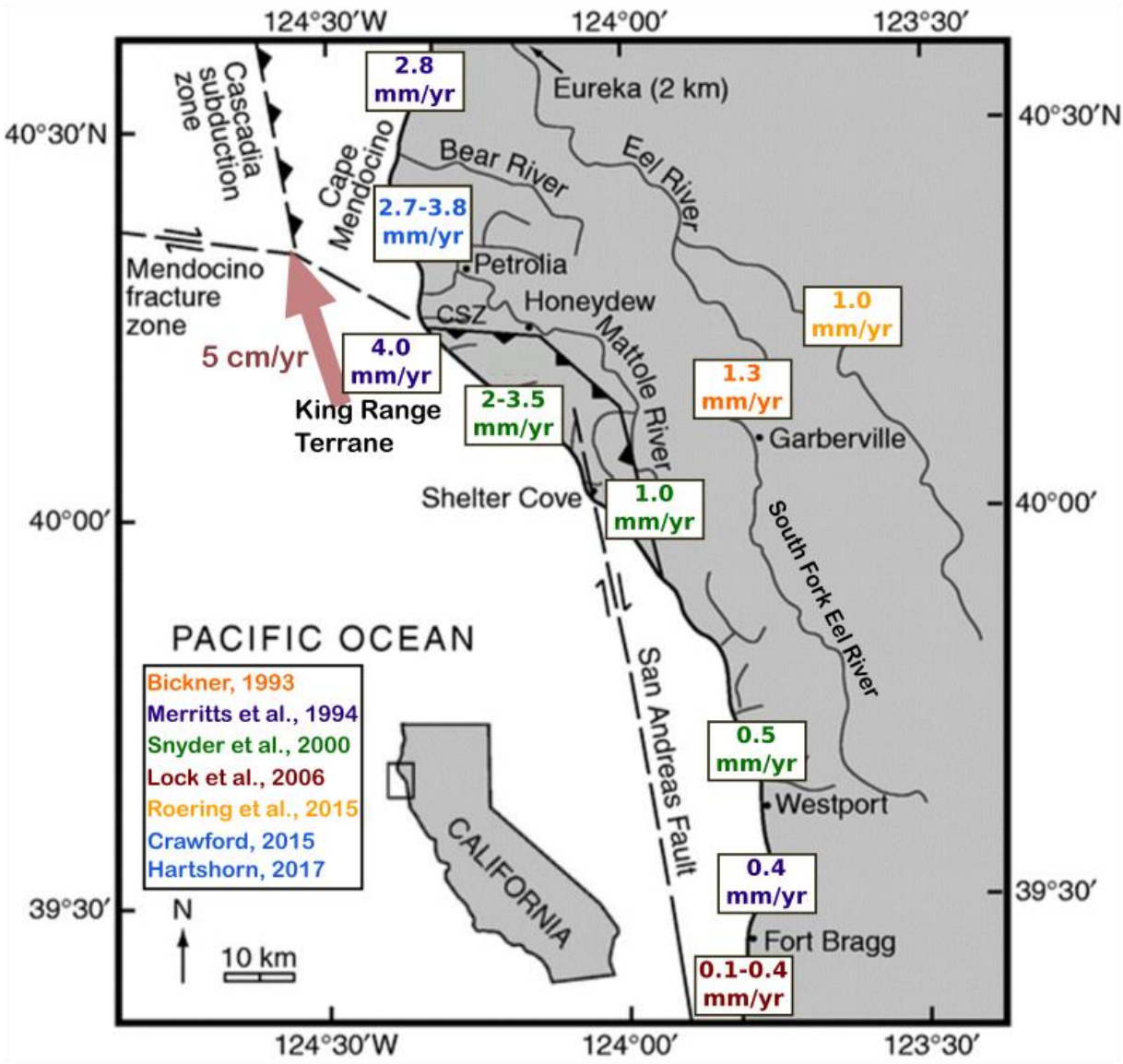

Figure 2.7: Inferred uplift rates for Northern California. Modified figure from Snyder et al., (2000) with marine terrace inferred uplift rates as calculated from Bickner, (1993), Merritts et al., (1994), Snyder et al., (2000), Lock et al., (2006), Roering et al., (2015), Crawford, (2015), and Hartshorn (2017). Bickner (1993) rates encompass an average rate from the last 80 ka. Merritts et al., (1994), and Snyder et al., (2000) rates encompass an average uplift rate from the late Pleistocene to Holocene. Rates inferred from Lock et al., (2006), and Roering et al., (2015) are modelled for ~125-75 ka. Lastly, rates from Crawford (2015) and Hartshorn (2017) represent modern rates of uplift.

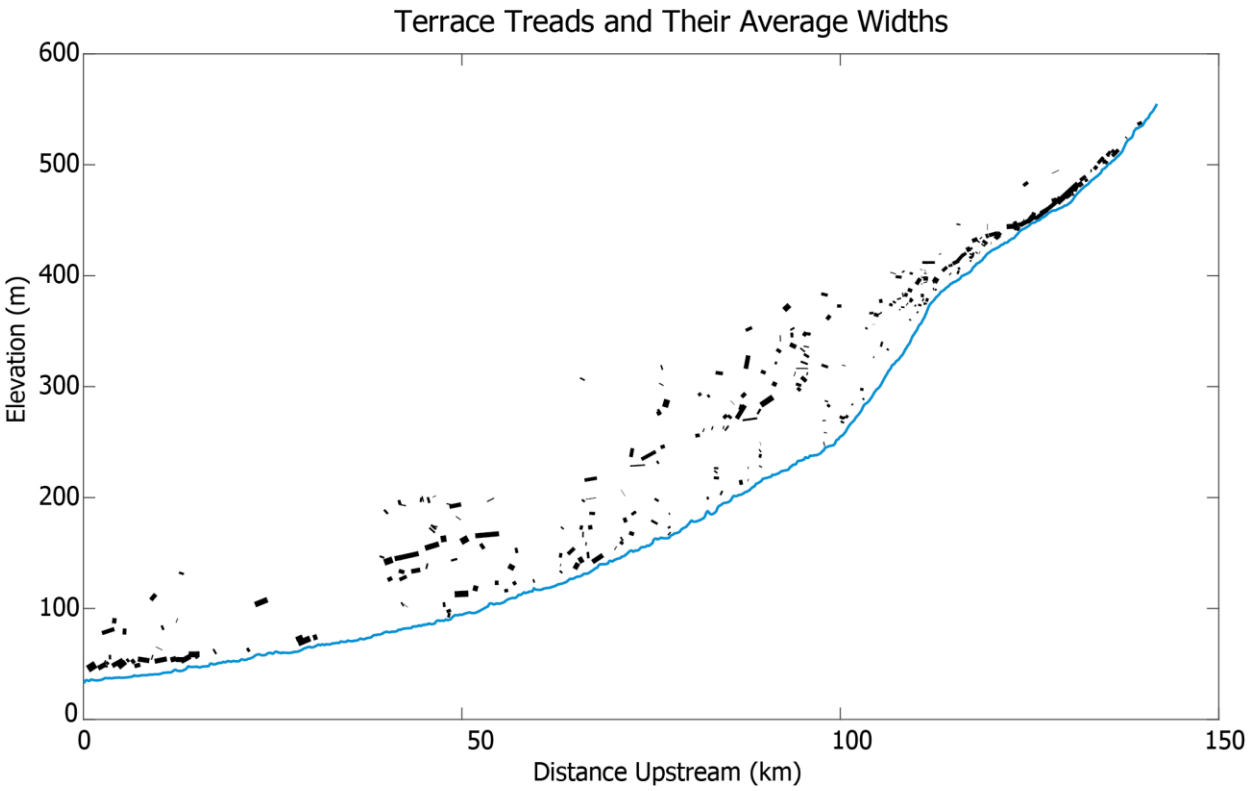

Figure 2.8: Strath terrace treads plotted along the longitudinal profile of the South Fork Eel River. The line thicknesses for each terrace is proportional to terrace width, logarithmically scaled.

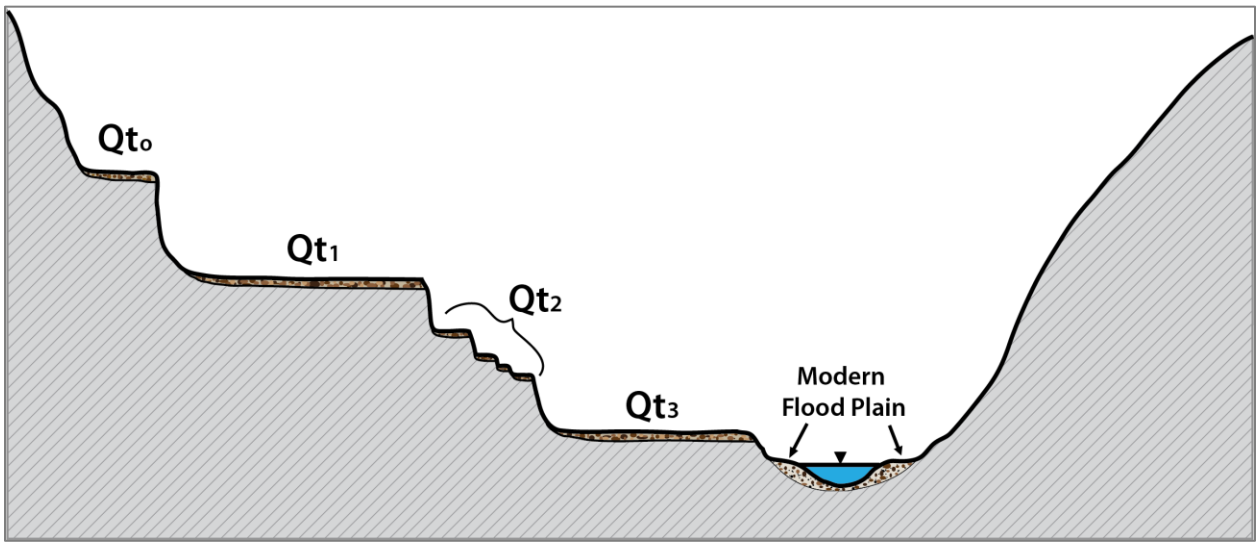

Figure 2.9: Hypothetical cross section of the river valley showing strath terrace generation placement and relative size of these features.

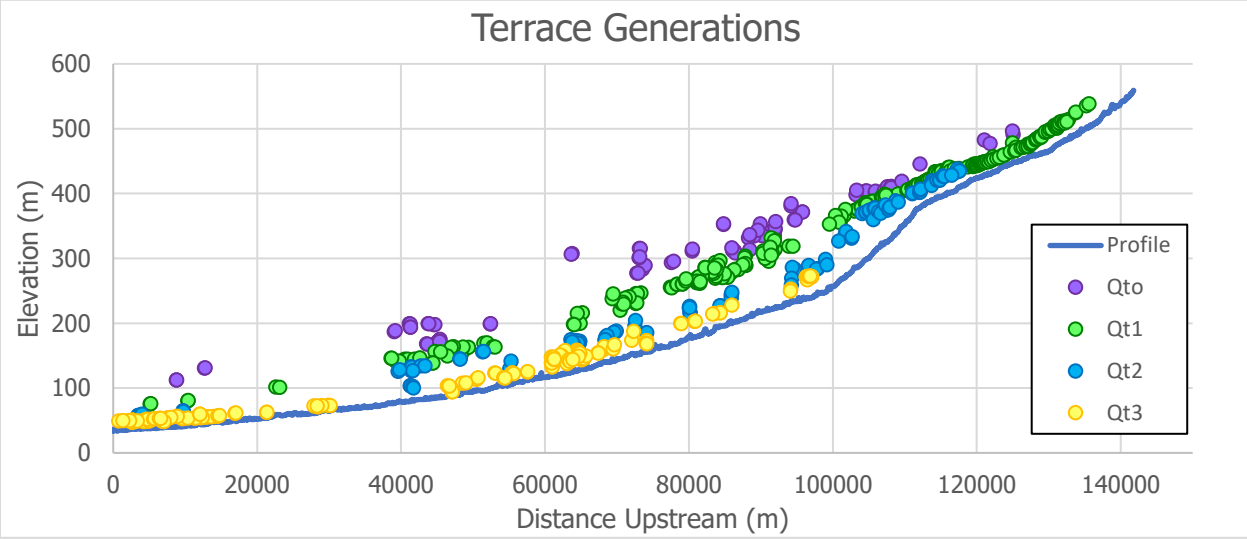

Figure 2.10: Simplified river valley profile line with terrace generations. Qt_o – oldest fluvial terraces far above the river; Qt_1 – uppermost continuous surface (ages were collected within this generation); Qt_2 – intermediate terraces; Qt_3 – youngest terraces which are closest to present day channel.

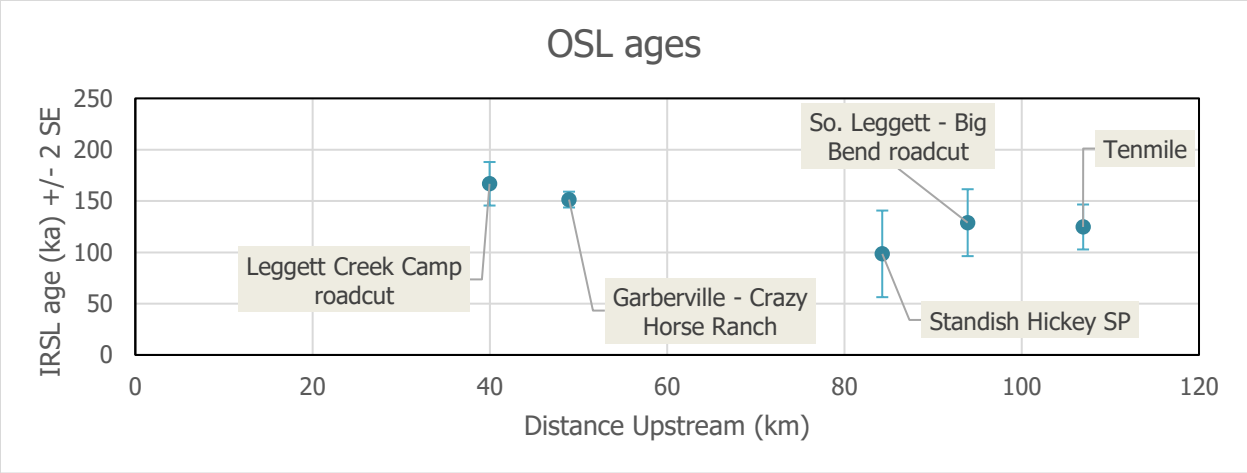

Figure 2.11: IRSL Terrace ages for the SFER with 2σ standard error. The basin wide average age is 139.74 ± 37.74. The age of terraces decreases with distance upstream.

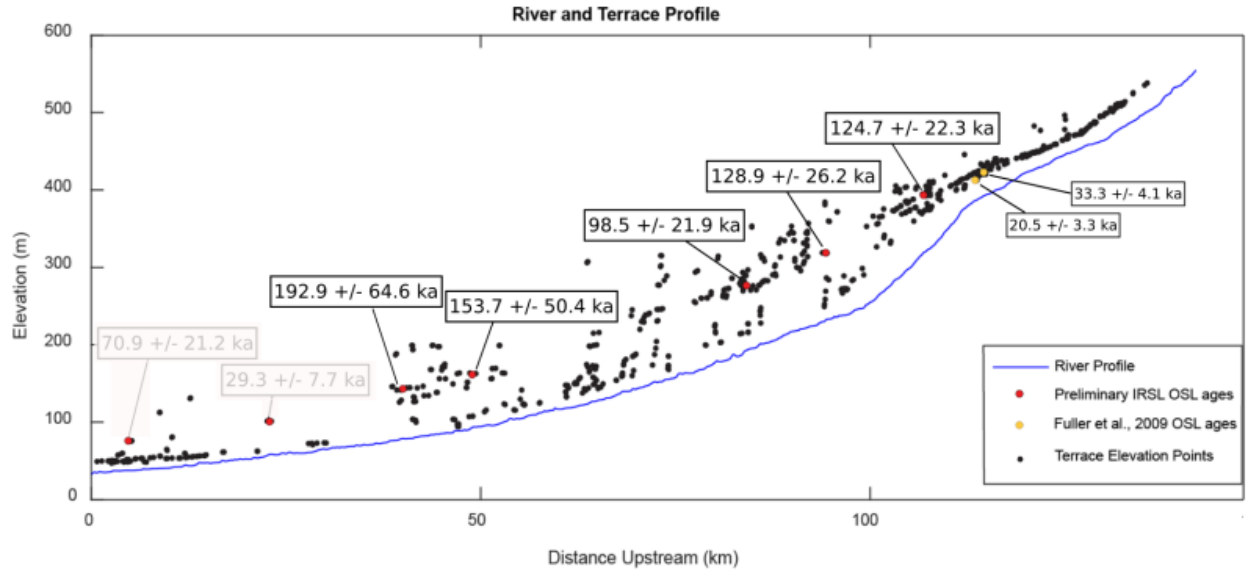

Figure 2.12: Terrace ages along the length of the SFER, along with Fuller et al., 2009 OSL terrace ages.

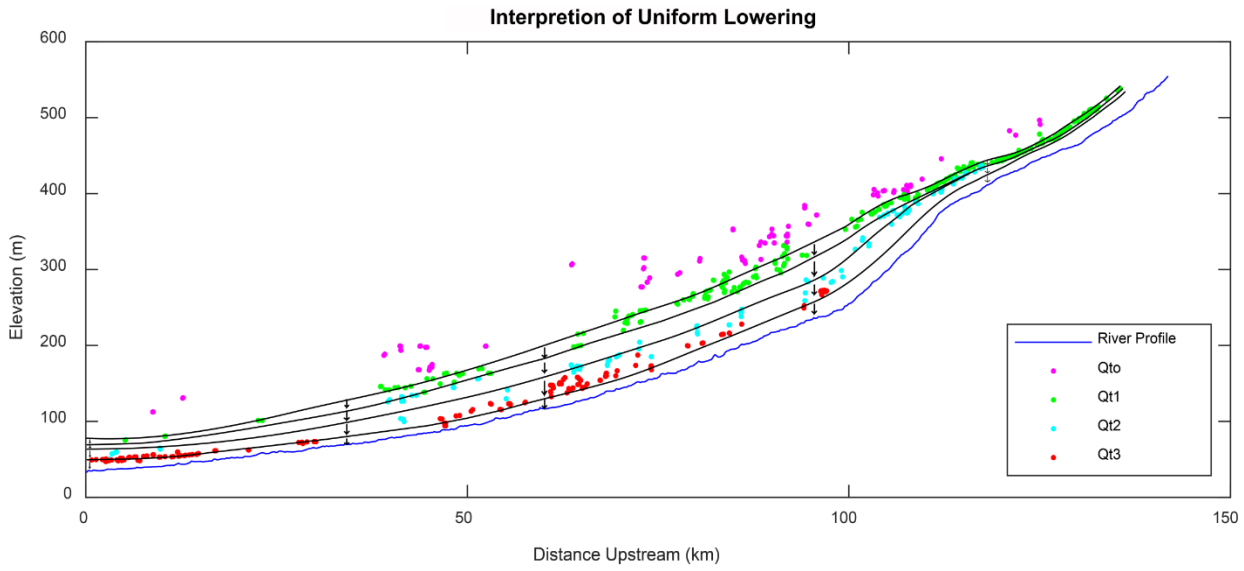

Figure 2.13: Interpretation of how uniform lowering within the SFER basin may have been accomplished. Where terraces within Qt_1 would yield similar ages. Four steps down through the basin likely occurred due to the placement of the intermediate terraces.

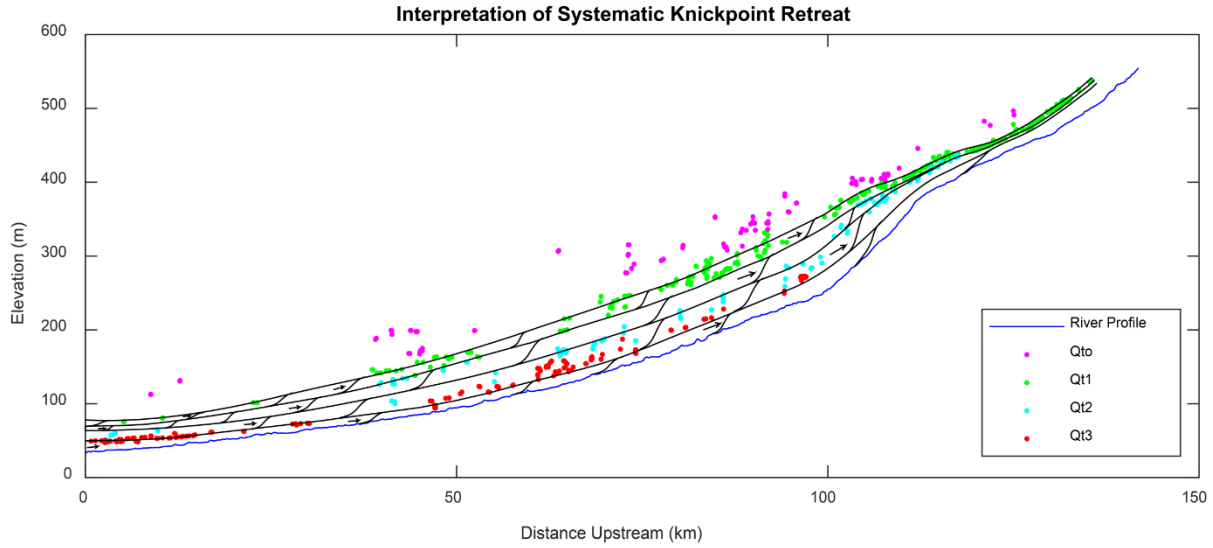

Figure 2.14: Interpretation of progressive knickpoint retreat within the SFER basin, where terrace ages within Qt_1 would decrease with distance upstream. Due to the placement of intermediate terraces, the singular retreat of one knickzone is unlikely.

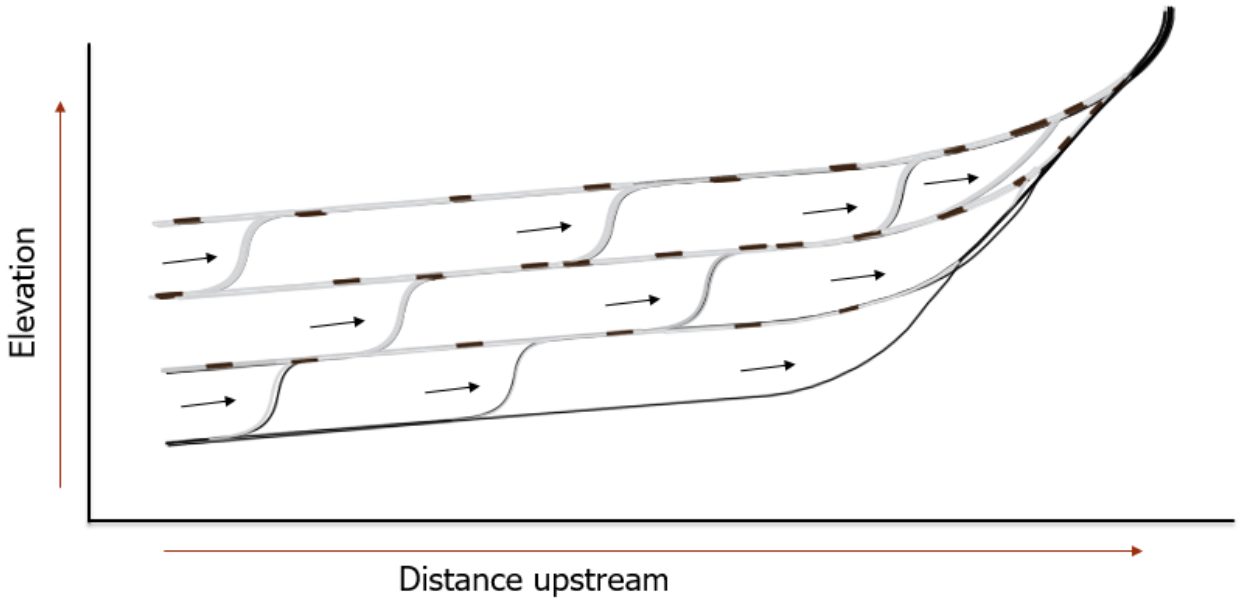

Figure 2.15: Diagram showing progressive knickpoint retreat within a basin. Multiple stages of the knickpoint/zone stepping back through time, and at varying starting channel locations.

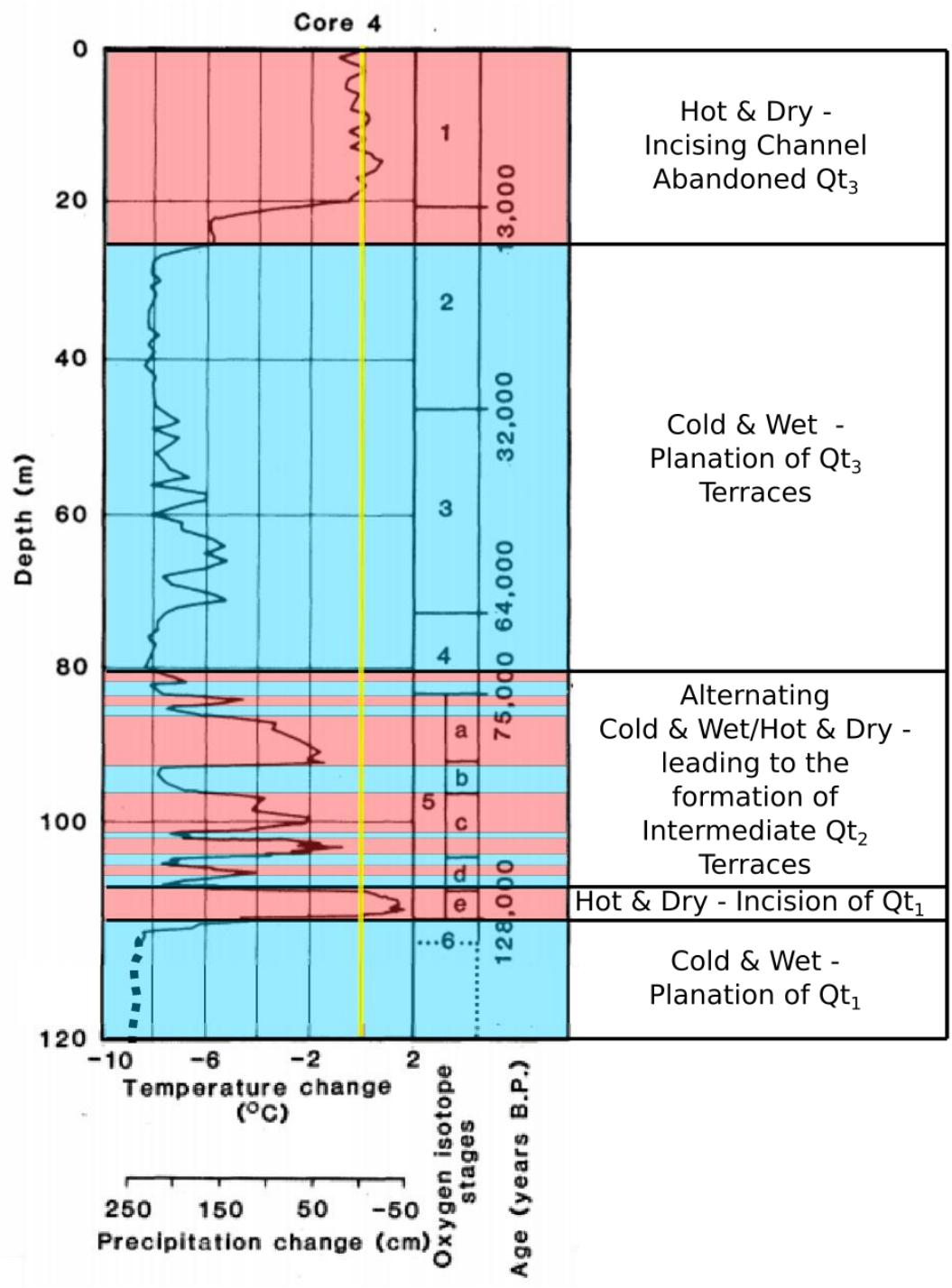

Figure 2.16: Reconstructed temperature and precipitation changes, plotted as a function of depth for Clear Lake core 4, modified from Adam and West, (1983). The reconstructed temperature and precipitation data denote how past conditions differed in comparison to modern day, which is represented by the yellow line. Time periods shaded blue represent glacial times when climate was cold and wet, increasing sediment production, channel aggradation and lateral planation of terraces. Time periods shaded red represent interglacial times when climate was hot and dry, decreasing sediment production, enabling vertical incision and terrace abandonment.

References

Adam, D.P., Sims, J.D., and Throckmorton, C.K., 1981, 130,000-yr continuous pollen record from Clear Lake, Lake County, California: Geology, v. 9, p. 373–377, doi: 10.1130/0091-7613(1981)9<373.

Adam, D.P., and West, J.G., 1983, Temperature and precipitation estimates through the last glacial cycle from Clear Lake, California, pollen data: Science, v. 219, p. 168–170.

Aitken, M.J., 1998, An Introduction to Optical Dating: The dating of Quaternary sediments by the use of photon-stimulated luminescence: New York, Oxford University Press, p. 267, doi: 10.1002/(SICI)1520-6548(200001)15:1<81::AID-GEA5>3.3.CO;2-Y.

Bateman, M.D., Boulter, C.H., Carr, A.S., Frederick, C.D., Peter, D., and Wilder, M., 2007, Preserving the palaeoenvironmental record in Drylands: Bioturbation and its significance for luminescence-derived chronologies: Sedimentary Geology, v. 195, p. 5–19, doi: 10.1016/j.sedgeo.2006.07.003.

Bennett, G.L., Roering, J.J., Mackey, B.H., Handwerger, A.L., Schmidt, D.A., and Guillod, B.P., 2016, Historic drought puts the brakes on earthflows in Northern California: Geophysical Research Letters, p. 5725–5731, doi: 10.1002/ 2016GL068378.

Berlin, M.M., and Anderson, R.S., 2009, Steepened channels upstream of knickpoints: Controls on relict landscape response: Journal of Geophysical Research: Solid Earth, v. 114, p. 1–20, doi: 10.1029/2008JF001148.

Bickner, F.R., 1993, A soil chronosequence of the Mitchell Ranch fluvial terraces on the South Fork Eel River: Age estimates and Tectonic Implications [MS thesis]: Humboldt, California State University, 81 p.

Blake Jr, M.C., Jayko, A.S., and Howell, D.G., 1981, Geology of a subduction complex in the Franciscan assemblage of Northern California: Oceanologica, p. 267–272.

Blum, M.D., and Törnqvist, T.E., 2000, Fluvial responses to climate and sea-level change: A review and look forward: Sedimentology, v. 47, p. 2–48, doi: 10.1046/j.1365-3091.2000.00008.x.

Bull, W.B., 1990, Stream-terrace genesis: implications for soil development: Geomorphology, v. 3, p 351-367, doi: 10.1016/0169-555X(90)90011-E.

Crawford, B., 2015, Geomorphic Map and Analysis of Uplifted Holocene Marine Terraces at the Southern Terminus of the Cascadia Subduction Zone: Cape Mendocino to Mouth of the Mattole River, Petrolia, CA [B.S. Thesis]: Humboldt, California State University, 46 p.

Crosby, B.T., and Whipple, K.X., 2006, Knickpoint initiation and distribution within fluvial networks: 236 waterfalls in the Waipaoa River, North Island, New Zealand: Geomorphology, v. 82, p. 16–38, doi: 10.1016/j.geomorph.2005.08.023.

Dietrich, W.E., 2014, Eel River Critical Zone Observatory July 2014 Lidar Survey: National Center for Airborne Laser Mapping, doi: 10.5069/G9MP517V.

Edwards, R.L., Gallup, C.D., and Cheng, H., 2003, Uranium-series Dating of Marine and Lacustrine Carbonates: Reviews in Mineralogy and Geochemistry, v. 52, p. 363–405, http://dx.doi.org/10.2113/0520363.

Finnegan, N.J., and Dietrich, W.E., 2011, Episodic bedrock strath terrace formation due to meander migration and cutoff: Geology, v. 39, p. 143–146, doi: 10.1130/G31716.1.

Foster, M.A., and Kelsey, H.M., 2012, Knickpoint and knickzone formation and propagation, South Fork Eel River, northern California: Geosphere, v. 8, p. 403–416, doi: 10.1130/GES00700.1.

Fuller, T.K., Perg, L.A., Willenbring, J.K., and Lepper, K., 2009, Field evidence for climate-driven changes in sediment supply leading to strath terrace formation: Geology, v. 37, p. 467–470, doi: 10.1130/G25487A.1.

Furlong, K.P., and Govers, R., 1999, Ephemeral crustal thickening at a triple junction: The Mendocino crustal conveyor: Geology, v. 27, p. 127–130, doi: 10.1130/0091-7613(1999)027<0127:ECTAAT>2.3.CO;2.

Gilbert, G.K., 1877, "Geology of the Henry Mountains", doi: 10.1038/022266c0.

Goni, M.F.S., Turon, J.-L., Eynaud, F., and Gendreau, S., 2000, European climatic response to millenial-scale changes in the atmosphere-ocean system during the Last Glacial period: Quaternary Research, v. 54, p. 394–403, doi: 10.1006/qres.2000.2176.

Guérin, G., Mercier, N., and Adamiec, G., 2011, Dose-rate conversion factors: update: Ancient TL, v. 29, p. 5–8.

Hancock, G.S., and Anderson, R.S., 2002, Numerical modelling of fluvial strath terrace formation in response to oscillating climate: Geological Society of American Bulletin, v. 114, p. 1131–1142, doi: 10.1130/0016-7606(2002)114<1131.

Hartshorn, E., 2017, Marine Terrace Formation Associated with Northern Migration of the Mendocino Triple Junction Uplift at Cape Mendocino, California [B.S. Thesis]: Humboldt, California State University, 55 p.

Kenworthy, M.K., Rittenour, T.M., Pierce, J.L., Sutfin, N.A., and Sharp, W.D., 2014, Luminescence dating without sand lenses: An application of OSL to coarse-grained alluvial fan deposits of the Lost River Range, Idaho, USA: Quaternary Geochronology, v. 23, p. 9–25, doi: 10.1016/j.quageo.2014.03.004.

Lock, J., Kelsey, H., Furlong, K., and Woolace, A., 2006, Late Neogene and Quaternary landscape evolution of the northern California Coast Ranges: Evidence for Mendocino triple junction tectonics: Bulletin of the Geological Society of America, v. 118, p. 1232–1246, doi: 10.1130/B25885.1.

Nelson, M.S., Gray, H.J., Johnson, J.A., Rittenour, T.M., Feathers, J.K., and Mahan, S.A., 2015, User Guide for Luminescence Sampling in Archaeological and Geological Contexts: Advances in Archaeological Practice, v. 3, p. 166–177, doi: 10.7183/2326-3768.3.2.166.

Maddy, D., 1997, Uplift-driven valley incision and river terrace formation in southern England: Journal of Quaternary Science, v. 12, p. 539–545, doi: 10.1002/(SICI)1099-1417(199711/12)12:6<539::AID-JQS350>3.3.CO;2-K.

McLaughlin, R., Ellen, S., Blake, M., Jayko, A., Irwin, W., Aalto, K., Carver, G., and Clarke Jr, S., 2000, Geology of the Cape Mendocino, Eureka, Garberville, and Southwestern part of the Hayfork 30x60 Minute Quadrangles and Adjacent Offshore Area, Northern California, Plate 3: Garberville Quadrangle: USGS.

Merritts, D., and Bull, W., 1989, Interpreting Quaternary uplift rates at the Mendocino triple junction, northern California, from uplifted marine terraces: Geology, v. 17, p. 1020–1024, doi: 10.1130/0091-7613(1989)017<1020:IQURAT>2.3.CO;2.

Merritts, D.J., Vincent, K.R., and Wohl, E.E., 1994, Long river profiles, tectonism, and eustasy: A guide to interpreting fluvial terraces: Journal of Geophyscial Research, v. 99, p. 1431–1450, doi: 10.1029/94JB00857.

Meyer, G.A., and Leidecker, M.E., 1999, Fluvial terraces along the Middle Fork Salmon River, Idaho, and their relation to glaciation, landslide dams, and incision rates: a preliminary analysis and river-mile guide: Museum, p. 219–235.

Montgomery, D.R., 2004, Observations on the role of lithology in strath terrace formation and bedrock channel width: American Journal of Science, v. 304, p. 454–476, doi: 10.2475/ajs.304.5.454.

Mountain, G.S., Burger, R.L., Delius, H., Fulthorpe, C.S., Austin, J.A., Goldberg, D.S., Steckler, M.S., Mchugh, C.M., Miller, K.G., Monteverde, D.H., Orange, D.L., and Pratson, L.F., 2007, The long-term stratigraphic record on continental margins: Continental Margin Sedimentation: From Sediment Transport to Sequence Stratigraphy, p. 381–458, doi: 10.1002/9781444304398.ch8.

Muhs, D.R., Simmons, K.R., Schumann, R.R., Groves, L.T., Mitrovica, J.X., and Laurel, D., 2012, Sea-level history during the Last Interglacial complex on San Nicolas Island, California: implications for glacial isostatic adjustment processes, paleozoogeography and tectonics: Quaternary Science Reviews, v. 37, p. 1–25, doi: 10.1016/J.QUASCIREV.2012.01.010.

Muhs, D.R., Wehmiller, J.F., Simmons, K.R., and York, L.L., 2003, Quaternary sea-level history of the United States: Developments in Quaternary Science, v. 1, p. 147–183, doi: 10.1016/S1571-0866(03)01008-X.

Murray, A.S., and Olley, J.M., 2002, Precision and accuracy in the optically stimulated luminescence dating of sedimentary quartz: a status review: Geochronometria, v. 21, p. 1-6.

Murray, A.S., and Wintle, A.G., 2000, Luminescence dating of quartz using an improved single-aliquot regenerative-dose protocol: Radiation Measurements, v. 32, p. 57–73.

National Center for Atmospheric Research, 2017, The Climate Data Guide: PRISM High-Resolution Spatial Climate Data for the United States: Max/min temp, dewpoint, precipitation: NCAR Climate Data Guide.

Ouimet, W.B., Whipple, K.X., Royden, L.H., Sun, Z., and Chen, Z., 2007, The influence of large landslides on river incision in a transient landscape: Eastern margin of the Tibetan Plateau (Sichuan, China): Geological Society of America Bulletin, v. 119, p. 1462–1476, doi: 10.1130/B26136.1.

Pazzaglia, F.J., 2013, Fluvial Terraces, in Shroder, J. ed.: Treatise on Geomorphology Elsevier Inc., v. 9, p. 379–412, doi: 10.1016/B978-0-12-374739-6.00248-7.

Penck, A., and Bruckner, E., 1909, Die Aplen im Eiszeitalter: 1199 p.

Perkins, J., 2009, South Fork Eel River, CA: Understanding Terrace Formation and Abandonment: National Center for Airborne Laser Mapping, doi: 10.5069/G93F4MH1.

Porter, S.C., 2001, Chinese loess record of monsoon climate during the last glacial-interglacial cycle: Earth-Science Reviews, v. 54, p. 115–128, doi: 10.1016/S0012-8252(01)00043-5.

Power, M.E., 2004, South Fork Eel River, CA Watershed Morphology: National Center for Airborne Laser Mapping, doi: 10.5069/G9639MPN.

Prescott, J.R., and Hutton, J.T., 1994, Cosmic ray contributions to dose rates for luminescence and ESR dating: Large depths and long-term time variations: Radiation Measurements, v. 23, p. 497–500.

Reneau, S.L., 2000, Stream incision and terrace development in Frijoles Canyon, Bandelier National Monument, New Mexico, and the influence of lithology and climate: Geomorphology, v. 32, p. 171–193, doi: 10.1016/S0169-555X(99)00094-X.

Rittenour, T.M., 2008, Luminescence dating of fluvial deposits: Applications to geomorphic, palaeoseismic and archaeological research: Boreas, v. 37, p. 613–635, doi: 10.1111/j.1502-3885.2008.00056.x.

Roering, J.J., Mackey, B.H., Handwerger, A.L., Booth, A.M., Schmidt, D.A., Bennett, G.L., and Cerovski-Darriau, C., 2015, Beyond the angle of repose: A review and synthesis of landslide processes in response to rapid uplift, Eel River, Northern California: Geomorphology, v. 236, p. 109–131, doi: 10.1016/j.geomorph.2015.02.013.

Sella, G.F., Dixon, T.H., and Mao, A., 2002, REVEL: A model for recent plate velocities from space geodesy: Journal of Geophysical Research: Solid Earth, v. 107, p. 11-30, doi: 10.1029/2000JB000033.

Snyder, N.P., Whipple, K.X., Tucker, G.E., and Merritts, D.J., 2000, Landscape response to tectonic forcing: Digital elevation model analysis of stream profiles in the Mendocino triple junction region, Northern California: Bulletin of the Geological Society of America, v. 112, p. 1250–1263, doi: 10.1130/0016-7606(2000)112<1250:LRTTFD>2.0.CO;2.

Stock, J.D., Montgomery, D.R., Collins, B.D., Dietrich, W.E., and Sklar, L., 2005, Field measurements of incision rates following bedrock exposure: Implications for process controls on the long profiles of valleys cut by rivers and debris flows: Bulletin of the Geological Society of America, v. 117, p. 174–194, doi: 10.1130/B25560.1.

Stokes, S., Bray, H.E., and Blum, M.D., 2001, Optical resetting in large drainage basins: Tests of zeroing assumptions using single-aliquot procedures: Quaternary Science Reviews, v. 20, p. 879–885, doi: 10.1016/S0277-3791(00)00045-7.

USFS, and BLM, 1996, South Fork Eel River Watershed Analysis.

Vandenberghe, J., and Maddy, D., 2001, The response of river systems to climate change: Quaternary International, v. 79, p. 1–3, doi: 10.1016/S1040-6182(00)00118-X.

Von-Blanckenburg, F., and Willenbring, J.K., 2014, Cosmogenic nuclides: dates and rates of earth-surface change: Elements, v. 10, p. 341–346, doi: 10.2113/gselements.10.5.341.

Waelbroeck, C., Labeyrie, L., Michel, E., Duplessy, J.C., McManus, J.F., Lambeck, K., Balbon, E., and Labracherie, M., 2002, Sea-level and deep water temperature changes derived from benthic foraminifera isotopic records: Quaternary Science Reviews, v. 21, p. 295–305, doi: 10.1016/S0277-3791(01)00101-9.

Wakabayashi, J., 2015, Anatomy of a subduction complex: architecture of the Franciscan Complex, California, at multiple length and time scales: International Geology Review, v. 6814, p. 37–41, doi: 10.1080/00206814.2014.998728.

Walker, M., 1986, Quaternary dating methods: West Sussex PO19 8SQ, England, John Wiley & Sons, Ltd, v. 58, 362 p., doi: 10.1016/0168-9622(86)90024-2.

Wang, Y., Amundson, R., Trumbore, S., No, A., Wang, Y., Amundson, R., and Trumbore, S., 1996, Radiocarbon Dating of Soil Organic Matter: Quaternary Research, v. 45, p. 282–288, doi: 10.1006/qres.1996.0029.

Wintle, A.G.A.G., 1997, Luminescence Dating: Laboratory Procedures and Protocols: p. 769-817, doi: 10.1016/S1350-4487(97)00220-5.

Wulf, S., 2013, Methods and applications of tephrochronology in sedimentary archives:, doi: 10.2312/GFZ.b103-14010.

Appendix 2.1

The OSL sampling procedures for bulk sampling, are based on the processes discussed in Kenworthy et al. (2014). Bulk sampling procedures is as accurate as traditional hammer-in pipe OSL methods for sediment collection, and work well for studies that are working within coarse alluvial deposits.

Terraces with >2 meters of sediment fill exposed along a natural cut face or outcrop of a terrace were targeted. Samples would be collected from interbedded sand lenses within the terrace, at a depth exceeding 1 meter, to minimize cosmogenic influence. When selection a sampling location, avoid as much botanical influence as possible to minimize possible contamination of light exposed grains. With coarse deposits, where driving metal tubes into the outcrop is difficult, sampling must be done at night by sampling directly from the deposit and separating the sand from the larger grains. Sampling must be done at night, because if the sample gets exposed to any sunlight, its age will be "reset" and will not give us an accurate age of how long the grain has buried in the terrace.

Once a good location is found, clear ~40-65 cm of sediment from the face of the outcrop, while digging down 40-100cm. Focusing on the sand-rich portions of the deposit, clear a radius of ~30 cm, to remove any loose materials. On the night of collection, under a tarp with a red headlamp light turned behind your head, clear another ~5 cm into the outcrop, to further clean the sampling area of material that may have been exposed to light earlier in the day.

Once the site is cleared off and light safe, collect 2 quart-sized baggies of sample material from the 30cm area. The first bag will contain the light sensitive fine to be dated. This light sensitive material triple wrapped in black trash bags after it has been collected underneath the tarp, and then stored in a light proof box for transportation and storage until processing. The

second bag will contain a mixture of the surrounding (30cm) sand/gravel/cobble to determine the elemental setting and mineralogy of the area (dose rate). A small, sealed film canister of sand will also be collected to determine the water content at the outcrop. The depth of burial, elevation, and latitude/longitude measurements must also be recorded.

Appendix 2.2

USU Luminescence Laboratory

Final Luminescence (IRSL) Age Report for the South Fork Eel River, Project #280

Table 1. Infrared Stimulated Luminescence (IRSL) Age Information

Sample num.	USU num.	Depth (m)	Grain size (μm)	Num. of aliquots[1]	Dose Rate (Gy/ka)	D_E[2] ± 2σ (Gy)	OD[3] (%)	**IRSL age[4] ± 2σ (ka)**
17KW_OS L6_W2	USU-2668	2.55	90-150	12 (14)	3.22 ± 0.36	142.1 ± 34.5	38.8 ± 9.3	**70.9 ± 21.2**
17KW_OS L7_Mer1	USU-2669	1.5	90-150	11 (14)	3.47 ± 0.39	64.6 ± 19.0	44.5 ± 11.1	**29.3 ± 7.7**
17KW_OS L8_LC2	USU-2670	3	90-150	15 (15)	3.04 ± 0.35	375.6 ± 80.9	39.8 ± 7.9	**166.8 ± 42.2**
17KW_OS L9_CH1	USU-2671	1.5	90-150	13 (14)	3.32 ± 0.38	324.6 ± 51.1	25.5 ± 6.2	**151.4 ± 32.6**
17KW_OS L10_SH2	USU-2672	2.8	90-150	13 (14)	3.55 ± 0.40	215.8 ± 54.3	41.7 ± 9.5	**98.5 ± 21.9**
17KW_OS L11_BB2	USU-2673	2.2	90-150	17 (20)	3.90 ± 0.49	299.8 ± 68.1	44.3 ± 8.4	**128.9 ± 26.2**
17KW_OS L12_TM1	USU-2674	1.2	63-150	17 (22)	4.75 ± 0.54	385.7 ± 50.3	22.9 ± 5.3	**124.7 ± 22.3**

[1] Age analysis using the IRSL (50°C) and elevated temperature (225°C) post-IR IRSL protocol of Buylaert et al. (2009). Number of aliquots used in age calculation and number of aliquots analyzed in parentheses.

[2] Equivalent dose (D_E) calculated using the Central Age Model (CAM) of Galbraith and Roberts (2012).

[3] Overdispersion (OD) represents variance in D_E data beyond measurement uncertainties, OD >20% may indicate significant scatter due to depositional or post-depositional processes.

[4] IRSL age on each aliquot corrected for fading following the method by Auclair et al. (2003) and correction model of Huntley and Lamothe (2001).

Table 2. Dose Rate Information

Sample num.	USU num.	In-situ H_2O (%)	Chem fraction[1]	K (%)[2]	Rb (ppm)[2]	Th (ppm)[2]	U (ppm)[2]	Cosmic (Gy/ka)
17KW_OSL6_W2	USU-2668	6.1	S (13%)	1.11±0.03	46.9±1.9	4.0±0.4	1.4±0.1	0.15±0.02
			P (35%)	1.02±0.03	43.6±1.7	4.8±0.4	1.5±0.1	
			C (52%)	1.26±0.03	45.5±1.8	5.8±0.5	1.6±0.1	
17KW_OSL7_Mer1	USU-2669	6.5	S (18%)	1.16±0.03	49.2±2.0	4.5±0.4	1.4±0.1	0.17±0.02
			P (28%)	1.22±0.03	46.9±1.9	5.6±0.5	1.6±0.1	
			C (54%)	1.60±0.04	56.4±2.3	7.5±0.7	2.1±0.2	
17KW_OSL8_LC2	USU-2670	7.3	S (5%)	0.95±0.02	44.2±1.8	4.1±0.4	1.5±0.1	0.15±0.01
			P (75%)	0.88±0.02	35.8±1.4	4.8±0.4	1.5±0.1	
			C (20%)	0.73±0.02	27.7±1.1	5.4±0.5	1.5±0.1	
17KW_OSL9_CH1	USU-2671	6.0	S (19%)	1.07±0.03	50.4±2.0	4.6±0.4	1.5±0.1	0.18±0.02
			P (44%)	0.93±0.02	40.0±1.6	4.8±0.4	1.5±0.1	
			C (37%)	1.22±0.03	49.5±2.0	6.3±0.6	1.6±0.1	
17KW_OSL10_SH2	USU-2672	6.1	S (35%)	1.20±0.03	51.2±2.0	4.5±0.4	1.6±0.1	0.15±0.02
			P (23%)	1.34±0.03	52.7±2.1	7.6±0.7	2.0±0.1	
			C (42%)	1.62±0.04	62.2±2.5	6.0±0.5	1.7±0.1	
17KW_OSL11_BB2	USU-2673	12.9	S (7%)	1.54±0.04	55.1±2.2	4.8±0.4	2.0±0.1	0.17±0.02
			P (33%)	1.35±0.03	56.7±2.3	6.2±0.6	2.0±0.1	
			C (60%)	1.45±0.04	49.6±2.0	9.0±0.8	2.1±0.1	
17KW_OSL12_TM1	USU-2674	6.3	S (5%)	1.81±0.05	82.8±3.3	6.3±0.6	2.3±0.2	0.19±0.02
			P (41%)	1.83±0.05	78.7±3.1	5.9±0.5	2.2±0.2	
			C (54%)	1.82±0.05	75.0±3.0	6.6±0.6	2.2±0.2	

[1] Dose rate (DR) fraction used for chemical analysis: S= sand, P= pebble, C= cobble. Gamma DR uses weighted average of fraction contributions (by % weight). Beta DR uses sand fraction only.

[2] Radioelemental concentrations determined by ALS Chemex using ICP-MS and ICP-AES techniques; dose rate is derived from concentrations by conversion factors from Guérin et al. (2011). Internal grain beta dose rate was determined assuming 12.5% K (Huntley and Baril, 1997) and 400ppm Rb (Huntley and Hancock, 2001) attenuated to grain size using Mejdahl (1979). Alpha contribution to dose rate determined using an efficiency factor, or 'a-value', of 0.15±0.015 after Balescu and Lamothe (1994) (Durcan et al., 2015).

Equivalent dose (D_E) Distributions: Probability density functions and radial plots

1. 17KW_OSL6_W2, USU-2668

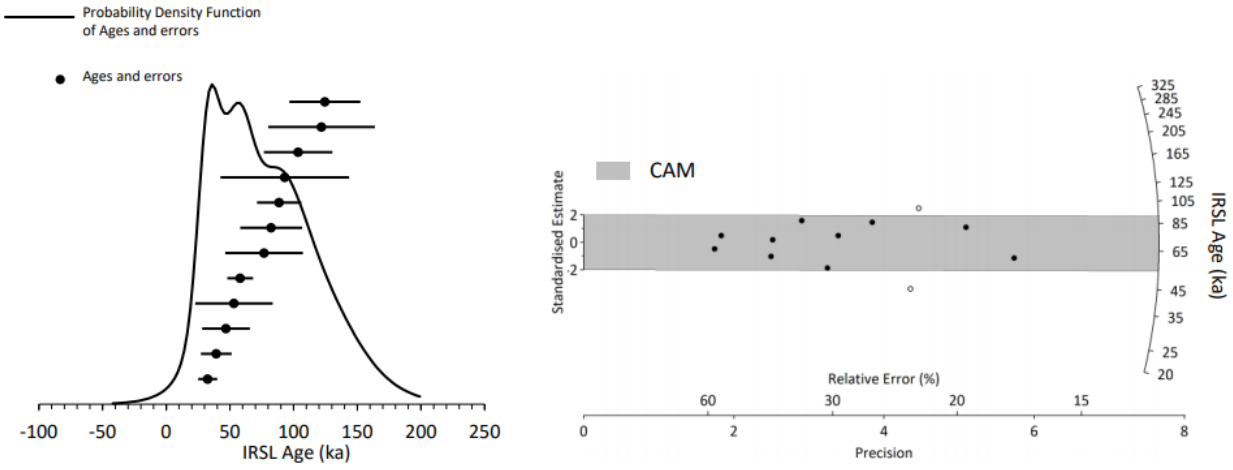

2. 17KW_OSL7_Mer1, USU-2669

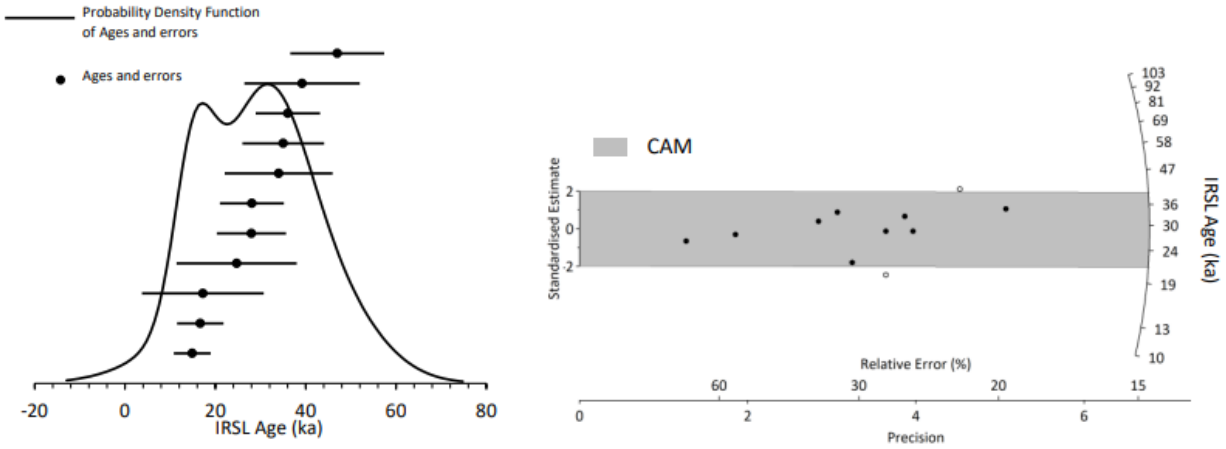

3. 17KW_OSL8_LC2, USU-2670

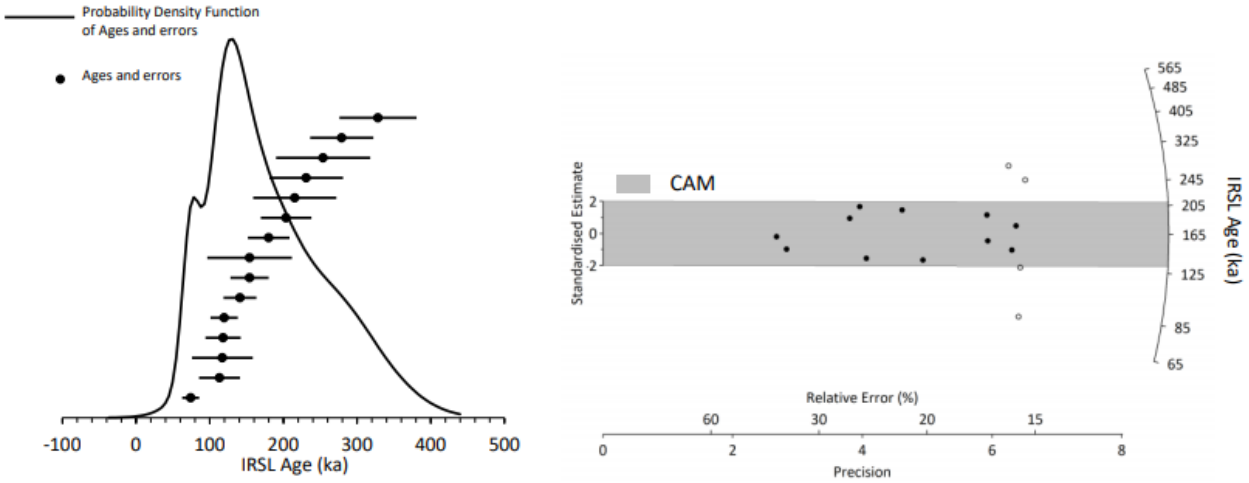

4. 17KW_OSL9_CH1, USU-2671

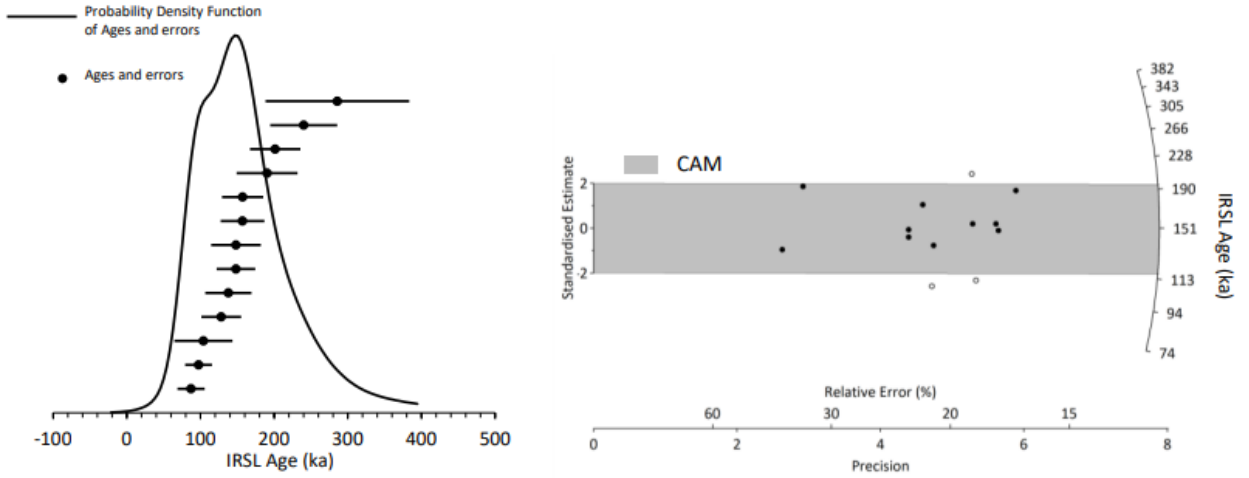

5. 17KW_OSL10_SH2, USU-2672

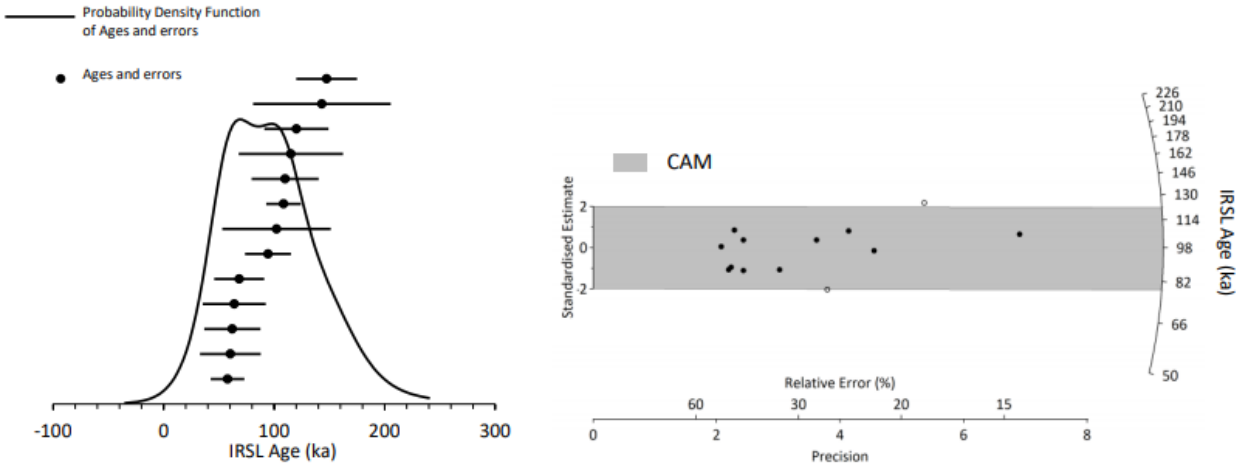

6. 17KW_OSL11_BB2, USU-2673

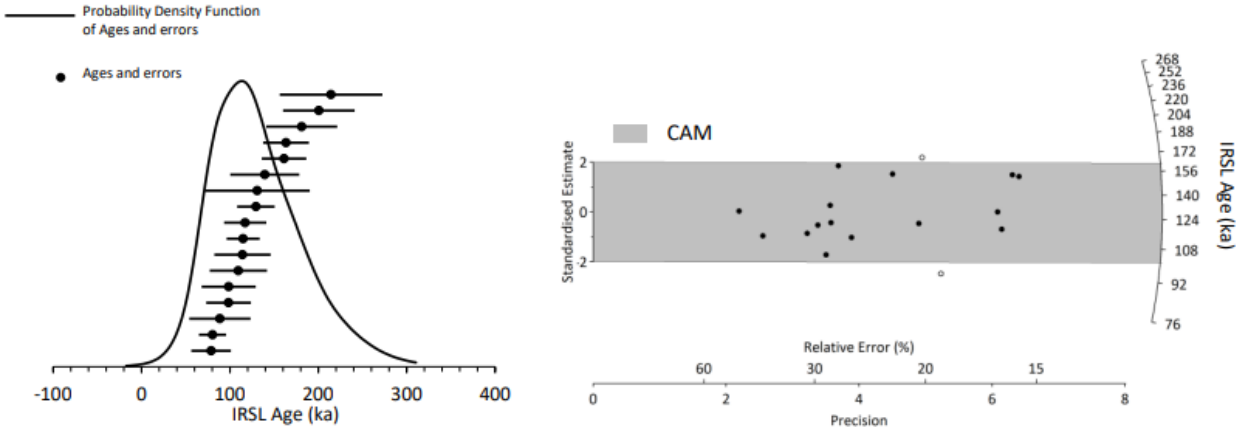

7. 17KW_OSL12_TM1, USU-2674

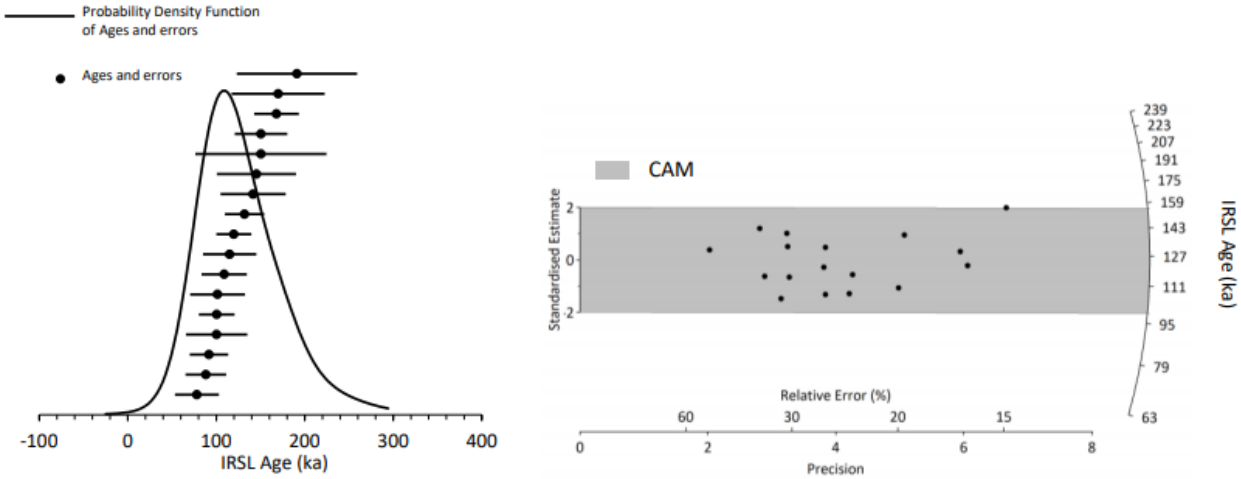

Chapter 3 : Longitudinal trends in hillslope failures reveal progressive adjustment following river incision along the South Fork Eel River, Northern California

Abstract

Hillslopes respond to rapid channel incision by generating mass movements. High resolution LiDAR is used to characterize mass movement bodies along the South Fork Eel River corridor, a system that is actively adjusting to base level change that initiated ~130 ka. Trends in percent area affected, number of mass movements, and roughness calculations show that the lower basin is more pervasively affected by mass movements than the area within the knickzone or upstream. Independent of basin location, the hillslopes upslope of terraces are buffered from the base level fall signal. These observations corroborate that base level fall has yet to propagate through the entire system. This pattern of hillslope response aligns with the suggested progressive knickpoint retreat model for incision through the lower basin. Through other work, it is clear that while river incision is focused around the knickzone, yet this work shows that the downstream hillslopes continue to respond to the base level fall long after the knickpoint has passed.

3.1 Introduction

River networks provide insight into how landscapes respond to changes in climate or tectonics, which impact relative base level and influence river incision and subsequent landscape transience (DiBiase et al., 2014). For example, if the relative base level of a channel drops due to either tectonic uplift or sea-level fall, a wave of incision transmits this signal upstream. This incision signal propagates upstream in the form of a knickpoint or knickzone, marking the erosional front of the upstream propagation of base level fall (Crosby and Whipple, 2006; Foster and Kelsey, 2012). These typically advance as an inflection point, separating the actively adjusting and adjusted landscape from the relict, unadjusted portion of the landscape (Schlunegger and Schneider, 2005).

As the river incises, this adjustment in base level is also "felt" by the surrounding hillslopes, as it causes over steepening, and undercuts slopes (Schlunegger and Schneider, 2005; Korup and Schlunegger, 2007; Ouimet et al., 2007; Highland and Bobrowsky, 2008; Dibiase et al., 2012). This destabilizes the surrounding hillslopes, causing mass wasting events to occur. This is due to the coupled relationship between hillslopes and the channel, so as the channel lowers, the connected hillslopes must adjust as well (Wohl, 2010). The strength of this connection affects both the temporal and spatial scale of how and when failures may occur. In poorly coupled systems the hillslope response may stay localized or only be seen at long time scales. In well coupled systems, hillslope response will be transmitted throughout the entire watershed as it lowers (Harvey, 2002; Savi et al., 2013).

The strength of coupling depends on several limiting factors, like the mechanical properties of the underlying bedrock and the ability of the river to erode these materials which affect the rate of river incision. Different lithologies have varying degrees of erodibility, which in

turn impacts the channel gradient and the propagation rate of knickpoints (Sklar and Dietrich, 2001; Goode and Wohl, 2010; Schlunegger et al., 2013). The strength of coupling can also be limited by the amount of soil cover (Mudd, 2016), as thick soil cover means more material is readily available for failure and hillslope adjustment. In landscapes with thin soil cover, less material is available for failure and the underlying bedrock itself must be eroded away to adjust to the changes within the channel. These relationships then affect the form of mass movement that are expected to occur within either domain. Landscapes with readily available material, thick soil cover, are likely to be dominated by rockfalls, rotational, and translational slides (Schlunegger et al., 2002, 2013). Landscapes with limited available material will have slower moving failures including creep, earthflows, and debris flows in concentrated areas like gullies (Schlunegger et al., 2002, 2013).

Much work has been done looking into the relationship between knickpoint incision and the hillslopes surrounding these erosional fronts (Gallen et al., 2011; Mackey et al., 2014; Anderson et al., 2015). These show that as knickpoints propagate upstream through a river network, increased erosion on the channel bed and surrounding banks occurs on the downstream edge of the knickpoint, and the hillslopes below the knickpoint steepen in response (DiBiase et al., 2014; Bennett et al., 2016). The hillslopes downstream of the inflection point then experience an increase in mass movements as erosion focuses adjacent to the channel, undermining the hillslope bases, leading to subsequent slope failures. Large landslides can also affect channels, as they can cause a temporary damming of the river, leading to a sudden change in channel slope and causing a temporary knickzone to form, furthering this feedback cycle (Ouimet et al., 2007).

Bennett et al. (2016) used aerial imagery to map debris slides within four major watersheds in northern California to study how landscapes may respond to tectonic uplift due to

the migration of the Mendocino Triple Junction (MTJ). Through mapping recent debris slides using aerial imagery, estimated contemporary mass movement erosion rates were compiled and compared to modeled uplift rates for the region, showing that the present day erosion rates from mass movements equaled those estimated by their model. This suggests that landslide erosion is one of the main mechanisms that landscapes use to adjust to equilibrium in response to tectonic uplift. Most studies however, do not look into how the hillslopes themselves continued to respond further downstream from knickpoints.

3.1.1 Study Overview and Rationale

Significant progress has been made on understanding knickpoint formation processes due to changes in base level (DiBiase et al., 2014), or formation of temporary knickpoints due to large landslides into a river system and how these knickpoints create a focused area of erosion on the adjoining hillslopes (Ouimet et al., 2007). The coupled relationship between rivers and their hillslopes has also been established (Harvey, 2002; Wohl, 2010; Savi et al., 2013), but little work has been done on this coupled relationship for hillslopes and how they respond to knickpoint propagation on larger temporal or spatial scales. Previous studies have addressed how wide floodplains can buffer interactions between channel and hillslope (Wohl, 2010), but none to our knowledge address how terraces separate these process domains. The aim of this study is to explore how hillslopes respond to base level change along the entire length of a river channel. To determine if hillslopes that have experienced base level fall are different from those that have not, and if they are different, do they differ systematically or in random manner.

The density, area, and type of mass movement throughout the basin can be compared along the length of the river, along with how these characteristics change with hillslope type. If the hillslopes that are shielded from base level fall signal by terraces respond in the same manner

as hillslopes that are directly connected to the channel. These characteristics can then be compared throughout the watershed; within the lower basin, which has experienced base level fall; within the knickzone, which is the area that is actively incising; and within the upper basin that has yet to experience base level fall.

Valley width can be used to determine which areas of a basin are actively experiencing base level fall, as the areas with higher rates tend to be narrow as vertical incision dominates (Montgomery, 2004). Valley width can also be used to characterize if a section of channel had been carved by fluvial or glacial processes (Amerson et al., 2008).

3.2 Study Area

The South Fork Eel River (SFER) is found within California's temperate Northern Coast Range, and spans ~1780 square kilometers as the second largest sub basin of the Eel River. The SFER is found within the accreted terrain of the Franciscan Complex, to the east of the Mendocino Triple Junction (McLaughlin et al., 2000; Lock et al., 2006; Bennett et al., 2016) (Figure 3.1). This accreted terrain is a mélange of material that consists primarily of greywackes, shales, conglomerates, sedimentary breccia, with greenstone, chert, and rare limestones (Wakabayashi, 2015).

The SFER is a bedrock dominated system, with numerous strath terraces along its entire length. These terraces, as described in chapter 2, are composed of four main treads – Qt_o, Qt_1, Qt_2, and Qt_3. The Qt_1 tread surface represents the uppermost continuous surface with terraces that young with distance upstream across a range of ages from 166.8 ± 42.2 ka to 124.7 ± 22.3 ka. It contains one prominent knickzone located ~135 kilometers upstream from its confluence with the main stem of the Eel River, between the tributary junctions of Tenmile and Rattlesnake

Creeks (Figure 3.2). The knickzone is ~10 kilometers in length, and extends from 250 to 400 meters above mean sea level (Fuller et al., 2009; Foster, 2010).

The SFER receives an annual average of ~200 cm of precipitation, as recorded from the monitoring stations in Garberville and Leggett, CA (National Center for Atmospheric Research, 2017). Precipitation is one of the major drivers within the watershed, with coast-facing ridges in the west receiving a majority of the moisture. Vegetation distribution within the SFER is strongly influenced by climate, lithology of bedrock and soils, and elevation. At present-day, these regions are dominated by Montane Hardwood Conifers, Douglas-fir, Redwood, and Montane Hardwood (USFS and BLM, 1996; California Department of Fish and Wildlife, 2014). The drier eastern side of the watershed is dominated by grasslands, white oak, and black oak woodlands (USFS and BLM, 1996). Various riparian plant communities can be found throughout the entire watershed (USFS and BLM, 1996). The SFER saw a significant increase in timber production beginning in the early 1900's, leading to an increase of sedimentation into the SFER and the removal of mature canopy cover for the region. In 1966, The Bureau of Land Management and U.S. Fish and Wildlife Service found that much of the watershed contains an early- to mid-mature canopy cover (USFS and BLM, 1996; California Department of Fish and Wildlife, 2016). Analysis of pollen within a core from Clear Lake, California shows that this vegetation has likely been dominant for the last 20,000 years. However, during the latest 130,000 years, records suggest that the climate was, on average, much colder (~8˚C) and wetter (~400 cm) (Adam et al., 1981; Adam and West, 1983). With this change in climate the region has also seen a shift in vegetation, with other coniferous species and pines being dominant.

3.3 Methods

This study relies entirely on topographic analysis made using 1m resolution LiDAR data collected by NCALM (Power, 2004; Perkins, 2009; Dietrich, 2014) in 2004, 2009, and 2014. LiDAR is essential for this analysis as it allows for a 'bare-earth' view (without vegetation) of the landscape. The SFER is a densely forested region, making it exceedingly difficult to map mass movements using aerial photos or even in the field. The 'bare-earth' view with LiDAR reveals how the topography, specifically the hillslopes, have responded to base level change. With LiDAR one can clearly see the hummocky topography of mass movements, along with the smooth 'melting' texture of hillslopes as they undergo creep processes. To cover the same area in the same level of detail using traditional methods would be tremendously time intensive, and difficult due to the steep terrain. Analysis for mass movements was completed using a combination of geostatistical and visualization tools in MATLAB and ArcGIS.

3.3.1 Valley Observations

3.3.1.1 Hillslope Classification

Hillslopes were classified into three primary categories based on topographic setting to determine how hillslope response changes along the channel; (1) no terraces present and directly connected to the river, (2) above Qt_1 and other terrace treads, and (3) above younger terrace tread type (Figure 3.3). The hillslopes above the various terrace treads are buffered from main river channel signals by the terraces themselves and therefore represent numerous stages of hillslope response. Since mainstem incision began after Qt_1 terrace tread surfaces were established, it is assumed that their hillslope form will be comparable to the relict landscape.

These were then further divided by their location within the basin; the lower basin, which encompasses the first 100 kilometers of the SFER and represents adjusted terrain; the knickzone,

which makes up the next ~10 kilometers and is actively adjusting; and the upper basin, which makes up the remaining ~60 kilometers and represents relict terrain. This was accomplished by first tracing the extent of hillslopes directly adjacent the river, extending up to the nearest ridgeline. This region was then divided into smaller sections as described above, while excluding terrace treads and the river channel itself. The hillslopes surrounding larger tributaries were categorized as directly connected to the channel as tributaries propagate the main channel signals up their own networks.

The hillslopes within the lower basin that are directly connected to the river are assumed to have minimal to no interference when adjusting to base level. While the hillslopes located above Qt_1 treads are assumed to be buffered from river incision by the terraces themselves. Preventing them from experiencing base level fall and preventing adjustment from taking place. Therefore, they are assumed to represent relict hillslopes within the lower basin. The third hillslope category encompasses all the hillslopes that are located within the knickzone. This section of the channel is actively adjusting to base level change, along with its hillslopes. The last section includes all the hillslopes located above the knickzone within the upper basin. This section of the channel has yet to experience main stem base level fall and represents the relict landscape.

3.3.1.2 Valley Width

To determine how valley width changes within the SFER, cross sections were made approximately every 1-kilometer along a simplified valley center line using 1-meter resolution LIDAR data. From these cross sections, a valley width was measured perpendicular to river flow. Measurements taken within meander bends were collected perpendicular to the general direction of river flow to better capture the true width. Valley width was determined by first

identifying the point where the hillside shifts from within the fluvial domain into hillslope domain, which was usually identified by a change in slope. This switch in domain typically occurred above terraces and above erosive banks along the river channel. The distance between these inflection points were then calculated from both river right and left to determine the valley width, hillslope type was also recorded for both sides of the river. These measurements were then binned and averaged by 10-kilometer-long ridgeline sections. These valley width measurements were then further subdivided into the several hillslope categories.

3.3.2 Mass Movement Digitization and Characterization

To determine how the hillslopes along the SFER have been responding to base level fall, mass movements along the main corridor of the river were characterized (Figure 3.4). Mass movements were first digitized using 1 m LiDAR, and identified by their hummocky topography and head/side scarps, which were distinct in contrast to the relatively smooth, creep-dominated surrounding hillslopes. The features were traced by hand in ArcMap, using a slope map as a guide. Only mass movements with clear boundaries (head and side scarps) were digitized and used within this study.

Once a mass movement had been identified a number of characteristics were recorded. These characteristics included the relative age with respect to its surrounding features, whether it was the oldest mass movement with younger mass movements cutting into its boundaries or vice versa. If it was a standalone feature it was difficult to determine its relative age. A primary movement type was also assigned, along with secondary or tertiary movement types if applicable for complex landslides. This was done by looking at the overall shape of the mass movement, the location of the head scarp, depositional materials, and rupture features as well as using the

criteria found in Highland and Bobrowsky, (2008). These movement types included translational slides, rotational slides, debris flow, earthflow, and areas of creep.

3.3.2.1 Percent Area and Number of Mass Movements

Once mass movements were digitized, the data set was subdivided into one of four hillslope classes: lower basin – no terrace, lower basin – above a Qt1 terrace, knickzone, and all hillslopes in the upper basin. The mass movements were then broken up into their respective river sections to determine what percent of the section area was affected by mass movements. For this calculation polygon area was re-calculated, to account for if any mass movements were cut by either hillslope type or by section boundaries. The total percent area covered by mass movements was then compiled for each section, along with the total number of MM bodies within each category.

3.3.2.2 Roughness Calculation for Mass Movement Bodies

Topographic roughness is often used to characterize or automate the mapping of mass movement bodies within a landscape (McKean and Roering, 2004; Booth et al., 2009; Grohmann et al., 2011; LaHusen et al., 2016). One method used to quantify topographic surface roughness is to measure the variability of slope and aspect of a DEM. This can be done by calculating the statistical variability of vector orientation, which are perpendicular to each cell within the DEM. The method used for this study was eigenvalue ratios, which determine the degree and amount of clustering of vectors within a user specified moving window, to determine how smooth a surface is (McKean and Roering, 2004). For this dataset, a sampling window size of 3x3 cells was used, with a cell size of 1-meter. The amount of clustering can be used as a proxy for how smooth a topographic surface is, with higher amounts of clustering representing smoother surfaces as the

resulting vectors would all be in a similar direction. Whereas, if the topography is relatively rough, the vectors would have a wide array of directions and therefore be less clustered.

This study uses these methods to determine how the roughness of geomorphic features within the SFER changes along its length. With modified code provided by McKean and Roering (2004), the amount smoothness of each individual mass movement was determined. Three mean eigenvalues were calculated for each MM, each value representing a different possible vector direction. Using the ratio of vector orientations in the X, Y directions, the amount of clustering can be determined for the hillslope surface.

3.4 Results

3.4.1.1 Coverage of Mass Movements – Number, Area Affected, Size

A total of 597 mass movement bodies were analyzed. There is large longitudinal variation in the number of mass movements found, their average size, and the total percent area that is being impacted by these features throughout the SFER. A majority of these mass movements are located on hillslopes that are directly connected to the river within the lower basin and throughout the knickzone (Figure 3.5A). These sections of channels have the highest density of mass movements per kilometer, with over four bodies per kilometer of channel. For the hillslopes above Qt1 terraces and within the upper basin, there were less than one mass movement per kilometer in these sections (Figure 3.6A). Section 4, in the lower basin, and section 10, just below the knickzone, have the largest total number of MM, with significant drops in mass movement count for the sections surrounding them.

The hillslopes that are directly connected to the river and the hillslopes within the knickzone have a larger percent area affected by mass movements than those that are either buffered by the Qt1 terraces or the hillslopes in the upper basin (Figure 3.6B & 3.5C). For

hillslopes in the lower basin that are directly connected to the river, approximately 12.9% of the area is affected by mass movements, with the first four sections of river being the most impacted by mass movements (Figure 3.5B). The hillslopes in the lower basin above a Qt1 terraces, only 3.2% of the area is affected by mass movements. 9.75% of the knickzone area is affected by mass movements, and within the upper basin only 1.4 % of the area is affected.

The upper basin has the lowest overall area affected by mass movements, but the mass movements within section 13 have the largest average size, with an average area of 0.19 ± 0.06 square kilometers (all uncertainties reported as 2σ of the standard error). Statistically, the lower basin has the largest area affected by MM, with the knickzone having the second largest area affected. While the hillslopes above Qt1 and in the upper basin have the smallest average area affected by MM and are statistically similar.

3.4.1.2 Valley Width

Valley width measurement shows that the valley is widest within the lower basin and narrows in the knickzone; width then increases slightly in the upper basin before it narrows again in the headwaters. There is a large amount of variation within these measurements (Figure 3.7), which can be attributed to the coarse 1 km binning of measurements at every 1 km along the center valley profile, along with the irregularity in terrace presence throughout the basin. For the first 40 kilometers of the SFER, the average width is analogous between sections, along with the amount of variation associated with these calculations. The channel is relatively straight with few terraces throughout. The remaining sections within the lower basin, have much more variability and contain numerous large terraces which are located along large meanders in the channel. Section 5 is especially dominated by expensive terraces along the 10-kilometer-long river section, leading to the considerable valley width measurements for this section of channel.

When comparing the several hillslope types, valley width is significantly wider in locations with Qt_1 terraces on either side of the river, with an average width of ~1200 ± 104 meters (Figure 3.6C). The knickzone has the narrowest overall valley width with an average of 170 ± 20 meters. Valley width in the upper and lower basins are slightly higher with average widths of ~350 ±80 meters and 245 ± 25 meters, respectively.

When looking at Figure 3.8A, which shows the average valley width by river section, the measurements within the lower basin are similar for the first 40 kilometers of the river, with a widening of the valley from 50-kilometers until just below the knickzone. This widening in valley width is concurrent with a shift in lithology from Central Franciscan Belt mélange to Coastal Franciscan Belt sediments. The knickzone then shows significant narrowing up into the beginning of the upper basin, before valley width then widens again before narrowing in the headwaters through the same Coastal Franciscan Belt sediments (Figure 3.1).

3.4.1.3 Primary Type of Movement

Translational slides are the dominant movement type, throughout the entire basin, regardless of the total number of MM within any section (Table 3.1 and Figure 3.11). Debris slides are the second most common MM type, showing an increase in numbers from 60 km up through the knickzone (% of total). Earthflows and translational slides are the dominant features in the lower basin (% of total). Out of the 597 mass movements used in this analysis, only 36 of these features were found above terraces – 6 above Qt_1 terraces.

3.4.1.4 Mass Movement Roughness

Roughness calculations show that mass movements become smoother with distance upstream, with the smoothest mass movements are found within the knickzone (Figure 3.9). There is a wide spread of amount clustering within the lower basin, near the mouth of the river,

which increases with distance upstream. Suggesting that the features within the lower basin have an overall roughness that is higher than the features found within the knickzone or the upper basin. When comparing hillslope types, the mass movements in the lower basin have the roughest surfaces (Figure 3.6D). The mass movements located above Qt_1 terraces are the next roughest, meaning they are smoother than those directly connected to the channel.

3.5 Discussion

3.5.1 Valley Width

The variance in average valley width along the channel is indicative of a valley that is adjusting to base level fall. Even though the valley narrows with overall distance upstream, it narrows within the knickzone before it widens again in the upper basin (Figure 3.10B). In a steady state landscape there would still upstream decreases in valley width, but it would consistently narrow with distance upstream (Figure 3.10A). The lower basin has experienced base level fall and is largely adjusted, leading to a wider valley that slowly narrows with distance up to the knickzone, before it abruptly narrows within the knickzone. Erosion is being focused within the knickzone, meaning that vertical erosion is dominant over lateral erosion, leading to the formation of this narrow canyon. Valley width then widens again within the upper basin, which represents the valley width of the relict landscape.

The width of the valley was significantly wider for the sections of channel that contained hillslopes above terraces by approximately a full order of magnitude with an average width of 1200 ± 100 meters (Figure 3.6C). This is expected because rivers widen their valleys when lateral erosion is greater than vertical incision, sometimes forming extensive floodplains that are later abandoned to preserve the terrace surfaces seen today. It is likely that the river was relatively stationary in elevation when carving the flood plain that would later form the Qt_1

terrace treads, as they are extensive features throughout the basin. The valley width for the lower basin, in locations where the hillslopes are directly connected to the channel (section 5-8), are significantly wider than within the knickzone or in the upper basin, with an average value of 350 ± 80 meters as compared to 170 ± 20 and 250 ± 26 meters, respectively. This could be a result of increasing stream power for the system, or due to the change in lithology from the lower basin into the knickzone and upper basin (Schanz and Montgomery, 2016). It is at section 5 that the SFER leaves the Coastal Franciscan Belt sediments, and begins to flow through the Central Franciscan Belt mélange. This mélange is composed of metamorphosed sediments and is more resistant than the sediments found further west in the Coastal belt.

3.5.2 Mass Movement Patterns

3.5.2.1 Basin Wide Response

The significant decrease in the percent area affected by mass movements in section 5 is likely a result of the sinuosity and presence of terraces. Section 5 is a highly sinuous section of channel with many terraces, which act as a buffer to the hillslopes, resulting in only 4% of the section being affected by mass movements. The number of mass movements increases through section 6 to section 10, just below the knickzone. The spike in the number of mass movements within section 10 could be due to focused erosion within the channel below the knickzone. As this is the tail end of the erosional front within the knickzone, which has mostly adjusted to base level change. The number of mass movements then decreases through the knickzone and into the upper basin. There is clear erosion into the hillslopes within the knickzone, but many of the MM are located along meander bends where erosion is more focused. Base level fall is being accomplished within the knickzone at present, therefore the relict upper basin has yet to experience base level fall. This relict landscape in turn shows very few mass movements, as the

hillslopes are relatively stable. The scarcity of mass movements within the upper basin could also be because only mass movements with clear boundaries were digitized and used. Implying that while there are only a few definable features, it is possible that there are more mass movements in the upper basin that are too old enough to have clear boundaries. That their scarps have been weathered and diffused through time.

Terraces are widespread throughout the SFER, buffering the hillslopes from incision. Only 36/597 mass movements are above terraces and only 6 above Qt1 throughout the whole basin. This indicates that terraces delay hillslope response to base level fall. This is particularly true for the upper basin, where terraces buffer the hillslopes even further from the small amount of incision that has occurred upstream of the knickpoint. This is important to consider when looking at the overall pattern of mass movements, as sections of the surrounding hillslopes are being buffered from mainstem base level fall. This impacts the overall number of mass movements occurring within the basin.

3.5.2.2 Variation in Hillslope Response

Over 12% of the hillslopes within the lower basin are affected by mass movements. The hillslopes that are within the knickzone, also have a high number of mass movements with 9.75% of the area being affected, as this section of the channel is actively adjusting (Figure 3.6B). There are a limited number of mass movements within the upper basin or above Qt_1 terraces. Base level fall has yet to propagate through the upper basin of the watershed, so the mass movements within this region represent the expected signal from weak lithology and high precipitation rates, with only 1.4% of the landscape affected by mass movements. The hillslopes above Qt_1 also represent relict topography, as the river cuts into the terrace and not the hillslope, which means the relative base level for the hillslope above the terrace is not changing because

the terrace tread elevation is staying constant. Since the area of hillslope being buffered by the terraces is relatively narrow, when mass movements do occur they have a greater effect on the area, resulting in approximately 3% of the buffered hillslopes being affected by mass movements. In general, we learn that incising landscapes that have the capacity to form and preserve terraces will take longer to re-equilibrate hillslopes following base level fall.

3.5.2.3 Type of Mass Movement Variation

Translational slides are the dominant type of mass movements throughout the basin, which typically occur in areas with readily available material (Figure 3.11). These features can move a lot of material quickly, compared to earthflows which can also cover a large area but move slowly. Debris flows were the next most common mass movement type and became more dominant in the areas below the knickzone (60-100 kilometers). The variation in the number and type of mass movements throughout the basin could be a result of changes in lithology, or due to the control exerted by stream power on the hillslopes themselves (sinuosity of the channel).

3.5.2.4 Roughness of Mass Movements

The roughness of mass movements adjacent to the SFER are rougher than the mass movements that occur on hillslopes within the upper basin (Figure 3.6D). Calculations also show that mass movements within the knickzone are smoother than those in the lower basin. This is likely because failures within the knickzone occur on steeper slopes and most materials are transported away, exposing the bedrock beneath, leaving behind less hummocky topography, which results in smoother surfaces. If this is true, then this would imply that soil coverage in the lower basin is thicker than in the knickzone for the smoother bedrock to become exposed. This

suggests that the hillslopes within the South Fork Eel River that have experienced base level fall earlier in time are significantly different from those that only recently have.

3.5.3 Basin-wide Response to Base Level Fall

3.5.3.1 River Response to Base Level Fall

As discussed in Chapter 2, terrace ages from the Qt_1 surface suggests a preliminary minimum central basin-wide age of 134 ± 29 thousand years. This central basin-wide age suggests that main stem incision within the SFER began after this time, and that the hillslopes within the lower basin have had ~134 ± 29 thousand years to adjust to base level change. The age progression of the Qt_1 terraces, along with the placement of intermediate terraces, suggests that lower basin incision was accomplished through progressive knickpoint retreat. As the Qt_1 terraces have two clusters of ages, which decrease with distance upstream, indicating that base level lowered incrementally, first at the outlet and later toward the headwaters.

3.5.3.2 Hillslope Response to Base Level Fall

The propagation of base level change through the lower basin destabilizes hillslopes, causing mass wasting events, which effectively re-equilibrate hillslopes. There is an overall decrease in the area affected by mass movements with distance upstream. The hillslopes in the lower basin that are directly connected to the SFER react more readily to these base level changes than the hillslopes that are buffered by terraces. Hillslopes located within the knickzone also show a high response to the incision that is actively occurring. The hillslopes in the upper basin represent the relict landscape, and a more natural response to high precipitation and weak lithologies. The pattern in which hillslopes are responding to base level change vary systematically along the channel, with a decreasing area affected by mass movements with

distance upstream. In combination with terrace age propagation, which decreases in age with distance upstream, it suggests that river incision was accomplished through knickpoint retreat through the lower basin, and the hillslopes reflect this behavior.

Some studies have looked how at hillslopes respond to change on a small scale, whether it is response to the propagation of a knickpoints (Ouimet et al., 2007; Gallen et al., 2011; DiBiase et al., 2014; Roering et al., 2015), or internal variations of mass movements themselves (McKean and Roering, 2004). Great work has been done on a section of hillslopes of the mainstem Eel River, just east of the SFER, on the spatial and temporal occurrence of mass movements and rock uplift rates (summarized in Roering et al., 2015). In their study area, mass movements are not random and instead occur in a way that best balances base level lowering, climatic changes, and lithologic variations. While that might be true on a smaller scale, it is important to apply this to a larger setting to see if it still holds true.

The work on the SFER looks at the large spatial scale changes along a similar environment, which base level changes are still propagating up through the surrounding hillslopes, as these features take additional time to adjust fully to changes. When studying landscape transience, more effort needs to be taken on the surrounding hillslopes as a whole to determine how the system continues to change through time. This can be done in the surrounding region to see how similar settings are responding to similar changes. If similar research is done on surrounding watersheds, more details on why there are differences spatially can be compared to determine if there is truly a pattern in how hillslopes respond to base level fall as it propagates up through a river network. This can also be done with other watersheds across the globe, to determine if there is a common trend on how hillslopes respond to base level fall on a basin wide scale.

3.6 Conclusions and Future Work

3.6.1 Summary

The variance in average valley width, from a wide lower basin that abruptly narrows into a canyon within a knickzone, which then widens again in the upper basin, is indicative of a channel that is experience transience and is adjusting to base level fall. The variability seen within valley width measurements is likely due to the coarse resolution of sampling and for the lower basin, a change in lithology from weak sediments into slightly more resistant mélange.

The hillslopes within the SFER that have experienced base level fall in the lower basin and within the knickzone differ from the hillslopes that are located in the upper basin or are buffered by terraces. There are significantly more mass movements present throughout the lower basin, which affect a greater overall hillslope area. The number of mass movements systematically decreases with distance upstream, suggesting that the hillslopes are responding to knickpoint retreat through the lower basin. That the hillslopes in the knickzone are actively adjusting, and the hillslopes in the upper basin have yet to experience significant base level fall.

This research can be applied to the surrounding region to determine if hillslopes within a similar setting respond in a similar way, and to determine what controls the spatial patterns of where mass movements occur. If other studies are done in a similar style globally, we can learn what trends hillslopes may follow when re-equilibrating to base level change.

3.6.2 Future Applications

To further understand how hillslopes respond to base level fall, determining how valley side-slope changes along the channel can support which parts of the channel are adjusting. As steeper slopes are less stable, and are likely adjusting. A more detailed geologic map, would allow for a more detailed analysis on what impacts the lithology has on how the system responds

to change. If valley width is greatly influenced by these changes in lithology, or if there is a relationship between the mass movement occurrence, type of mass movement, roughness characteristics and the type of bedrock and bedding plans. Future work would also benefit from similar analysis within other watersheds within the Franciscan Complex to determine if this same pattern is seen. As the surrounding region is likely affected by the same disturbances as the SFER, so a comparison between sites in the surrounding region would be beneficial to determine if their hillslopes follow a similar trend or not. To determine if a change in total watershed area has a larger impact than the small scale changes in similar mélange lithology. Comparing similar watersheds would help in determining how large of a role does lithology play in hillslope response to base level fall with knickpoint retreat.

Chapter 3 Tables

Table 3.1: Number of mass movements by type for each section. Data showing the style of mass movements relative to their distance along the South Fork Eel River. Each section represents 10 km of length along the valley width profile.

SECTION #	TRANSLATIONAL	ROTATIONAL	EARTHFLOW	CREEP	DEBRIS FLOW	TOTAL MM
1	30	8	7	0	2	47
2	21	11	16	1	1	50
3	11	1	11	2	4	29
4	45	14	24	5	6	94
5	19	1	5	0	2	27
6	22	4	8	1	4	39
7	22	3	3	4	9	41
8	27	3	3	1	11	45
9	23	8	2	0	13	46
10	43	2	4	3	21	73
11	15	11	1	1	16	44
12	7	4	1	1	8	21
13	0	0	2	0	0	2
14	3	0	0	0	0	3
15	0	0	0	0	0	0

Chapter 3 Figures

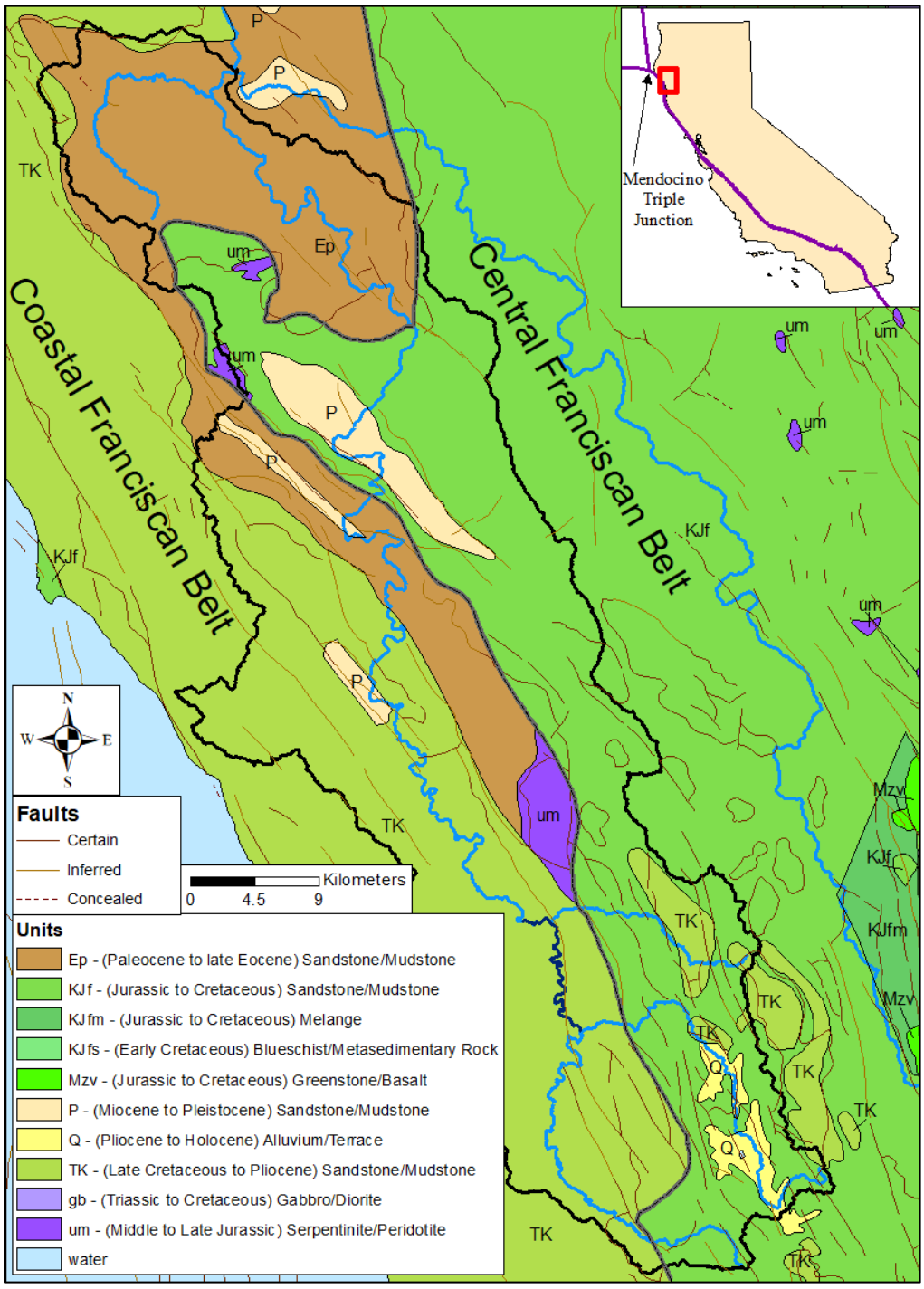

Figure 3.1: Geologic map of the SFER watershed and surrounding areas. Lithology within the Franciscan is inconsistent and highly variable throughout the area (Wakabayashi, 2011). Terraces are present in both the mixed sandstones and mudstones of Triassic and Jurassic ages.

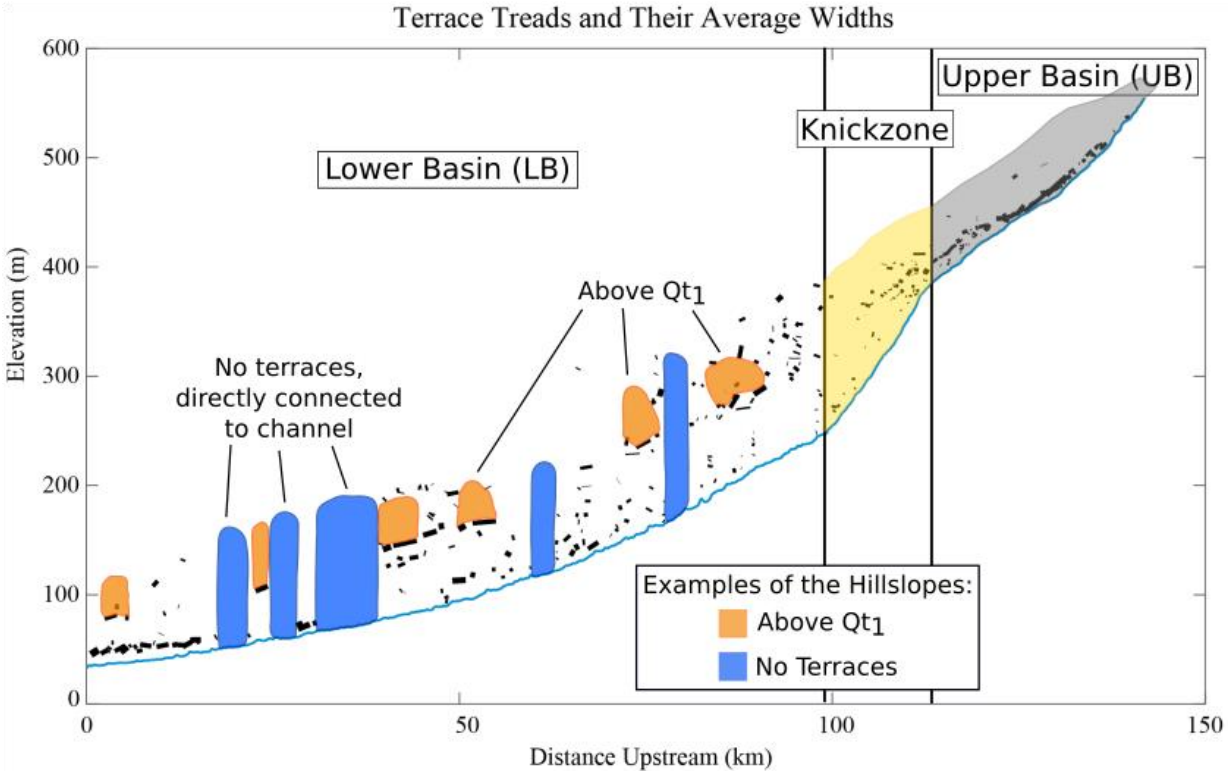

Figure 3.2: Strath terrace treads plotted along the longitudinal profile of the South Fork Eel River, with colored hillslope domains. The line thicknesses for each terrace is proportional to terrace width, logarithmically scaled. The primary hillslope categories for the lower basin (LB) are: above Qt_1 terrace treads (orange), directly connected to the SFER without any terraces (blue), above other terrace treads (no shading). The hillslopes were analyzed as a group within knickzone (yellow) and the upper basin (UB - grey).

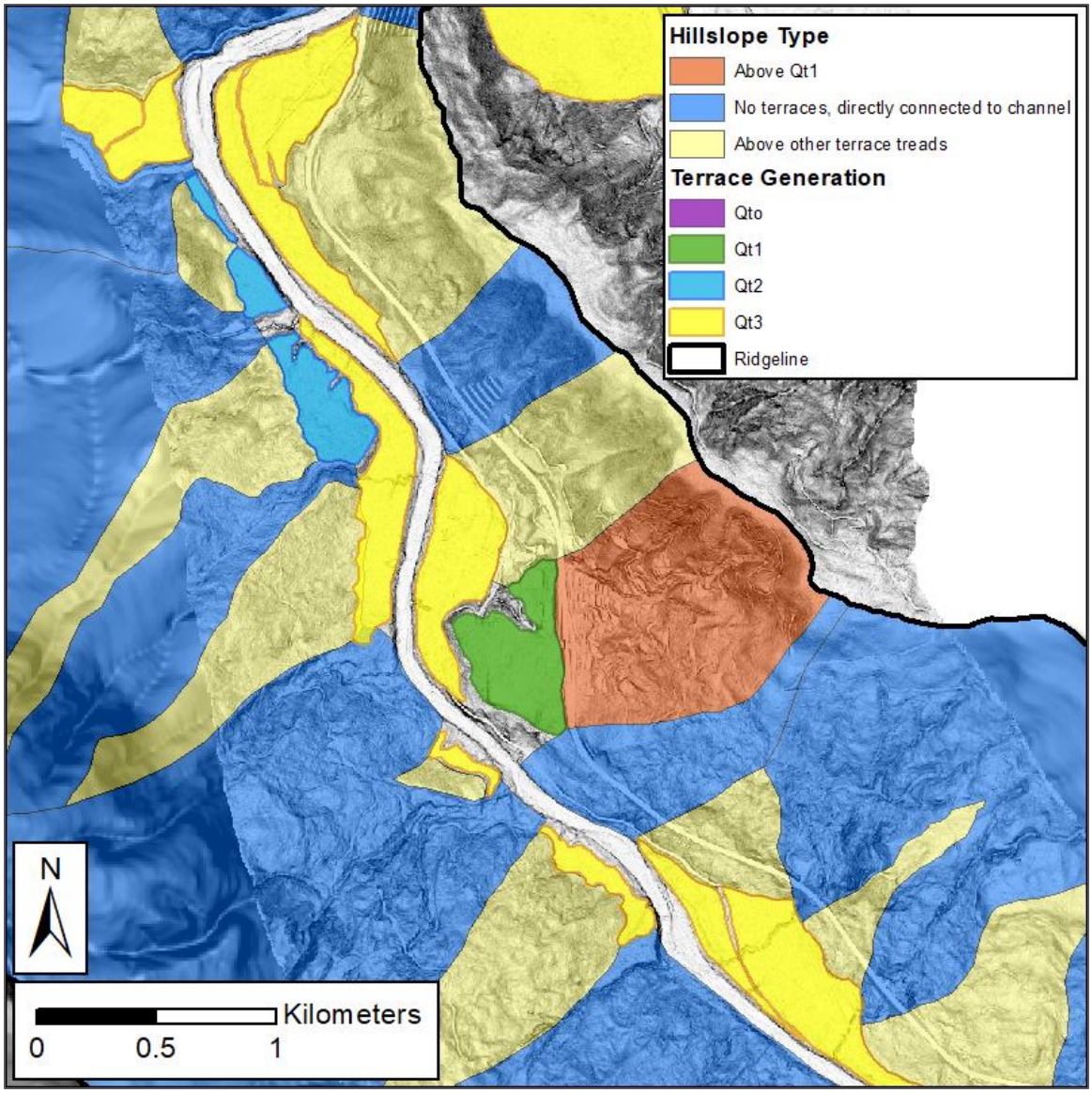

Figure 3.3: Example of the various hillslope types along the lower basin of the SFER near the mouth, along with some examples of the different terrace generations.

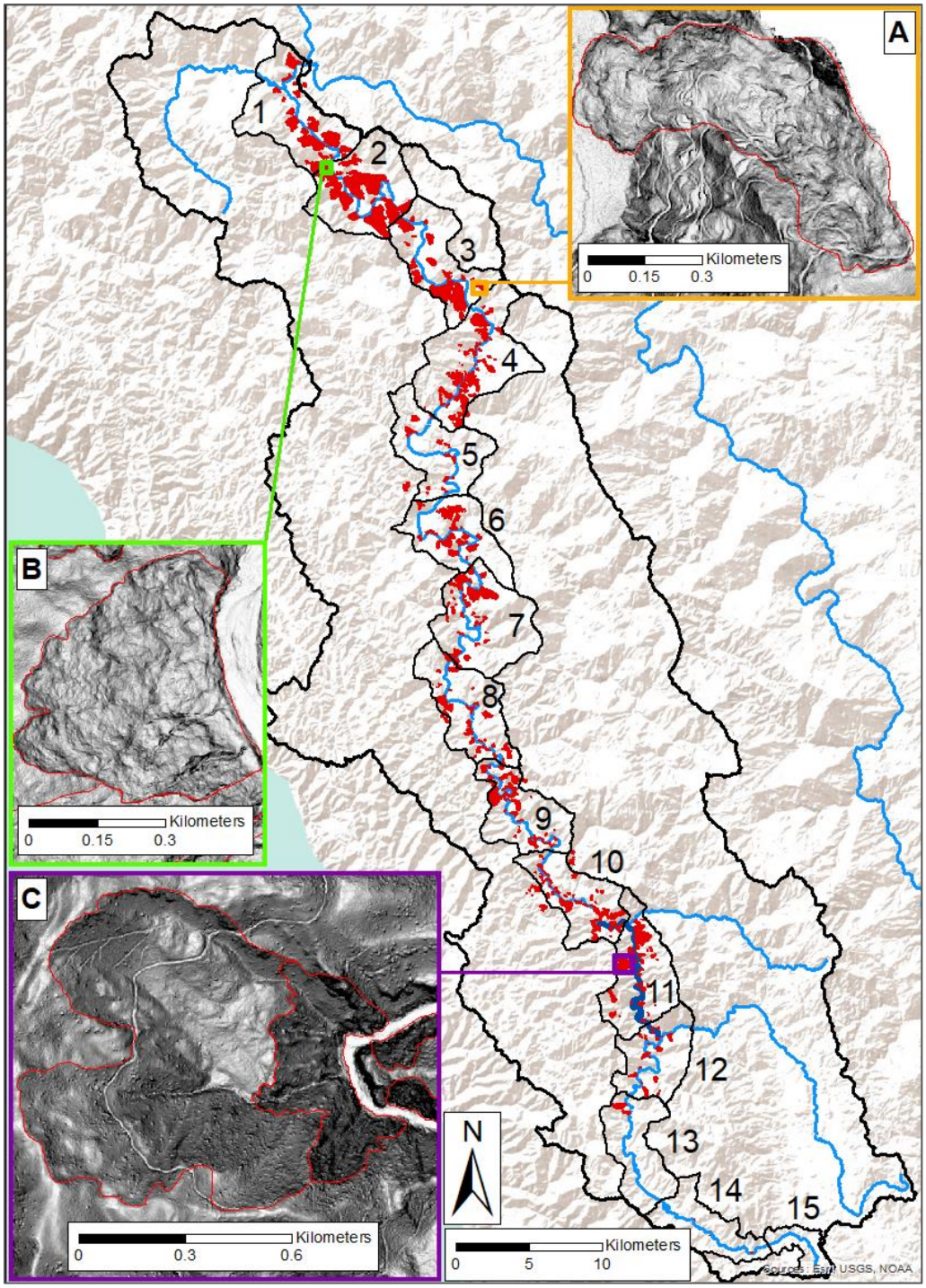

Figure 3.4: Locations of mass movements along the SFER identified in this study. SFER knickzone is in dark blue. Small framed images are examples of the identifying features of mass movements. A (Orange): Debris flow, with minor rotation. B (green): Translational slide with some rotation. C (Purple): Larger translational slide with some rotation, and a debris flow. Ridgeline sections are outlined in black with corresponding section number.

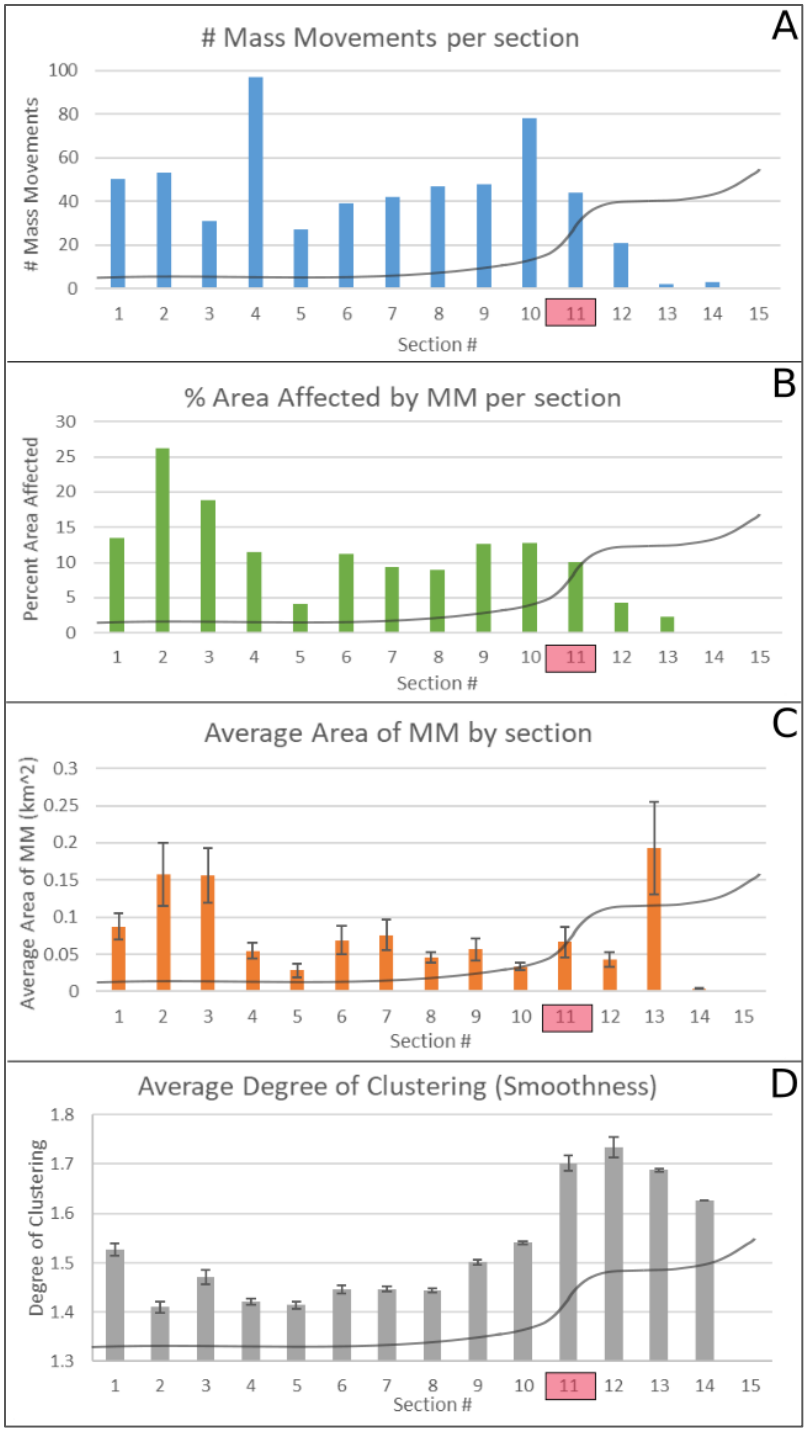

Figure 3.5: Mass movement metrics per section along the SFER. Section 11 contains the knickzone, which is marked using the red box. Simplified channel profile in grey across datasets. A) The total number of mass movements within each section along the SFER. B) Percent area affected by mass movement for each section. C) Average area of mass movements by section, with standard error of 2σ. D) The average degree of vector clustering for mass movement bodies which is used as a proxy for how smooth a DEM surface is.

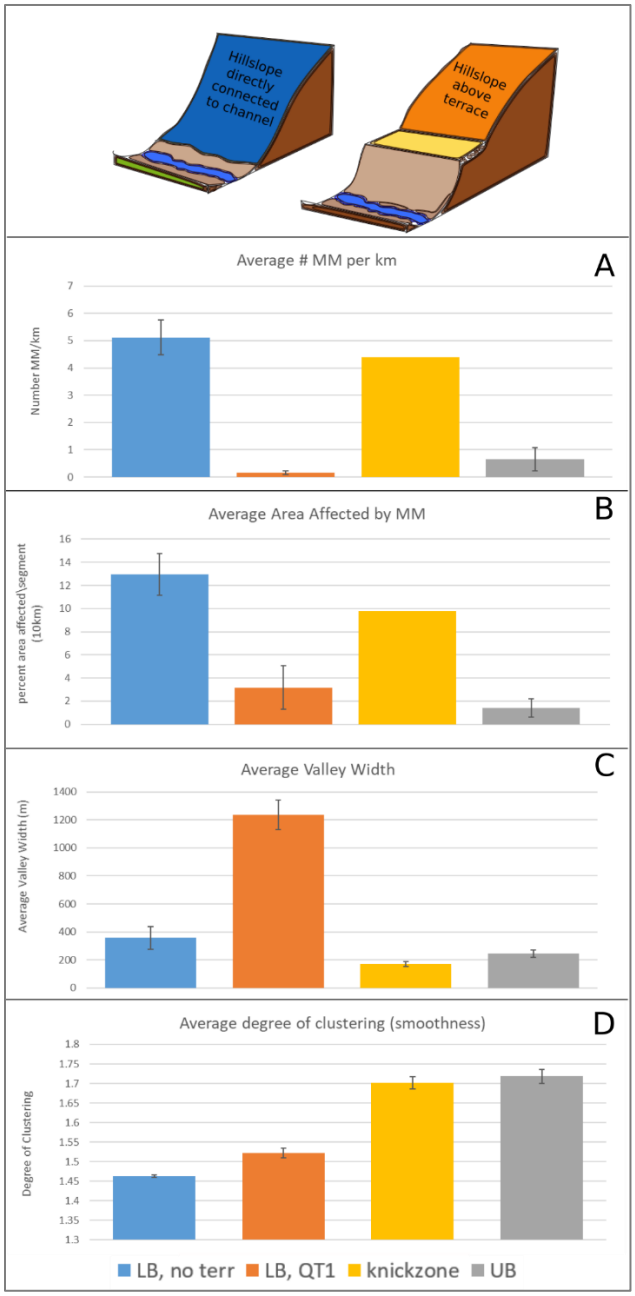

Figure 3.6: Mass movement metrics by hillslope category in the SFER. *LB, no terr* – hillslopes in the lower basin which are directly connected to the channel; *LB, QT1* – hillslopes in the lower basin which are located above Qt_1 terraces (see inset above graphs); *knickzone* – all hillslopes within the knickzone; *UB* – all hillslopes within the upper basin. A) The total number of mass movements for each hillslope category. All plots indicate a standard error of 2σ. B) Average percent area affected by mass movement for each hillslope category. C) Average valley width for each hillslope category. D) The average degree of vector clustering for mass movement bodies within each hillslope category, which is used as a proxy for how smooth the surface is. The knickzone does not contain error bars for A or B, as values are binned by 10 kilometer sections of river for these calculations, and the knickzone falls into one bin.

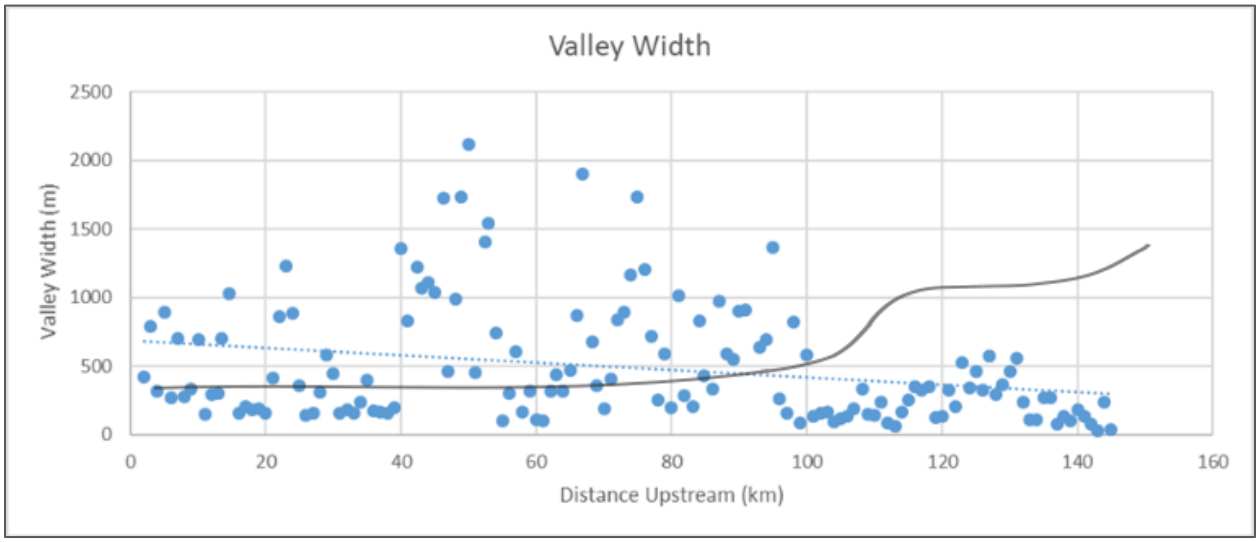

Figure 3.7: Individual valley width measurements, plotted against distance upstream. Valley width becomes less variable in and above the knickzone. The knickzone is located between 100-110 kilometers. Simplified channel profile in grey.

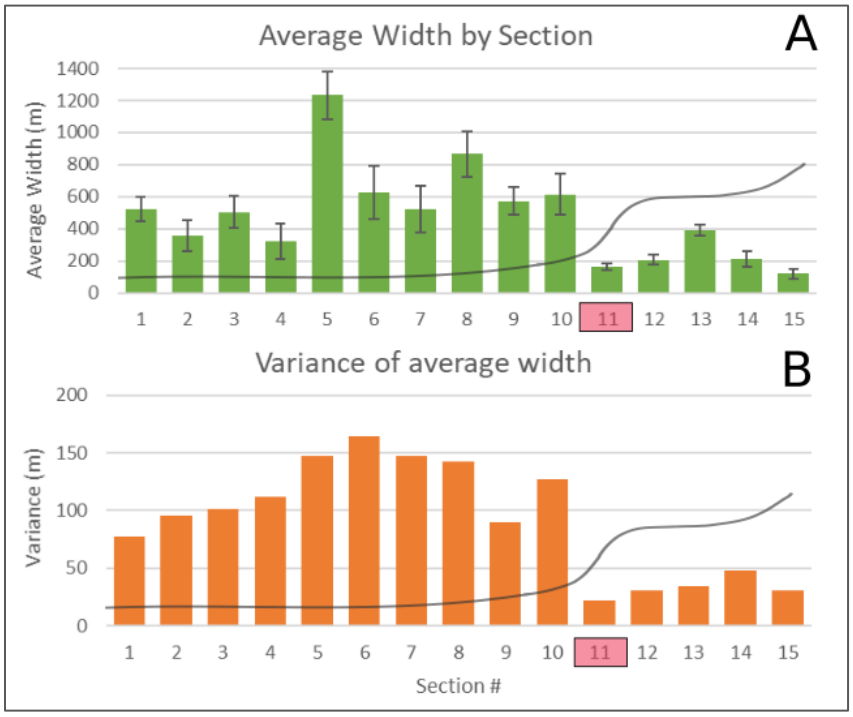

Figure 3.8: Average valley width by section ± 2 sigma. A) Valley width measurements by section, and B) the associated variation/error on these averages. Simplified channel profile in grey. Knickzone is marked by a red box in section 11.

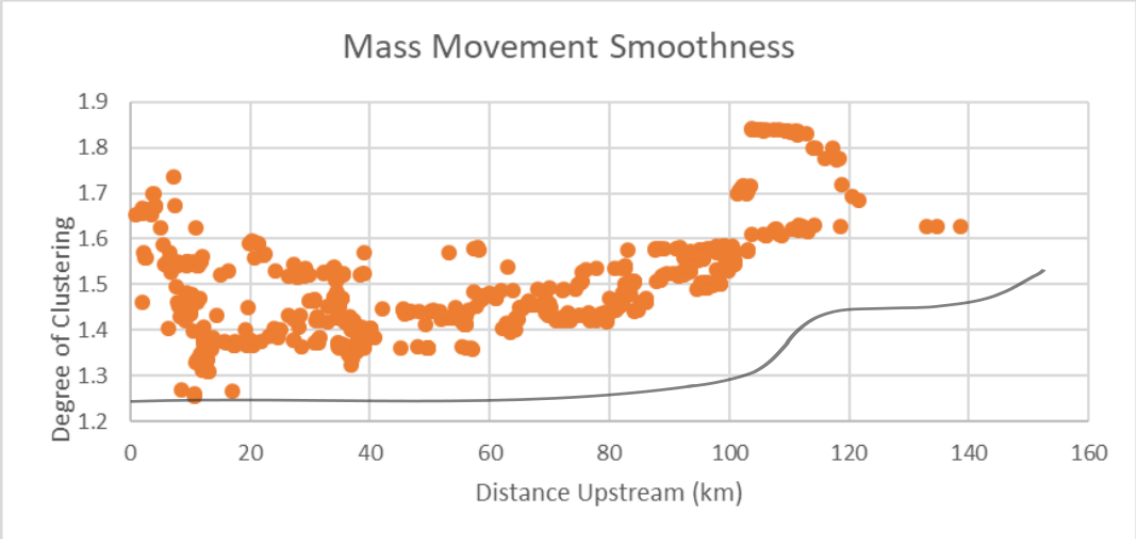

Figure 3.9: Individual roughness value calculations (degree of clustering) for each mass movement with distance upstream. The knickzone is located between 100-110 kilometers. This figure shows that there is a lot of variation in the degree of clustering within the lower basin, and overall mass movements become smoother with distance upstream. Simplified channel profile in grey.

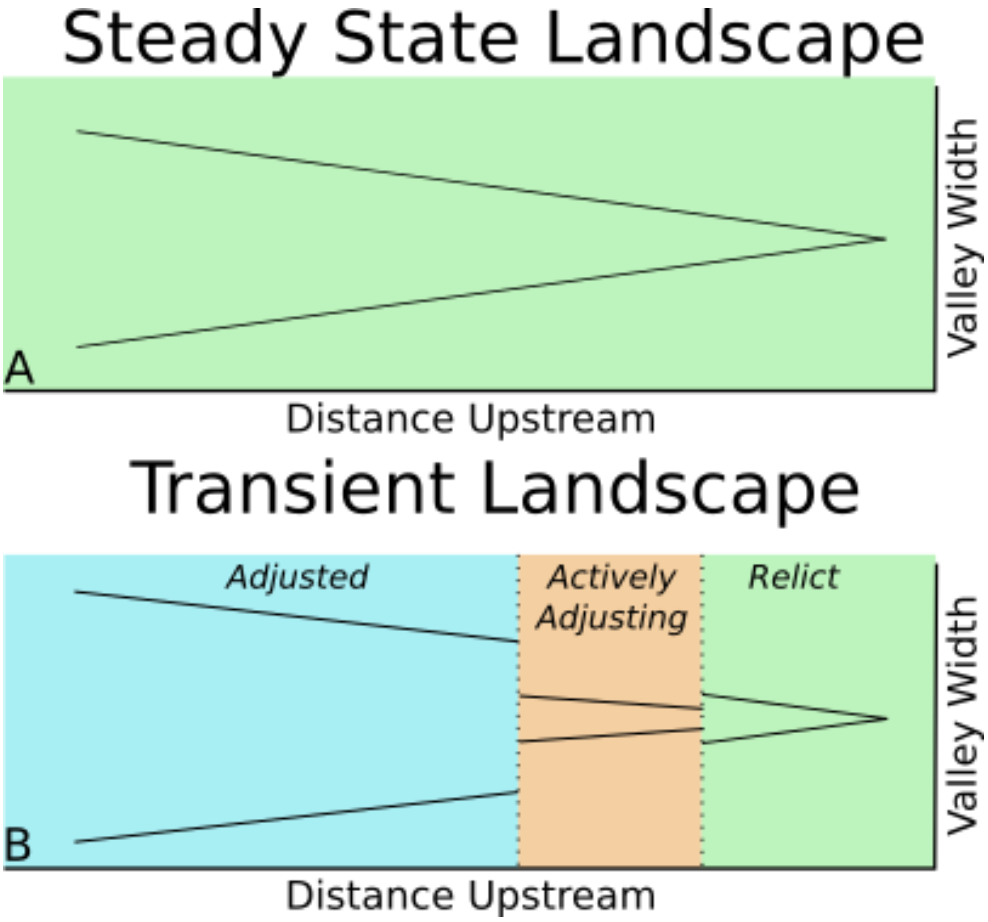

Figure 3.10: Conceptual model of valley width changes in either a steady state landscape or a transient landscape. A) Steady state landscapes have a linear relationship for decreasing valley width with distance upstream. B) A transient landscape has changing valley widths for the various sections of channel. A wide valley with that slowly decreases with distance upstream, which has adjusted to new base level conditions. The section of channel that is actively adjusting is abruptly narrower than the adjusted landscape. Finally the relict section of the channel has not undergone base level fall yet and still represents previous base level valley width conditions.

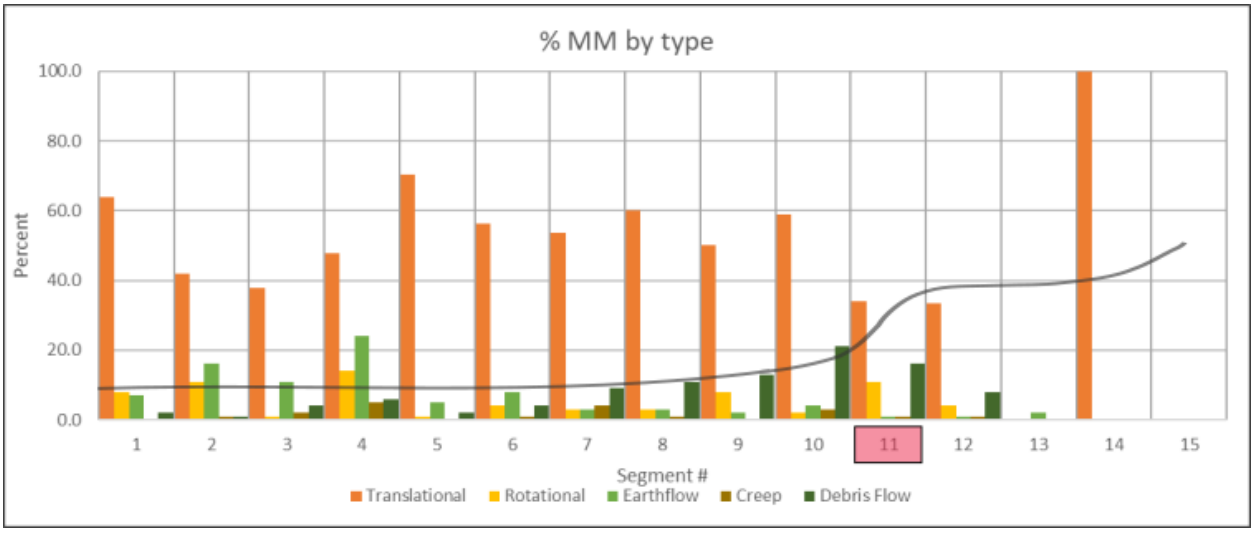

Figure 3.11: Mass movement percentages by type within each channel section. The knickzone is boxed in red, and the simplified channel profile is in grey.

References

Adam, D.P., Sims, J.D., and Throckmorton, C.K., 1981, 130,000-yr continuous pollen record from Clear Lake, Lake County, California: Geology, v. 9, p. 373–377, doi: 10.1130/0091-7613(1981)9<373.

Adam, D.P., and West, J.G., 1983, Temperature and precipitation estimates through the last glacial cycle from Clear Lake, California, pollen data: Science, v. 219, p. 168–170.

Amerson, B.E., Montgomery, D.R., and Meyer, G., 2008, Relative size of fluvial and glaciated valleys in central Idaho: Geomorphology, v. 93, p. 537–547, doi: 10.1016/j.geomorph.2007.04.001.

Anderson, S.W., Anderson, S.P., and Anderson, R.S., 2015, Exhumation by debris flows in the 2013 Colorado front range storm: Geology, v. 43, p. 391–394, doi: 10.1130/G36507.1.

Bennett, G.L., Miller, S.R., Roering, J.J., and Schmidt, D.A., 2016, Landslides, threshold slopes, and the survival of relict terrain in the wake of the Mendocino Triple Junction: Geology, v. 44, p. 363–366, doi: 10.1130/G37530.1.

Booth, A.M., Roering, J.J., and Perron, J.T., 2009, Automated landslide mapping using spectral analysis and high-resolution topographic data: Puget Sound lowlands, Washington, and Portland Hills, Oregon: Geomorphology, v. 109, p. 132–147, doi: 10.1016/j.geomorph.2009.02.027.

California Department of Fish and Wildlife, 2014, South Fork Eel River Watershed Overview: p. 186.

California Department of Fish and Wildlife, 2016, Study Plan: Habitat and Instream Flow Evaluation for Anadromous Salmonids in the South Fork Eel River and Tributaries, Humboldt and Mendocino Co.

Crosby, B.T., and Whipple, K.X., 2006, Knickpoint initiation and distribution within fluvial networks: 236 waterfalls in the Waipaoa River, North Island, New Zealand: Geomorphology, v. 82, p. 16–38, doi: 10.1016/j.geomorph.2005.08.023.

DiBiase, R.A., Heimsath, A.M., and Whipple, K.X., 2012, Hillslope response to tectonic forcing in threshold landscapes: Earth Surface Processes and Landforms, v. 37, p. 855–865, doi: 10.1002/esp.3205.

DiBiase, R.A., Whipple, K.X., Lamb, M.P., and Heimsath, A.M., 2014, The role of waterfalls and knickzones in controlling the style and pace of landscape adjustment in the western San Gabriel Mountains, California: Bulletin of the Geological Society of America, v. 127, p. 539–559, doi: 10.1130/B31113.1.

Dietrich, W.E., 2014, Eel River Critical Zone Observatory July 2014 Lidar Survey: National Center for Airborne Laser Mapping, doi: 10.5069/G9MP517V.

Foster, M.A., 2010, Knickpoints in tributaries of the south fork Eel River, Northern California [M.S. Thesis]: Humboldt, California State University, 97 p.

Foster, M.A., and Kelsey, H.M., 2012, Knickpoint and knickzone formation and propagation, South Fork Eel River, northern California: Geosphere, v. 8, p. 403–416, doi: 10.1130/GES00700.1.Fuller, T.K., Perg, L.A., Willenbring, J.K., and Lepper, K., 2009, Field evidence for climate-driven changes in sediment supply leading to strath terrace formation: Geology, v. 37, p. 467–470, doi: 10.1130/G25487A.1.

Gallen, S., Wegmann, K., Frankel, K., Hughes, S., Lewis, R., Lyons, N., Paris, P., Ross, K., Bauer, J., and Witt, A., 2011, Hillslope response to knickpoint migration in the Southern Appalachians: Implications for the evolution of post-orogenic landscapes: Earth Surface Processes and Landforms, v. 36, p. 1254–1267, doi: 10.1002/esp.2150.

Goode, J.R., and Wohl, E., 2010, Substrate controls on the longitudinal profile of bedrock channels: Implications for reach-scale roughness: Journal of Geophysical Research: Earth Surface, v. 115, p. 1–14, doi: 10.1029/2008JF001188.

Grohmann, C.H., Smith, M.J., and Riccomini, C., 2011, Multiscale analysis of topographic surface roughness in the Midland Valley, Scotland: IEEE Transactions on Geoscience and Remote Sensing, v. 49, p. 1200–1213, doi: 10.1109/TGRS.2010.2053546.

Harvey, A.M., 2002, Effective timescales of coupling within fluvial systems: Geomorphology, v. 44, p. 175–201, doi: 10.1016/S0169-555X(01)00174-X.

Highland, L.M., and Bobrowsky, P., 2008, The Landslide Handbook — A Guide to Understanding Landslides: USGS, v. Circular 1, 0-129 p., doi: Circular 1325.

Korup, O., and Schlunegger, F., 2007, Bedrock landsliding, river incision, and transience of geomorphic hillslope-channel coupling: Evidence from inner gorges in the Swiss Alps: Journal of Geophysical Research: Earth Surface, v. 112, doi: 10.1029/2006JF000710.

LaHusen, S.R., Duvall, A.R., Booth, A.M., and Montgomery, D.R., 2016, Surface roughness dating of long-runout landslides near Oso, Washington (USA), reveals persistent postglacial hillslope instability: Geology, v. 44, p. 111–114, doi: 10.1130/G37267.1.

Lock, J., Kelsey, H., Furlong, K., and Woolace, A., 2006, Late Neogene and Quaternary landscape evolution of the northern California Coast Ranges: Evidence for Mendocino triple junction tectonics: Bulletin of the Geological Society of America, v. 118, p. 1232–1246, doi: 10.1130/B25885.1.

Mackey, B.H., Scheingross, J.S., Lamb, M.P., and Farley, K.A., 2014, Knickpoint formation, rapid propagation, and landscape response following coastal cliff retreat at the last interglacial sea-level highstand: Kaua'i, Hawai'i: Bulletin of the Geological Society of America, v. 126, p. 925–942, doi: 10.1130/B30930.1.

McKean, J., and Roering, J., 2004, Objective landslide detection and surface morphology mapping using high-resolution airborne laser altimetry: Geomorphology, v. 57, p. 331–351, doi: 10.1016/S0169-555X(03)00164-8.

McLaughlin, R., Ellen, S., Blake, M., Jayko, A., Irwin, W., Aalto, K., Carver, G., and Clarke Jr, S., 2000, Geology of the Cape Mendocino, Eureka, Garberville, and Southwestern part of the Hayfork 30x60 Minute Quadrangles and Adjacent Offshore Area, Northern California, Plate 3: Garberville Quadrangle: USGS.

Montgomery, D.R., 2004, Observations on the role of lithology in strath terrace formation and bedrock channel width: American Journal of Science, v. 304, p. 454–476, doi: 10.2475/ajs.304.5.454.

Mudd, S.M., 2016, Detection of transience in eroding landscapes: Earth Surface Processes and Landforms, doi: 10.1002/esp.3923.

National Center for Atmospheric Research, 2017, The Climate Data Guide: PRISM High-Resolution Spatial Climate Data for the United States: Max/min temp, dewpoint, precipitation: NCAR Climate Data Guide, https://climatedataguide.ucar.edu/climate-data/prism-high-resolution-spatial-climate-data-united-states-maxmin-temp-dewpoint. (accessed February 2018).

Ouimet, W.B., Whipple, K.X., Royden, L.H., Sun, Z., and Chen, Z., 2007, The influence of large landslides on river incision in a transient landscape: Eastern margin of the Tibetan Plateau (Sichuan, China): Geological Society of America Bulletin, v. 119, p. 1462–1476, doi: 10.1130/B26136.1.

Perkins, J., 2009, South Fork Eel River, CA: Understanding Terrace Formation and Abandonment: National Center for Airborne Laser Mapping, doi: 10.5069/G93F4MH1.

Roering, J.J., Mackey, B.H., Handwerger, A.L., Booth, A.M., Schmidt, D.A., Bennett, G.L., and Cerovski-Darriau, C., 2015, Beyond the angle of repose: A review and synthesis of landslide processes in response to rapid uplift, Eel River, Northern California: Geomorphology, v. 236, p. 109–131, doi: 10.1016/j.geomorph.2015.02.013.

Savi, S., Schneuwly-Bollschweiler, M., Bommer-Denns, B., Stoffel, M., and Schlunegger, F., 2013, Geomorphic coupling between hillslopes and channels in the Swiss Alps: Earth Surface Processes and Landforms, v. 38, p. 959–969, doi: 10.1002/esp.3342.

Schanz, S.A., and Montgomery, D.R., 2016, Lithologic controls on valley width and strath terrace formation: Geomorphology, v. 258, p. 58–68, doi: 10.1016/j.geomorph.2016.01.015.

Schlunegger, F., Detzer, K., and Olsson, D., 2002, The evolution towards steady state erosion in a soil-mantled drainage basin: Semi-quantitative data from a transient landscape in the Swiss Alps: Geomorphology, v. 43, p. 55–76, doi: 10.1016/S0169-555X(01)00120-9.

Schlunegger, F., Norton, K., and Caduff, R., 2013, Hillslope processes in Temperate Environments: Treatise on Geomorphology, v. 7, p. 337–354, doi: 10.1016/B978-0-12-374739-6.00183-4.

Schlunegger, F., and Schneider, H., 2005, Relief-rejuvenation and topographic length scales in a fluvial drainage basin, Napf area, Central Switzerland: Geomorphology, v. 69, p. 102–117, doi: 10.1016/j.geomorph.2004.12.008.

Sklar, L.S., and Dietrich, W.E., 2001, Sediment and rock strength control on river incision into bedrock: Geology, v. 29, p. 1087–1090, doi: 10.1130/0091-7613(2001)029<1087:SARSCO>2.0.CO.

Stern, R.J., 2004, Subduction initiation: spontaneous and induced: Earth and Planetary Science Letters, v. 226, p. 275–292, doi: 10.1016/j.epsl.2004.08.007.

USFS, and BLM, 1996, South Fork Eel River Watershed Analysis.

Wakabayashi, J., 2015, Anatomy of a subduction complex: architecture of the Franciscan Complex, California, at multiple length and time scales: International Geology Review, v. 6814, p. 37–41, doi: 10.1080/00206814.2014.998728.

Wakabayashi, J., 2011, Mélanges of the Franciscan Complex, California: Diverse structural settings, evidence for sedimentary mixing, and their connection to subduction processes: Geological Society of America Special Papers, v. 480, p. 117–141, doi: 10.1130/2011.2480(05).

Wohl, E., 2010, A brief review of the process domain concept and its application to quantifying sediment dynamics in bedrock canyons: Terra Nova, v. 22, p. 411–416, doi: 10.1111/j.1365-3121.2010.00950.x.

Chapter 4 : Conclusions and Recommendations

4.1 Terraces and Landscape Transience

As landscapes respond to changes in forcings, they leave behind remnants of their previous form. These remnants include strath terraces, which represent segments of the abandoned river bed that were isolated when the channel incises down into bedrock. The placement of terraces along a channel in combination with ages of fill, can be used to determine the timing of river incision and characterize how incision may have been accomplished. The South Fork Eel River (SFER) contains numerous alluvium mantled strath terraces. Four terrace steps were identified within the SFER. Qt_o, represents the oldest terraces which are scattered throughout and are located far above the current river channel. The next terrace step, Qt_1, represents the upper-most prominent longitudinally discontinuous surface within the basin. Below Qt_1 are intermediate terraces, Qt_2, which are scattered throughout the lower basin and have no clear tread along the length of the basin. The final step, Qt_3, represent the terraces that are located just above the present-day channel.

Processed feldspar grains from the lower basin, using post-infrared infrared stimulated luminescence (pIR-IRSL) methods, yield a terrace abandonment age of at least 134 ± 29 ka. This age suggests that conditions for the SFER changed around 134 kya, causing mainstem incision to begin.

Individual Qt_1 terrace ages may show an overall decrease in age with distance upstream. This age progression suggests that progressive knickpoint retreat is the dominant form of river incision for the SFER. This implies that multiple steps of knickpoint retreat occurred through the lower basin up to the present day knickzone, where it became hung up at its current location. This hang up at the knickzone location is likely due to a decrease in stream power from the

diminished drainage area of the upper SFER at Tenmile Creek. A change in lithology may also be impacting incision at this location, along with the presence of a fault that runs through the center of the knickzone.

4.2 Hillslopes and Landscape Transience

There is a coupled relationship between rivers and their surrounding hillslopes; as a river responds to a change, the hillslopes must also adjust. Hillslope adjustment can be characterized by the spatial distribution and characteristics of mass movement bodies (MM), along with valley width variation. The spatial distribution of MM shows that with distance upstream there is a decrease in the number and total area affected by instability. Hillslopes that are directly connected to the river channel or within the knickzone show a greater response to incision than hillslopes that are buffered by Qt_1 terraces, or hillslopes within upper basin. Terraces likely act as a buffer, preventing the hillslopes from experiencing base level fall. Whereas the upper basin represents the relict landscape that has not undergone the 60 meters of incision. The type of MM also vary with distance upstream. Translational slides dominate throughout the entire basin, with debris flows increasing in occurrence from mid-lower basin up through the knickzone. MM roughness also decreases with distance upstream, implying that the features within the lower basin are more active than those further upstream, or that more material is available for movement within the lower basin. As the MM within the lower basin have a strong hummocky texture, and the MM within the knickzone and upper basin have a smoother texture.

Valley width narrows with distance upstream, with the knickzone staying fairly narrow, before the valley opens up again just above the knickzone. Valley width then declines again into the headwaters of the SFER. The largest variation in valley width is within the lower basin and where Qt_1 terraces dominate the river. This signifies that the lower basin has undergone a larger

amount of lateral river erosion in comparison to the knickzone, where vertical incision dominates. The increase in valley width above the knickpoint shows that the upper basin still represents the relict landscape conditions. The observed variation with distance upstream in the mass movement occurrence and characteristics, along with valley width changes, provides additional support that river incision was accomplished through progressive knickpoint retreat.

4.3 Opportunities for Future Work

To gain further understanding into how incision was accomplished throughout the SFER, additional terrace ages would be beneficial. Resampling of the Weott terrace, at a greater depth and better location could yield more confident results. Sampling of a Qt_1 terrace within the upper basin, above the knickpoint, would allow for a more complete basin-wide average age for terraces within that region. Lastly, the sampling of a flight of intermediate terraces would be extremely beneficial for determining the rate of river incision within the lower basin.

Slope analysis of MM and the hillslopes as a whole would be valuable, as slope can also be used to determine which areas of the basin are over steepened and adjusting to change versus areas with lower slope angles that have likely adjusted already. This large MM dataset could also be looked at in greater detail and compared against sinuosity, lithology, slope, valley width, etc. to determine what other controls there may be on the type or location of MM bodies.

More detailed geologic maps would also be highly valuable, as the coarse resolution of geology in the region makes it difficult to evaluate how the lithology of the watershed changes, and may be impacting the results we see. To determine if certain lithology's do erode more easily in certain sections of the watershed, either with distance upstream or if the Coastal Franciscan Belt terrain weathers differently than the Central Franciscan Belt terrain.

4.4 Project Limitations and Lessons

Some limitations that arose for the terrace data, included the limited number of terrace samples that were able to be collected. While many landowners were extremely accommodating with access to their property, some locations we were unable to get permissions for sampling (especially the intermediate terraces). Some locations were also less than ideal, as shown with the young ages for the Weott and Miranda terraces. Terrace strath and fill contacts where difficult to discern, along with having less defined flat terrace treads at sample locations. Weott and Miranda terraces had more rounded edges and treads at the sampling locations.

It was also difficult only being able to collect samples after sunset, limiting the number of samples could be collected at a time. Typically a maximum of two locations a night, depending on the difficulty of access and distance to sample location. The processing steps for feldspars also take longer than for quartz when their natural dose rate is being determined, as the charge stored within feldspars naturally decay overtime, and additional post-processing is required.

The limited extent of LiDAR along the SFER corridor limited the extent that MM could be studied, as these features cannot be discerned using the 10m DEM up to the nearest ridgelines.

References

Adam, D.P., and West, J.G., 1983, Temperature and precipitation estimates through the last glacial cycle from Clear Lake, California, pollen data: Science, v. 219, p. 168–170.

Muhs, D.R., Simmons, K.R., Schumann, R.R., Groves, L.T., Mitrovica, J.X., and Laurel, D., 2012, Sea-level history during the Last Interglacial complex on San Nicolas Island, California: implications for glacial isostatic adjustment processes, paleozoogeography and tectonics: Quaternary Science Reviews, v. 37, p. 1–25, doi: 10.1016/J.QUASCIREV.2012.01.010.